Coordination Chemistry Reviews
219–221 (2001) 605–663

COORDINATION
CHEMISTRY
REVIEWS

www.elsevier.com/locate/ccr

# Review of metal 1-azaallyl complexes

Catherine F. Caro, Michael F. Lappert *, Philippe G. Merle

*The Chemistry Laboratory, School of Chemistry, Physics & Environmental Science,*
*University of Sussex, Brighton BN1 9QJ, UK*

Received 21 November 2000; accepted 16 February 2001

Dedicated to Professor A.B.P. Lever, as a mark of esteem and (for M.F.L.) of valued friendship

## Contents

---

* Corresponding author. Tel.: +44-1273-678316; fax: +44-1273-677196.
*E-mail address:* m.f.lappert@sussex.ac.uk (M.F. Lappert).

0010-8545/01/$ - see front matter © 2001 Elsevier Science B.V. All rights reserved.
PII: S0010-8545(01)00361-7

---

## Abstract

This review provides a comprehensive survey relating to the synthesis, characterisation and reactivity of main group and d- and f-block metal 1-azaallyl complexes. Section 1 introduces the topic and defines the scope of the article, Section 2 considers general methods of preparation and Section 3 discusses the diversity of bonding modes of the 1-azaallylmetal complexes. Section 4 provides a group by group account of metal 1-azaallyls. Section 5 describes in outline the chemistry of related complexes, namely 2-pyridylalkylmetal and related metal complexes. Finally, we provide a table summarising data on individual metal 1-azaallyls. © 2001 Elsevier Science B.V. All rights reserved.

*Keywords:* Metal 1-azaallyl complexes; Bonding modes; Four-membered metalloacycles

---

## 1. Introduction and scope

Metal–$\eta^3$-allyl complexes are well known and play an important part in many metal-mediated reactions [1–6]; a key feature for C–C bond formation is the ease of $\eta^3$–$\eta^1$-slippage making available a vacant site [7]. Recently, the chemistry of metal heteroallyls has generated much interest because of the asymmetric bonding due to the differing electronic properties of the heteroatoms, N, P or O. Transition metal complexes of $\eta^3$-1-oxaallyls and $\eta^3$-1-phosphaallyls are well documented [8–14], as well as metal-1,3-diazaallyls complexes containing two terminal nitrogens (e.g. benzamidinates) [15,16], and 2-azaallyls [17–19]. Metal 1-azaallyl complexes have received less attention, although there is a long-standing interest in lithium-1-azaallyls (albeit, prepared in situ and not generally structurally characterised), because of their synthetic utility [20]. Thus, they are useful reagents in organic synthesis undergoing a number of C–C bond-forming reactions with electrophiles, e.g. in controlled aldol condensation reactions or regioselective $\alpha$-functionalisation of ketones [20–24]. They have considerable advantages over enolates in that they generally react with electrophiles much faster than they undergo proton transfer with the resulting imines; therefore, monoalkylation is not complicated by concomitant side reactions [20,25]. The anion was found to be more stable in the *syn* rather than the *anti*-conformation; theoretical modelling indicated that the *syn* preference arose not just from homoaromaticity and chelate effects but also to minimise electrostatic repulsion between the lone pair of electrons on the nitrogen and the partial negative charge on the terminal carbon atom [26,27].

The 1-azaallyl ligand **I**, related to the allyl ligand **II**, consists of an N⋯C⋯C backbone, shown here in the $\eta^3$-mode, i.e. with a delocalised negative charge; the range of known 1-azaallyl ligands is shown in Fig. 1. A closely similar class of compounds is the alkyl-functionalised pyridyls **III**, related to the benzyl anion **IV**. However, they are not ‘true’ 1-azaallyls in that the nitrogen cannot bear a negative charge unless the pyridine ring loses its aromaticity (which, almost invariably, is not the case). Section 5 discusses the metal complexes synthesised from these and related ligands. The group R throughout this article refers to $SiMe_3$.

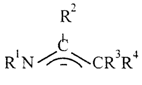
**I**

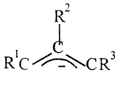
**II**

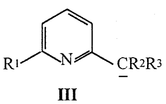
**III**

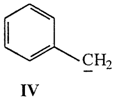
**IV**

## 2. General methods of preparation of 1-azaallylmetal complexes

Two principal routes exist for the preparation of lithium 1-azaallyls. The first involves deprotonation of an aldimine, ketimine or similar unsaturated species, Eq. (1) [20]. A series of such structurally authenticated complexes has been reported [21].

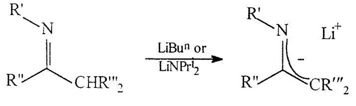
(1)

R', R'' or R''' = H, alkyl or aryl

The second route to alkali metal 1-azaallyls is by insertion of an alkali metal bis(trimethylsilyl)methyl (≡ $MCHR_2$, $R = SiMe_3$) (or a related compound) into an α-H-free nitrile R′CN (R′ = ᵗBu), e.g. Eq. (2) [28,29] (for insertion of an isonitrile, see Scheme 3). Lithium 1-azaallyls are good ligand-transfer reagents and have been used in the synthesis of numerous main group, as well as d- and f-block metal 1-azaallyls, see, e.g. Refs. [29–33].

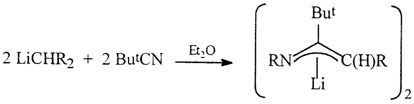
(2)

Other methods for the synthesis of transition metal 1-azaallyls include (i) the reaction of $[Mo_2(CO)_4(\eta^5\text{-}C_5H_5)_2]$ with a substituted 2-azirine [34]; (ii) thermal isomerisation of a Mo or W alkyl containing an isonitrile ligand, or of an $\eta^2$-iminoacyl complex [35–40]; (iii) decarbonylation of a Group 6 metal $\eta^2$-imine [41]; (iv) cleavage of a cyclopropane by a zirconocene-$\eta^2$-imine [42]; (v) a β-hydride

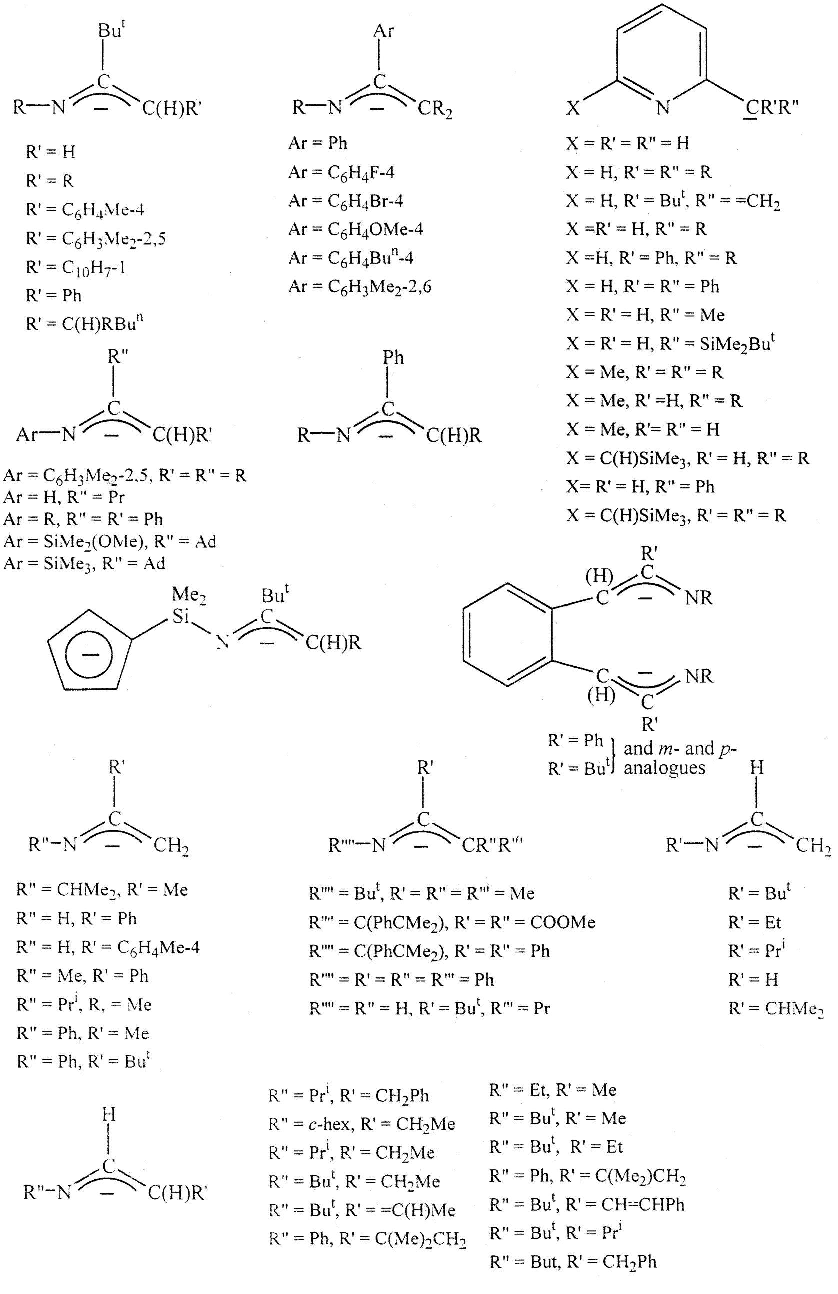

Fig. 1. Known 1-azaallyl ligands (R = $SiMe_3$).

transfer to an unstable zirconocene $\eta^2$-imine [43]; (vi) thermolysis of a vanadium imido complex [44]; (vii) β- and γ-dehydrogenation of a coordinated amine in a ruthenium complex [45,46]; or oxidative addition of a 1-azaallyl iodide to nickel or palladium [47]. Further details are discussed in later sections.

The most convenient synthetic route to an f-block metal 1-azaallyl (Section 4.13) was by an alkali metal halide elimination reaction between a lanthanide or actinide halide and the appropriate Group 1 metal 1-azaallyl. The insertion reaction of $[\text{Yb}(\text{CHR}_2)_2(\text{OEt}_2)]_2$ ($\text{R} = \text{SiMe}_3$) with two equivalents of ${}^t\text{BuCN}$, analogous to the lithium case (cf. Eq. (2)), has also been reported.

## 3. Bonding modes and structural features of 1-azaallylmetal complexes

The 1-azaallyl ligand can bind to a metal in one of five major ways **A**–**E**, depending on the nature of the substituent groups on the ligand, the nature of the metal and the presence or absence of neutral coligand(s). Configuration **A** is the most common; the presence of sterically hindering groups on the $\text{N}{\cdots}\text{C}{\cdots}\text{C}$ backbone serves to afford thermally stable compounds of metals in a low-coordination environment (mononuclear metal(II) complexes of a Groups 2, 13 or 14 element, Co, Ni, Sm or Yb [32,48,49]). The extent of asymmetrical bonding is dependent upon the nature of the substituent groups. The enamido configuration **C** is favoured usually in complexes containing bulky 1-azaallyl ligands or where a strong neutral donor such as thf is present, as in $[\text{Li}\{\mu\text{-N(R)C(Ph)C(H)R}\}(\text{thf})]_2$ [28]. The bridging mode **D** has been observed in metal(I) complexes $[\text{M}\{\mu\text{-CR}_2(\text{C}_5\text{H}_4\text{N-2})\}]_2$ (Li, Cu, Ag or Au) or $[\text{M}\{\mu\text{-N(R)C}({}^t\text{Bu})\text{C(H)R}\}]_2$ ($\text{M} = \text{Cu}$ or Au, $\text{R} = \text{SiMe}_3$) [50] forming eight-membered metallacycles with the trimethylsilyl groups assisting in the stabilisation of the two-coordinate metal environments. Finally, the lithium complexes $[\text{Li}\{\mu\text{-N(R)C}({}^t\text{Bu})\text{C(H)R}\}]_2$ [28,29] and $[\text{Li}\{\mu\text{-C(H)R}(\text{C}_5\text{H}_4\text{N-2})\}(\text{OEt}_2)]_2$ [48,51–53] demonstrate the 1-azaallyl ligand behaving in the chelating/bridging mode **E**.

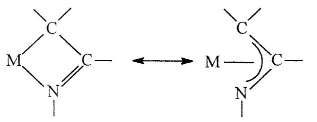

**A** **B**
(**Terminal**, η3-, Iminoalkyl)

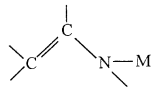

**C**
(**Terminal**,η1-,Enamido)

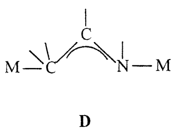

**D**
(*C*,*N*-**Bridging**)

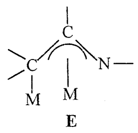

**E**
(*C*,*N*-**Bridging/Chelating**)

## 4. 1-Azaallylmetal complexes

### 4.1. Introduction

The following sections are concerned with metal 1-azaallyls in the literature and also include some unpublished work from the University of Sussex. A summary is provided in Table 1.

### 4.2. Group 1 metal 1-azaallyls

#### 4.2.1. Synthesis and structures of lithium 1-azaallyls

Organolithium reagents are useful synthons in preparative organic chemistry [20]. Only recently, however, the structure and bonding in these complexes has been studied. The structures (e.g. degree of association in solution and solid state, or covalency) are dependent markedly upon the solvent used and steric and electronic effects [54]. Monomeric structures are found generally when the lithium tends towards coordinative saturation, as in complexes containing bi and tri-dentate chelating agents, e.g. tmen or pmdeta.

The 1-azaallyl ligand **I** belongs to a wider family: the allyls **II**, the carboxylates **V**, the enolates (1-oxaallyls) **VI** and the amidinates (1,3-diazaallyls) **VII**. As mentioned in Section 1, studies of the 1-azaallyl ligand have been scarce compared to its isoelectronic counterparts **V**–**VII**. In the last decade, research on bis(trimethylsilyl)methyllithium and its derivatives has yielded a range of 1-azaallyl complexes exhibiting diverse bonding modes **A**–**E** [28].

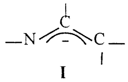
**I**


**V**

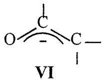
**VI**

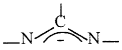
**VII**

Originally, lithium 1-azaallyls were generated in situ and their structures formulated as $\mathrm{LiC(H)_2CR''{=}NR''}$ or $\mathrm{Li^+[CH_2\overset{...}{-}CR''\overset{...}{-}NR''']^-]^-}$ ($R''$ and $R''' =$ alkyl or aryl) [20]. Research by Raston et al. (see Section 5) provided structurally characterised examples of lithium 2-pyridylalkyls and these were proposed as models for lithium 1-azaallyls [51–53]. Since then, several examples of $\eta^3$-allyl-type bonding have been reported for lithium imines [55], amides [56], indolenides [25,57], enolates [58], and hydrazones [59,60]. For example, the *N*-lithiated compounds $[\mathrm{Li\{N(Ph)C(^tBu){=}CH_2\}}]_2$ [57] and $[\mathrm{Li\{N(Ph)C_6H_9\}(NH^iPr_2)}]_2$ [56] both exhibited evidence of $\pi$-bonding implicating the 1,2 bond of the aromatic ring in the former, while the latter compound showed bonding to the cyclohexene double bond.

The first fully characterised example of a lithium 1-azaallyl, prepared by insertion of an $\alpha$-H-free nitrile $\mathrm{R'CN}$ into $\mathrm{LiCHR_2}$ ($\mathrm{R = SiMe_3}$), was $[\mathrm{Li\{\overline{\mu\text{-}N(R)C(R')C}(H)R\}}]_2$ ($\mathrm{R' = {}^tBu}$) [29]. Mulvey et al. had previously proposed the structure $[\mathrm{\overline{M\{N(H)C(^tBu)C}(H)C_3H_7\}(HMPA)_{\mathit{x}}}]_n$ ($\mathrm{M = Li}$, $x = 1$; $\mathrm{M = Na}$, $x = 2$) for related complexes on the basis of NMR spectroscopy [61], but this was confirmed only recently by the X-ray structure, showing $\eta^3$-NCC bonding; ab initio

Table 1

Summary of data on metal 1-azaallyl complexes (MS, mass spectrometry; EA, elemental analyses; $^x$M correspond to NMR-active nuclei, UV–vis, electronic spectroscopy; El, electrochemistry; R = SiMe$_3$, R′ = Si$^t$Bu$_3$, Ad = adamantyl, Cp = $\eta^5$-C$_5$H$_5$, Cp* = $\eta^5$-C$_5$Me$_5$, tmen = (Me$_2$NCH$_2$)$_2$, pmdeta = (Me$_2$NCH$_2$CH$_2$)$_2$NMe, HMPA = OP(NMe$_2$)$_3$)

| Complex | Characterisation | Bonding mode [a] | Comments | References |
|---|---|---|---|---|
| *Group 1* | | | | |
| [Li{N(H)C($^t$Bu)C(H)C$_3$H$_7$}(HMPA)]$_2$ | $^1$H, $^{13}$C, EA and X-ray | C | Dimer | [62] |
| [Li{N(H)C($^t$Bu)CH$_2$}(HMPA)]$_2$ | $^1$H, $^{13}$C, EA and X-ray | E | Dimer, *N*-bridged | [62] |
| [Li{μ-N(R)C($^t$Bu)C(H)R}]$_2$ | $^1$H, $^{13}$C, MS, EA and X-ray | E | Dimer | [28,29,31] |
| [Li{μ-N(SiMe$_2$OMe)C(Ad)C(H)R}]$_2$ | $^1$H, $^{13}$C, $^7$Li, EA and X-ray | C | Dimer, three-coord. Li (N,N,O) | [64] |
| [Li$_3${$\eta^5$-C$_5$H$_4$Si(Me)$_2$NC($^t$Bu)C(H)R}$_2$(tmen)] | $^1$H, $^{13}$C, EA and X-ray | B | | [63] |
| [Li{N(Ph)C($^t$Bu)CH$_2$}(OEt)$_2$]$_2$ | $^1$H, $^{13}$C, $^7$Li and X-ray | C | Dimer | [57] |
| [Li{N(R)C(Ph)=CH$_2$}(OEt$_2$)]$_n$ | $^1$H, $^{13}$C, $^7$Li, $^{29}$Si and EA | C | | [81] |
| [Li{N(R)C(Ph)CR$_2$}]$_2$ | $^1$H, $^{13}$C, $^7$Li, $^{29}$Si, MS and EA | | | [81] |
| [Li{N(R)C($^t$Bu)CH$_2$}]$_3$ | $^1$H, $^{13}$C, $^7$Li, EA and X-ray | B | | [90] |
| [Li{N(R)C(Ph)CR$_2$}(thf)] | $^1$H, $^{13}$C, MS and EA | | | [33,65] |
| [Li{N(R)C(C$_6$H$_4$F-4)CR$_2$}(thf)] | $^1$H, $^{13}$C, MS and EA | B | | [65] |
| [Li{N(R)C(C$_6$H$_4$Br-4)CR$_2$}(thf)] | $^1$H, $^{13}$C, MS, EA and X-ray | B | Monomer, $\eta^3$ | [65] |
| [Li{N(R)C(C$_6$H$_4$OMe-4)CR$_2$}(thf)] | $^1$H, $^{13}$C, MS and EA | | | [65] |
| [Li{N(R)C(C$_6$H$_4^t$Bu-4)CR$_2$}(thf)] | $^1$H, $^{13}$C, MS and EA | | | [65] |
| [Li{N(R)C(C$_6$H$_3$Me$_2$-2,6)CR$_2$}(thf)] | $^1$H, $^{13}$C, $^7$Li, EA and MS | | | [28] |
| [Li{μ-N(R)C($^t$Bu)C(H)R}(thf)]$_2$ | $^1$H, $^{13}$C, $^7$Li, MS and X-ray | C | Dimer, enamide | [28] |
| [Li{μ-N(R)C(Ph)C(H)R}(thf)]$_2$ | $^1$H, $^{13}$C, $^7$Li, MS, EA and X-ray | C | | [28] |
| [Li{μ-N(R)C(Ad)C(H)R}]$_2$ | $^1$H, $^{13}$C, $^7$Li, $^{29}$Si, MS, EA and X-ray | C | | [66] |
| [Li{N(R)C($^t$Bu)C(H)CH(R)$^n$Bu}]$_2$ | $^1$H, $^{13}$C, $^7$Li, MS, EA and X-ray | | Dimer | [28,29] |
| [Li{N(H)C($^t$Bu)C(H)C$_3$H$_7$}(HMPA)] | $^1$H, $^{13}$C, $^7$Li, IR and EA | A–B | | [61] |
| [Li{N(C$_6$H$_3$Me$_2$-2,6)C(R)C(H)R}(tmen)] | $^1$H, $^{13}$C, and $^7$Li | C | Enamide | [67] |
| [Li{N(R)C(Ph)C(H)R}(tmen)] | $^1$H, $^{13}$C, and $^7$Li | C | Enamide | [67,84] |
| [Li$_2${N(R)C($^t$Bu)CH}$_2$C$_6$H$_4$-1,2(tmen)$_2$] | $^1$H, $^{13}$C, EA and X-ray | B | | [30,167] |

Table 1 (*Continued*)

| Complex | Characterisation | Bonding mode [a] | Comments | References |
|---|---|---|---|---|
| [Li$_2${N(R)C($^t$Bu)CH}$_2$(C$_6$H$_4$-1,3 or -1,4)(tmen)$_2$] | $^1$H, $^{13}$C, EA and X-ray | B | | [70] |
| [Li$_2${N($^t$Bu)C(R)CH}$_2$C$_6$H$_4$-1,2(tmen)$_2$] | $^1$H, $^{13}$C, EA and X-ray | B | | [70] |
| [Li$_2${N(R)C(Ph)CH}$_2$C$_6$H$_4$-1,2(tmen)$_2$] | $^1$H, $^{13}$C, MS, EA and X-ray | B | | [70] |
| [Li{N(R)C(Ph)CH$_2$}(NCPh)]$_n$ | $^1$H, $^{13}$C, $^7$Li, $^{29}$Si and EA | | | [81] |
| [Li{N(C$_6$H$_3$Me$_2$-2,6)C(R)C(H)Ph}(tmen)] | $^1$H, $^{13}$C, $^7$Li, EA, MS and X-ray | C | | [70] |
| [Li{N(C$_6$H$_3$Me$_2$-2,6)C(R)C(H)R}(tmen)] | $^1$H, $^{13}$C, $^7$Li, EA, MS and X-ray | C | | [67,70] |
| [Li{N($^t$Bu)(R)C(H)Ph}(tmen)] | $^1$H, $^{13}$C, $^7$Li, EA and MS | C | | [28] |
| [Li{N(R)C(Ph)C(H)R}(tmen)] | $^1$H, $^{13}$C, $^7$Li, MS and EA | | | [28] |
| [Li{N(R)C(Ph)C(H)R}(pmdeta)] | $^1$H, $^{13}$C, $^7$Li, MS and EA | | | [28] |
| [Li{μ-CR$_2$(C$_5$H$_4$N-2)}]$_2$ | $^1$H, $^{13}$C, X-ray | D | Binuclear | [51–53] |
| [Li{CR$_2$(C$_5$H$_4$N-2)}(tmen)] | $^1$H, $^{13}$C, $^7$Li and X-ray | B | Monomer | [52,53] |
| [Li{μ-C(H)R(C$_5$H$_4$N-2)}(tmen)]$_2$ | $^1$H, $^{13}$C, $^7$Li and X-ray | C | Dimer | [53] |
| [Li{μ-C(H)R(C$_5$H$_4$N-2)}(OEt$_2$)]$_2$ | $^1$H, $^{13}$C, $^7$Li and X-ray | E | Binuclear | [52,53] |
| [Li{μ-C(R)Ph(C$_5$H$_4$N-2)}(tmen)]$_2$ | $^1$H, $^{13}$C and X-ray | C | Dimer | [129] |
| [Li{C(SiMe$_2^t$Bu)H(C$_5$H$_4$N-2)}(tmen)]$_2$ | $^1$H, $^{13}$C and X-ray | C | Dimer | [129] |
| [Li{C(Ph)R(C$_5$H$_4$N)-2}(tmen)] | $^1$H, $^{13}$C and X-ray | C | Monomer | [129] |
| [Li{CR$_2$(C$_5$H$_3$NMe-6)-2}] | $^1$H | | | [143] |
| [Li{C(H)R(C$_5$H$_3$N(CHR$_2$-6)-2}(tmen)] | $^1$H and $^{13}$C | | | [143] |
| [Li{C(H)R(C$_5$H$_4$N-2)}{NC$_5$H$_4$C(H)R$_2$-2}]$_2$ | $^1$H, $^{13}$C, $^7$Li and X-ray | E | | [51–53] |
| [Li{CR$_2$(C$_5$H$_4$N-2)}{NC$_5$H$_4$C(H)R$_2$-2}] | $^1$H, $^{13}$C and X-ray | B | Binuclear | [52,53] |
| [Li{N(R)C(C$_6$H$_3$NMe$_2$-2,6)CR$_2$}(NCPh)] | $^1$H, $^{13}$C, $^7$Li, EA and MS | | | [112] |
| [Li{C(H)R(C$_5$H$_4$N-2)}(−)-sparteine] | $^1$H, $^{13}$C, $^7$Li and X-ray | B | | [53] |
| [Li$_2${(CHR)$_2$(C$_5$H$_3$N-2,6)}(tmen)$_2$] | X-ray | B | | [130] |
| [Li{C(H)R(C$_5$H$_3$NMe-6)-2}(pmdetu)] | $^1$H, $^{13}$C, $^7$Li, EA, X-ray | C | | [174] |
| [Na{N(H)C($^t$Bu)C(H)C$_3$H$_7$}(HMPA)$_2$]$_2$ | $^1$H, $^{13}$C, EA and X-ray | C | Dimer | [62] |
| [Na{N(R)C(Ph)C(H)R}]$_n$ | $^1$H, $^{13}$C, EA and MS | | | [79] |
| [Na{N(R)C($^t$Bu)C(H)R}]$_n$ | $^1$H, $^{13}$C and MS | | | [79] |

Table 1 (*Continued*)

| Complex | Characterisation | Bonding mode [a] | Comments | References |
|---|---|---|---|---|
| $[\mathrm{Na\{N(H)C(^tBu)C(H)C_3H_7\}(HMPA)_2}]$ | $^1$H, $^{13}$C, $^7$Li, IR, EA and X-ray | A–B | | [61] |
| $[\mathrm{Na\{NC_5H_4(CPh_2)\text{-}2\}(thf)_3}]$ | $^1$H, $^{13}$C, IR, EA and X-ray | C | | [131] |
| $[\mathrm{Na\{C(H)R(C_5H_4N\text{-}2)(L)\}_2}]$ | $^1$H, $^{13}$C, EA, X-ray | C | | [174] |
| $[\mathrm{K\{N(R)C(Ph)C(H)R\}}]_n$ | $^1$H, $^{13}$C, MS, EA and X-ray | A | Polymeric dimer | [79] |
| $[\mathrm{K\{N(R)C(^tBu)C(H)R\}}]_n$ | $^1$H, $^{13}$C and MS | | | [29,79] |
| $[\mathrm{K\{N(R)C(^tBu)C(H)Ph\}}]_n$ | $^1$H, $^{13}$C, EA and MS | | | [84] |
| $[\mathrm{K\{N(R)C(^tBu)C(H)C_6H_4Me\text{-}4\}}]_n$ | $^1$H, $^{13}$C, MS and EA | | | [84] |
| $[\mathrm{K\{N(R)C(^tBu)C(H)C_6H_3Me_2\text{-}2,5\}}]$ | $^1$H, $^{13}$C, MS and EA | | | [89] |
| $[\mathrm{K\{N(R)C(^tBu)C(H)C_{10}H_7\text{-}1\}}]_n$ | $^1$H, $^{13}$C, MS and EA | | | [84,89] |
| $[\mathrm{K\{NC_5H_4(CPh_2)\text{-}2\}(pmdeta)}]$ | $^1$H, $^{13}$C, IR, EA and X-ray | C | | [131] |
| $[\mathrm{K_2\{N(R)C(^tBu)CH\}_2C_6H_4\text{-}1,2(tmen)_2}]$ | $^1$H, $^{13}$C and X-ray | B | Polymeric | [70,167] |
| $[\mathrm{K_2\{N(R)C(^tBu)CH\}_2C_6H_4\text{-}1,4(tmen)_2}]$ | $^1$H, $^{13}$C, EA and X-ray | B | Dimeric | [70,167] |
| $[\mathrm{K\{C(H)R(C_5H_4N\text{-}2)\}(pmdeta)}]$ | $^1$H, $^{13}$C, X-ray | | | [174] |
| $[\mathrm{Cs\{N(R)C(^tBu)C(H)R\}}]$ | $^1$H, $^{13}$C, $^{29}$Si, $^{133}$Cs | | | [172] |
| *Group 2* | | | | |
| $[\mathrm{Mg\{CR_2(C_5H_4N\text{-}2)\}_2}]$ | $^1$H, $^{13}$C, MS, EA and X-ray | A | Distorted tetrahedral | [80] |
| $[\mathrm{Mg\{N(R)C(^tBu)C(H)R\}_2}]$ | $^1$H, $^{13}$C, $^{29}$Si, MS, EA and X-ray | A | Planar Mg | [81] |
| $[\mathrm{Mg\{C(H)R(C_5H_4N\text{-}2)\}_2(HMPA)_2}]$ | $^1$H, $^{13}$C, X-ray | C | | [174] |
| $[\mathrm{Ca\{N(R)C(^tBu)C(H)R\}_2(thf)_2}]$ | $^1$H, $^{13}$C, $^{29}$Si, MS and EA | | | [81] |
| $[\mathrm{Sr\{N(R)C(^tBu)C(H)R\}_2(thf)_2}]$ | $^1$H, $^{13}$C, $^{29}$Si, MS and EA | | | [81] |
| $[\mathrm{Ba\{N(R)C(^tBu)C(H)R\}_2(thf)_2}]$ | $^1$H, $^{13}$C, $^{29}$Si, MS and EA | | | [81] |
| *Group 4* | | | | |
| $[\mathrm{Ti\{N(Ph)C(H)CPh_2\}(OH)Cp_2}]$ | $^1$H, $^{13}$C and IR | | | [83] |
| $[\mathrm{Ti\{N(Ph)C(H)CPh_2\}(Cl)Cp_2}]$ | $^1$H, $^{13}$C and IR | | | [83] |
| $[\mathrm{Ti\{N(Ph)C(H){=}CPh_2\}(H)Cp_2}]$ | $^1$H, $^{13}$C and IR | | Enamide | [83] |
| $[\mathrm{Ti\{N(R)C(^tBu)C(H)R\}Cp_2}]$ | MS, EA | | Paramagnetic | [47] |

Table 1 (*Continued*)

| Complex | Characterisation | Bonding mode [a] | Comments | References |
|---|---|---|---|---|
| $[Zr\{(\eta^5\text{-}C_5H_4Si(Me)_2NC(^tBu)C(H)R\}_2]$ | $^1H$, $^{13}C$ and EA | B | | [63] |
| *rac*-$[Zr\{(N(R)C(^tBu)C(H)R\}_2Cl_2]$ | $^1H$, $^{13}C$, MS, EA and X-ray | B | Diastereospecific | [29–31,82] |
| $[Zr\{(N(R)C(^tBu)CH\}_2C_6H_4\text{-}2)Cl_2]$ | $^1H$, $^{13}C$, EA, MS and X-ray | B | Good catalyst | [31,84,85,167] |
| $[Zr\{(N(R)C(^tBu)C(H)R)(\mu\text{-}Cl)Cl_2\}_2]$ | $^1H$, $^{13}C$, EA, MS and X-ray | B | | [31,85] |
| $[Zr\{N(R)C(Ph)C(H)Ph\}Cl_3]$ | $^1H$, $^{13}C$, EA, MS and X-ray | B | | [85] |
| $[Zr\{(N(R)C(^tBu)C(H)Ph\}Cl_3]$ | $^1H$, $^{13}C$, EA, MS and X-ray | B | Good catalyst | [29–31,85] |
| $[Zr\{C(H)R(C_5H_4N\text{-}2)\}Cp_2]$ | $^1H$, $^{13}C$, MS and EA | | | [136] |
| $[Zr\{C(H)R(C_5H_4N\text{-}2)\}Cp_2Cl]$ | $^1H$, $^{13}C$, MS, EA, EPR and X-ray | B | | [136] |
| $[Zr\{N(Ph)C(H)C(H)C(Me)_2CH_2\}Cp_2]$ | $^1H$ | | Bycyclopropane cleavage | [42] |
| $[Zr\{N(R)C(Ph)C(H)(C_5H_4N\text{-}2)\}_2Cl_2]$ | $^1H$, $^{13}C$, EA and MS | | | [168] |
| $[Zr\{N(R)C(Ph)C(R)(C_5H_4N\text{-}2)\}_2Cl_2]$ | $^1H$, $^{13}C$, EA and MS | | | [168] |
| $[Zr\{N(R)C(Ph)C(H)(C_9H_6N\text{-}2)\}_2Cl_2]$ | $^1H$, $^{13}C$, EA and MS | | | [168] |
| $[Zr\{N(R)C(Ph)C(R)(C_9H_6N\text{-}2)\}_2Cl_2]$ | $^1H$, $^{13}C$, EA and X-ray | C | | [168] |
| $[Zr\{N(R)C(Ph)C(H)(C_5H_4N\text{-}2)\}Cl_3]$ | $^1H$, $^{13}C$, EA and MS | | | [168] |
| $[Zr\{N(R)C(Ph)C(R)(C_5H_4N\text{-}2)\}Cl_3]$ | $^1H$, $^{13}C$, EA and MS | | | [168] |
| $[Zr\{N(R)C(^tBu)C(H)(C_5H_4N\text{-}2)\}_2Cl_2]$ | $^1H$, $^{13}C$, EA and X-ray | C | | [168] |
| $[Zr\{N(Ph)C(Me)CH_2\}Cp_2H]$ | $^1H$ | | Fluxional azaallyl | [43] |
| $[Zr\{CH_2(C_5H_3NMe\text{-}6)\text{-}2\}_2Cp_2]$ | $^1H$, $^{13}C$, EA and X-ray | B | | [137,139] |
| $[Zr\{N(C_6H_3Me_2\text{-}2,6)C(H){=}C(H)(C_5H_3NMe\text{-}6)\}_2Cp_2]$ | $^1H$, $^{13}C$, EA and X-ray | | | [137,139] |
| $[Zr\{N(C_6H_3Me_2\text{-}2,6)C(H){=}C(H)(C_5H_3NMe\text{-}6)\}\text{-}(CH_2C_6H_3Me_2\text{-}2,6)Cp_2]$ | $^1H$, $^{13}C$ and EA | | | [137,139] |
| $[Zr\{CH_2(C_5H_3NMe\text{-}6)\text{-}2\}Cp_2][BPh_4]$ | $^1H$, $^{13}C$, EA and IR | B | | [72] |
| $[Zr\{CH_2(C_5H_3NMe\text{-}6)\text{-}2\}Cp_2(thf)][BPh_4]$ | $^1H$, $^{13}C$ and EA | B | | [72,87] |
| $[Zr\{2,3\text{-benzoquinolinato}\}Cp_2(thf)][BPh_4]$ | $^1H$, $^{13}C$ and EA | | | [87] |
| $[Zr\{\eta^2\text{-phenazinyl}\}Cp_2(thf)][BPh_4]$ | $^1H$, $^{13}C$ and EA | | | [87] |
| $[Zr\{N(R)C(Ph)C(H)CH_2B(C_6F_5)_3\}Cp_2]$ | $^1H$, $^{13}C$ and $^{19}F$ | | Zwitterionic | [88] |

Table 1 (*Continued*)

| Complex | Characterisation | Bonding mode [a] | Comments | References |
|---|---|---|---|---|
| [Zr{$\eta^2$-acridinyl}$Cp_2$(thf)][$BPh_4$] | $^1$H, $^{13}$C and EA | | | [87] |
| [Hf{$CH_2(C_5H_3NMe$-6)$CH_2(C_5H_3NMe$-6)}$Cp_2$] | $^1$H, $^{13}$C and EA | | | [137,139] |
| [Hf{N($C_6H_3Me_2$-2,6)C(H)=C(H)($C_5H_3NMe$-6)}$_2Cp_2$] | $^1$H, $^{13}$C and EA | | | [137,139] |
| [Hf{N($C_6H_3Me_2$-2,6)C(H)=C(H)($C_5H_3NMe$-6)}-($CH_2C_6H_3Me_2$-2,6)$Cp_2$] | $^1$H, $^{13}$C and EA | | | [137,139] |
| [Hf{$\eta^2$-N($C_6H_3Me_2$-2,6)=CC(H)($C_5H_4N$-2)}(Ph)}$Cp_2$Cl] | $^1$H, $^{13}$C and EA | | | [137,139] |
| [Hf{N(R)C($^t$Bu)C(H)($C_5H_4N$-2)}$_2Cl_2$] | $^1$H, $^{13}$C, EA and X-ray | C | | [168] |
| [Hf{$CH_2(C_5H_3NMe$-6)-2}$_2$($OC_6H_3^tBu_2$-2,6)$_2$] | $^1$H, $^{13}$C, EA and X-ray | B | | [135] |
| *Group 5* | | | | |
| [V(N{Si(Bu$^t$)$_2$C(Me)$_2CH_2$}C(Et)C(H)Et)(=NR′)(HNR′)] | $^1$H, $^{13}$C, $^{51}$V, IR and EA | | | [44] |
| [V(N{Si(Bu$^t$)$_2$C(Me)$_2CH_2$}C(Me)C(H)Me)(=NR′)(HNR′)] | $^1$H, $^{13}$C, $^{51}$V, IR, EA and X-ray | B | Asymmetric bonding | [44] |
| [Nb{N(R)C($^t$Bu)$CH_2$}($\eta^5$-$C_5H_4SiMe_3$)$_2$] | $^1$H, $^{13}$C | | | [90] |
| [Nb{N(R)C($^t$Bu)$CH_2$}Cl($\eta^5$-$C_5H_4SiMe_3$)$_2$] | IR, ESR and EA | | | [90] |
| *Group 6* | | | | |
| [MoCp(CO)$_2$]$_2$[{$\eta^1$:$\eta^3$-$CH_2$C(H)NNC(H)$CH_2$}] | $^1$H, $^{13}$C, MS and EA | | | [41] |
| [Mo{N(H)C(Ph)$CH_2$}Cp(CO)$_2$] | $^1$H, $^{13}$C, IR and EA | | | [34] |
| [Mo{N(H)C($C_6H_4Me$-4)$CH_2$}Cp(CO)$_2$] | $^1$H, $^{13}$C, IR, EA and X-ray | B | Labile H, *endo* config. | [34] |
| [Mo{N(Me)C(Ph)$CH_2$}Cp(CO)$_2$] | $^1$H, $^{13}$C, IR and EA | | | [34] |
| [Mo{N(Me)C(Me)C($NEt_2$)}Cp*(CO)$_2$] | $^1$H, $^{13}$C, IR and EA | B | | [92] |
| [Mo{N(Et)C(H)$CH_2$}Cp*(CO)$_2$] | $^1$H, $^{13}$C, MS, EA and IR | | | [37] |
| [Mo{N(Et)C(H)C(H)Me}Cp*(CO)$_2$] | $^1$H, $^{13}$C, MS, EA and IR | | | [37] |
| [Mo{N($^i$Pr)C(H)$CH_2$}Cp(CO)$_2$] | $^1$H, $^{13}$C, IR, MS and EA | | | [41] |
| [Mo{N($^i$Pr)C(Me)$CH_2$}Cp(CO)$_2$] | $^1$H, $^{13}$C, IR, MS, EA and X-ray | B | Bound *C*, *N* to Mo | [41] |
| [Mo{N($^t$Bu)C(H)$CH_2$}Cp*(CO)$_2$] | $^1$H, $^{13}$C, IR, EA and X-ray | B | N-bound ligand in *syn* orientation | [35,39] |

Table 1 (*Continued*)

| Complex | Characterisation | Bonding mode [a] | Comments | References |
|---|---|---|---|---|
| $\mathrm{[Mo\{N({}^{t}Bu)C(H)CH_2\}Cp(CO)_2]}$ | $^{1}$H, $^{13}$C, EA and IR | B | | [38] |
| $\mathrm{[Mo\{N({}^{t}Bu)C(H)CH_2\}(\eta^5\text{-}C_5H_4Me)(CO)_2]}$ | $^{1}$H, $^{13}$C, IR and EA | | | [35,39] |
| $\mathrm{[Mo\{N({}^{t}Bu)C(H)CH_2\}Cp^*(CO)_2]}$ | $^{1}$H, $^{13}$C, IR and EA | | | [35,39] |
| $\mathrm{[Mo\{N({}^{t}Bu)C(H)CH_2\}(\eta^5\text{-}C_9H_7)(CO)_2]}$ | $^{1}$H and $^{13}$C | | | [40] |
| $\mathrm{[Mo\{\eta^3\text{-}N(H)C(H)CH_2\}(CO)_2(NCMe)_3][BF_4]}$ | $^{1}$H, $^{13}$C and EA | B | Cationic | [93] |
| $\mathrm{[Mo\{C(H)Me(C_5H_4N\text{-}2)\}_2Cp_2]}$ | $^{1}$H, $^{13}$C, IR and EA | | | [138] |
| $\mathrm{[W\{N(Me)C(Me)C(NEt_2)\}Cp^*(CO)_2]}$ | $^{1}$H, $^{13}$C, IR, EA and X-ray | B | | [92] |
| $\mathrm{[W\{N(Et)C(H)CH_2\}Cp^*(CO)_2]}$ | $^{1}$H, IR, EA and X-ray | B | | [36] |
| $\mathrm{[W\{N(Et)C(H)C(H)Me\}Cp^*(CO)_2]}$ | $^{1}$H, IR and EA | | | [36] |
| $\mathrm{[W\{N({}^{i}Pr)C(Me)CH_2\}Cp(CO)_2]}$ | $^{1}$H, $^{13}$C, IR and EA | | | [39] |
| $\mathrm{[W\{N({}^{i}Pr)C(Me)CH_2\}Cp^*(CO)_2]}$ | $^{1}$H, $^{13}$C, IR and EA | | | [39] |
| $\mathrm{[W\{N({}^{t}Bu)C(Me)CH_2\}Cp(CO)_2]}$ | $^{1}$H, $^{13}$C, IR and EA | | | [39] |
| $\mathrm{[W\{N({}^{t}Bu)C(Me)CH_2\}Cp^*(CO)_2]}$ | $^{1}$H, $^{13}$C, IR and EA | | | [39] |
| $\mathrm{[W\{N({}^{t}Bu)C(H)CH_2\}(\eta^5\text{-}C_9H_7)]}$ | $^{1}$H, $^{13}$C and EA | | | [40] |
| $\mathrm{[W\{N({}^{t}Bu)CMe_2\}(Me)({}^{t}Bu)\{N({}^{t}Bu)CMe{=}CMe_2\}]}$ | $^{1}$H, $^{13}$C, EA, MS, IR and X-ray | C | Enamide | [169] |
| *Group 8* | | | | |
| $\mathrm{[Fe\{CR_2(C_5H_4N\text{-}2)\}_2]}$ | EA, MS, $\mu_{\mathrm{eff}}$ and X-ray | A | Chelating ligands | [132,141] |
| $\mathrm{[Fe\{CR_2(C_5H_4N\text{-}2)\}Cl(tmen)]}$ | EA, $\mu_{\mathrm{eff}}$ and X-ray | C | | [141] |
| $\mathrm{[Fe\{N(R)C({}^{t}Bu)C(H)R\}_2]}$ | EA, MS, CV, $\mu_{\mathrm{eff}}$ and X-ray | B | Monomer | [89] |
| $\mathrm{[Fe\{N(R)C({}^{t}Bu)C(H)C_6H_4Me\text{-}4\}_2]}$ | EA, MS, CV, $\mu_{\mathrm{eff}}$ and X-ray | B | Monomer | [89] |
| $\mathrm{[Fe\{N(R)C({}^{t}Bu)C(H)C_{10}H_7\text{-}1\}]_2}$ | EA, MS, CV, $\mu_{\mathrm{eff}}$ and X-ray | C | Enamide | [89] |
| $\mathrm{[Fe\{C(Ph)R(C_5H_4N\text{-}2)\}_2]}$ | MS, EA and $\mu_{\mathrm{eff}}$ | | | [141] |
| $\mathrm{[Fe\{C(H)(SiMe_2{}^{t}Bu)C_5H_4N\text{-}2)\}_2]_2}$ | EA and X-ray | D | Dimer | [141] |
| $\mathrm{[Fe\{C(R)Ph(C_5H_4N\text{-}2)\}Cl(tmen)]}$ | EA, $\mu_{\mathrm{eff}}$ and X-ray | A | | [141] |
| $\mathrm{[Fe_2\{\mu\text{-}N\{C(Ph)CMe_2\}C(CO_2Me)C(CO_2Me)\}(CO)_6]}$ | $^{1}$H, $^{13}$C, MS, UV, EA, IR and X-ray | B | | [94] |
| $\mathrm{[Fe_2N\{C(Ph)CMe_2\}C(Ph)C(Ph)(CO)_6]}$ | $^{1}$H, MS, IR, UV and EA | | | [94] |

Table 1 (*Continued*)

| Complex | Characterisation | Bonding mode [a] | Comments | References |
|---|---|---|---|---|
| [FeMn{μ-N(Bu$^t$)C(H)C(H)N(H)Bu$^t$}(CO)$_6$] | $^1$H, $^{13}$C, IR, MS and EA | B | η$^3$ to Fe | [96] |
| [Fe$_2${μ-N($^t$Bu)C(H)C(H)}(CO)$_6$] | $^1$H, $^{13}$C, IR, MS, EA and X-ray | B | | [97,98] |
| [Fe$_2${N($^t$Bu)C(H)C(CH=CHPh)}(CO)$_6$] | $^1$H, $^{13}$C, IR, MS and EA | | | [99,100] |
| [Fe$_2${μ-N(Ph)C(H)C(H)}(CO)$_6$] | $^1$H, $^{13}$C, IR, MS and EA | | | [97,98] |
| [(RuCp*)$_2${N($^i$Pr)C(Me)CH$_2$}(μ-H)] | $^1$H, $^{13}$C, IR and X-ray | B | Two Ru environments | [45,46] |
| [(RuCp*)$_2${N($^i$Pr)C(Me)CH$_2$}(μ-H)(CO)] | $^1$H, $^{13}$C and IR | | | [46] |
| [(RuCp*)$_2${N($^i$Pr)C(Me)CH$_2$}(μ-H)(PMe$_2$Ph)] | $^1$H, $^{13}$C and $^{31}$P | | | [46] |
| [(RuCp*)$_2${N($^i$Pr)C(Me)CH$_2$}(μ-H)(PMePh$_2$)] | $^1$H, $^{13}$C and $^{31}$P | | | [46] |
| [(RuCp*)$_2${N($^i$Pr)C(Me)CH$_2$}(μ-H)P(OEt)$_3$] | $^1$H, $^{13}$C and $^{31}$P | | | [46] |
| [(RuCp*)$_2${N($^i$Pr)C(Me)CH$_2$}(μ-H)(PMe$_3$)] | $^1$H, $^{13}$C and $^{31}$P | | | [46] |
| [Ru$_2${N($^t$Bu)C(H)C(H)$^i$Pr}(CO)$_5$PPh$_3$] | $^1$H, $^{13}$C, IR and EA | | | [106] |
| [Ru$_2${N($^i$Pr)C(H)C(H)N($^i$Pr)C(O)CH$_2$C(O)CH$_2$}(CO)$_5$] | $^1$H, $^{13}$C, IR and X-ray | B | | [106,107] |
| [Ru$_2${N($^i$Pr)C(H)C(H)$^i$Pr}(CO)$_6$] | $^1$H, $^{13}$C, IR, EA, MS and X-ray | | | [95,104] |
| [Ru$_2${N($^t$Bu)C(H)C(H)$^i$Pr}(CO)$_6$] | $^1$H, $^{13}$C, IR, EA and MS | | | [95,104] |
| [Ru$_2${N($^t$Bu)C(H)C(H)CH$_2$Ph}(CO)$_6$] | $^1$H, $^{13}$C, IR, EA and MS | | | [95,104] |
| [Ru$_2${N($^t$Bu)C(H)CEt$_2$}(CO)$_6$] | $^1$H, $^{13}$C, IR and X-ray | B | | [105] |
| [Ru$_2${N(C$_6$H$_{11}$)C(H)C(H)$^i$Pr}(CO)$_6$] | $^1$H, $^{13}$C, IR, EA and MS | | | [95,104] |
| [Os$_3$(μ-H)Sn{CR$_2$(C$_5$H$_4$N-2)}(CO)$_{10}$] | $^1$H, $^{13}$C, EA and X-ray | A | | [155] |
| *Group 9* | | | | |
| [Co{CR$_2$(C$_5$H$_4$N-2)}$_2$] | MS, EA, CV, $\mu_{\mathrm{eff}}$ and X-ray | A | Planar Co(II) | [109,110] |
| [Co{C(Ph)R(C$_5$H$_4$N-2)}$_2$] | MS, EA, CV, $\mu_{\mathrm{eff}}$ and X-ray | A | Planar Co(II) | [109,110] |
| [Co{C(H)(SiMe$_2^t$Bu)(C$_5$H$_4$N-2)}$_2$]$_2$ | MS, EA, CV, $\mu_{\mathrm{eff}}$ and X-ray | D | Co$_2$R$_2$ ring-chair shape | [109,110] |
| [Co{N(R)C($^t$Bu)C(H)R}$_2$] | EA, $\mu_{\mathrm{eff}}$ and MS | | | [89] |
| [Co{N(R)C($^t$Bu)C(H)C$_6$H$_4$Me-4}$_2$] | CV, EA, MS, $\mu_{\mathrm{eff}}$ and X-ray | B | Monomer | [89] |

Table 1 (*Continued*)

| Complex | Characterisation | Bonding mode [a] | Comments | References |
|---|---|---|---|---|
| *Group 10* | | | | |
| $[\mathrm{Ni}\{N(R)C(^tBu)C(H)C_6H_4Me\text{-}4\}_2]$ | $^1$H, $^{13}$C, EA, MS and X-ray | B | Three isomers in solution | [89] |
| $[\mathrm{Ni}\{N(R)C(^tBu)C(H)R\}_2]$ | $^1$H, $^{13}$C, EA and MS | | | [89] |
| $[\mathrm{Ni}\{N(R)C(Ph)C(H)R\}_2]$ | $^1$H, $^{13}$C and X-ray | B | Two isomers in solution | [79] |
| $[\mathrm{Ni}\{N(R)C(Ph)C(H)R\}\{\eta^3\text{-}CH_2C(H)CH_2\}]$ | $^1$H and $^{13}$C | | | [79] |
| $[\mathrm{Ni}\{N(R)C(^tBu)C(H)R\}_2]$ | $^1$H, $^{13}$C, EA and MS | | | [47] |
| $[\mathrm{Ni}\{N(R)C(^tBu)C(H)R\}I(PPh_3)\}]$ | $^1$H, $^{13}$C, EA, MS and X-ray | B | Monomer | [47] |
| $[\mathrm{Ni}\{CR_2(C_5H_4N\text{-}2)\}_2]$ | $^1$H, $^{13}$C, MS, IR and EA | | | [143] |
| $[\mathrm{Ni}\{CR_2(C_5H_4N\text{-}2)\}Cp]$ | $^1$H, $^{13}$C, MS, EA and X-ray | A | Unequal $\eta^5$–Cp coord. | [142] |
| $[\mathrm{Ni}\{C(H)R(C_5H_4N\text{-}2)\}Cp]$ | $^1$H, $^{13}$C, MS and EA | | | [142] |
| $[\mathrm{Ni}\{CR_2(C_5H_4N\text{-}2)\}(\eta^5\text{-}C_5H_3R_2\text{-}1,3)]$ | $^1$H, $^{13}$C, MS and EA | | | [142] |
| $[\mathrm{Pd}\{N(R)C(Ph)C(H)R\}_2]$ | $^1$H and $^{13}$C | | | [79] |
| $[\mathrm{Pd}\{N(R)C(^tBu)C(H)R\}I]$ | $^1$H and $^{13}$C | | | [47] |
| $[\mathrm{Pd}\{N(R)C(^tBu)C(H)R\}I(PPh_3)]$ | $^1$H, $^{13}$C, $^{31}$P, EA and MS | | | [47] |
| *Group 11* | | | | |
| $[\mathrm{Cu}\{CR_2(C_5H_4N\text{-}2)\}]_2$ | $^1$H, $^{13}$C, EA, MS and X-ray | D | Eight-membered ring | [51,52,118,144] |
| $[\mathrm{Cu}\{\mu\text{-}N(R)C(^tBu)C(H)R\}]_2$ | $^1$H, $^{13}$C, MS, EA and X-ray | D | Dimer | [31,50] |
| $[\mathrm{Cu}\{C(H)R(C_5H_4N\text{-}2)\}]_4$ | X-ray | D | Tetramer | [118] |
| $[\mathrm{Cu}\{N(R)C(Ph)CR_2\}]_2$ | $^1$H, $^{13}$C, EA, MS, X-ray, UV–vis and El | D | Dimer | [112] |
| $[\mathrm{Cu}\{CR_2(C_5H_3NMe\text{-}6)\text{-}2\}]_2$ | $^1$H, $^{13}$C and EA | | | [48,145] |
| $[\mathrm{Cu}\{N(R)C(^tBu)C(H)R\}(PPh_3)]$ | $^1$H, $^{13}$C, MS, EA, X-ray, UV–vis and El | C | Monomer, enamide | [112] |
| $[\mathrm{Li}(DME)_3][\mathrm{Cu}\{N(R)C(^tBu)C(H)R\}_2]$ | $^1$H, $^{13}$C, MS, EA, X-ray, UV–vis and El | C | Monomer, sep. ion pair | [112] |
| $[\mathrm{Ag}\{CR_2(C_5H_4N\text{-}2)\}]_2$ | X-ray | D | Thermally stable | [48,118,144] |
| $[\mathrm{Ag}\{CR_2(C_5H_3NMe\text{-}6)\text{-}2\}]_2$ | $^1$H, $^{13}$C and EA | | | [48,145] |

Table 1 (*Continued*)

| Complex | Characterisation | Bonding mode [a] | Comments | References |
|---|---|---|---|---|
| $[Ag\{C(H)R(C_5H_4N\text{-}2)\}]_2$ | $^1H$, $^{13}C$ and EA | | | [48,145] |
| $[Au\{CR_2(C_5H_4N\text{-}2)\}]_2$ | $^1H$, $^{13}C$ and X-ray | D | | [48,118] |
| $[Au\{CR_2(C_5H_3NMe\text{-}6)\text{-}2\}]_2$ | $^1H$, $^{13}C$ and EA | | | [48,145] |
| $[Au\{N(R)C(Ph)CR_2\}]_2$ | $^1H$, $^{13}C$, MS, EA, X-ray, UV–vis and EI | D | | [112] |
| *Group 12* | | | | |
| $[Zn\{CR_2(C_5H_4N\text{-}2)\}]_2$ | $^1H$, $^{13}C$, MS and X-ray | A | Distorted tetrahedral | [80] |
| $[Zn\{C(H)R(C_5H_3NMe\text{-}6)\text{-}2\}_2]$ | $^1H$, $^{13}C$, MS, EA and X-ray | A | | [48,145,146] |
| $[Zn\{C(H)R(C_5H_3NMe\text{-}6)\text{-}2\}Cl]_2$ | $^1H$, $^{13}C$, MS and EA | | | [48,145,146] |
| $[Cd\{CR_2(C_5H_4N\text{-}2)\}]_2$ | $^1H$, $^{13}C$, MS and X-ray | A | Distorted tetrahedral | [80] |
| $[Cd\{C(H)R(C_5H_3NMe\text{-}6)\text{-}2\}_2]$ | X-ray | A | | [48,145,146] |
| *rac*-$[Cd\{C(H)R(C_5H_3NMe\text{-}6)\text{-}2\}_2(tmen)]$ | X-ray | A | Large C–Cd–C angle | [48,145,146] |
| $[Hg\{CR_2(C_5H_4N\text{-}2)\}]_2$ | $^1H$, $^{13}C$, MS, EA and X-ray | A | CN of 2 for Hg | [80] |
| $[Hg\{C(H)R(C_5H_3NMe\text{-}6)\text{-}2\}_2]$ | X-ray | A | | [48,145,146] |
| $[Hg\{CR_2(C_5H_4N\text{-}2)\}Cl]_2$ | X-ray | A | | [48,145,146] |
| $[Hg\{C(H)R(C_5H_3NMe\text{-}6)\text{-}2\}Cl]_2$ | X-ray | | Near linear coord. | [48,145,146] |
| *Group 13* | | | | |
| $[Al\{N(R)C(Ad)C(H)R\}\{N(R)C(Ad)C(H)R\}Me]$ | $^1H$, $^{13}C$, $^{29}Si$, $^{27}Al$ MS, EA and X-ray | B+C | | [66] |
| $[Al\{N(R)C(Ph)CR_2\}Me_2]$ | $^1H$, $^{13}C$, $^{29}Si$, $^{27}Al$, MS and EA | | | [120] |
| $[Al\{N(R)C(Ph)CR_2\}MeCl]$ | $^1H$, $^{13}C$, $^{29}Si$, $^{27}Al$, MS and EA | | | [120] |
| $[Al\{N(R)C(Ph)CR_2\}Cl_2]$ | $^1H$, $^{13}C$, $^{29}Si$, $^{27}Al$, MS, EA and X-ray | B | | [120] |
| $[Al\{N(R)C(Ph)CR_2\}Br_2]$ | $^1H$, $^{13}C$, $^{29}Si$, $^{27}Al$, MS and EA | | | [120,121] |
| $[Al\{N(R)C(Ph)CR_2\}F(\mu\text{-}F)]_2$ | $^1H$, $^{13}C$, $^{29}Si$, $^{27}Al$, MS, EA and X-ray | B | Dimer | [120] |
| $[Al\{N(R)C(Ph)CR_2\}I_2]$ | $^1H$, $^{13}C$, $^{29}Si$, $^{27}Al$, MS and EA | | | [120] |

Table 1 (*Continued*)

| Complex | Characterisation | Bonding mode [a] | Comments | References |
|---|---|---|---|---|
| $[Al\{N(R)C(Ph)CR_2\}H(\mu\text{-}H)]$ | $^1H$, $^{13}C$, $^{29}Si$, $^{27}Al$, MS, EA and X-ray | | | [121] |
| $[Al\{N(R)C(Ph)CR_2\}(\mu\text{-}E)]$ (E = Se or Te) | $^1H$, $^{13}C$, $^{29}Si$, $^{27}Al$, MS, EA and X-ray | | | [121] |
| $[Al\{N(R)C(Ph)CR_2\}MeCl(thf)]$ | $^1H$, $^{13}C$, $^{29}Si$, $^{27}Al$, MS and EA | | | [120] |
| $[Al\{N(R)C(Ph)CR_2\}Cl_2(thf)]$ | $^1H$, $^{13}C$, $^{29}Si$, $^{27}Al$, MS, EA and X-ray | C | | [120] |
| $[Al\{N(R)C(Ph)CR_2\}I\text{-}Al\{N(R)C(Ph)CR_2\}Cl]$ | $^1H$, $^{13}C$, $^{29}Si$, MS, EA and X-ray | B | Dinuclear Al–Al | [122] |
| $[Al\{N(R)C(^tBu)C(H)R\}\{N(R)C(^tBu){=}C(H)R\}Me]$ | $^1H$, $^{13}C$, $^{29}Si$, $^{27}Al$, MS, EA and X-ray | B + C | | [119] |
| $[Al\{N(R)C(^tBu)C(H)R\}Me_2]$ | $^1H$, $^{13}C$, $^{29}Si$, $^{27}Al$, MS and EA | | | [119] |
| $[Al\{N(R)C(Ph)C(H)R\}Me_2]$ | $^1H$, $^{13}C$, $^{29}Si$, $^{27}Al$, MS and EA | C | | [119] |
| $[Al\{N(R)C(Ph)C(H)R\}_2Me(thf)]$ | $^1H$, $^{13}C$, $^{29}Si$, $^{27}Al$, MS and EA | C | | [119] |
| $[Al\{CR_2(C_5H_4N\text{-}2)\}_2Cl]$ | $^1H$, $^{13}C$, MS, IR and X-ray | A | | [48,149,150] |
| $[Al\{CR_2(C_5H_3NMe\text{-}6)\text{-}2\}_2Cl]$ | X-ray | A | Distorted trig.bipy | [48,145,146] |
| $[Al\{CR_2(C_5H_3NMe\text{-}6)\text{-}2\}Cl_2]$ | X-ray | A | | [48,145,146] |
| $[Al\{CR_2(C_5H_4N\text{-}2)_2\}][AlCl_4]$ | $^1H$, IR and X-ray | A | | [48,149,150] |
| $[Ga\{N(R)C(Ph)CR_2\}Cl_2]$ | $^1H$, $^{13}C$, $^{29}Si$, MS, IR, EA and X-ray | B | Monomeric | [122] |
| $[Ga\{N(R)C(Ph)CR_2\}Cl]_2$ | $^1H$, $^{13}C$, $^{29}Si$, MS, IR, EA and X-ray | B | Dinuclear | [122] |
| $[Ga\{CR_2(C_5H_4N\text{-}2)\}_2Cl]$ | $^1H$, $^{13}C$ and MS | | | [48,150] |
| $[Ga\{CR_2(C_5H_3NMe\text{-}6)\text{-}2\}_2Cl]$ | $^1H$, $^{13}C$ and EA | | | [48] |
| $[Ga\{CR_2(C_5H_4N\text{-}2)\}_2GaCl_4]$ | $^1H$, IR and X-ray | A | | [48,150] |
| $[In\{N(R)C(Ph)CR_2\}Br]_2$ | $^1H$, $^{13}C$, $^{29}Si$, MS, IR, EA and X-ray | B | Dinuclear | [122] |
| $[In\{CR_2(C_5H_4N\text{-}2)\}_2Cl]$ | X-ray | A | Fluxional in solution | [48] |
| $[In\{CR_2(C_5H_3NMe\text{-}6)\text{-}2\}_2Cl]$ | X-ray | A | | [48,145] |
| $[In\{CR_2(C_5H_3NMe\text{-}6)\text{-}2\}Cl_2]$ | $^1H$, $^{13}C$ and EA | | | [48] |
| *Group 14* | | | | |
| $[Si\{CR_2(C_5H_4N\text{-}2)\}(H)Cl_2]$ | $^1H$, $^{13}C$, $^{29}Si$, MS and X-ray | A | Strong Si–N interaction | [151] |

Table 1 (*Continued*)

| Complex | Characterisation | Bonding mode [a] | Comments | References |
|---|---|---|---|---|
| $[\overline{\mathrm{Si}\{\mathrm{CR}_2(\mathrm{C}_5\mathrm{H}_4\mathrm{N}}\text{-}2)\}(\mathrm{Me})\mathrm{Cl}_2]$ | $^{1}$H, $^{13}$C, $^{29}$Si and MS | | | [151] |
| $[\overline{\mathrm{Si}\{\mathrm{CR}_2(\mathrm{C}_5\mathrm{H}_4\mathrm{N}}\text{-}2)\}(\mathrm{Me})_2\mathrm{Cl}]$ | $^{1}$H, $^{13}$C and EA | | | [48,145] |
| $[\overline{\mathrm{Si}\{\mathrm{CR}_2(\mathrm{C}_5\mathrm{H}_3\mathrm{N}}\mathrm{Me}\text{-}6)\text{-}2\}_2(\mathrm{H})\mathrm{Cl}_2]$ | $^{1}$H, $^{13}$C, $^{29}$Si and MS | | | [151] |
| *rac*-$[\overline{\mathrm{Si}\{\mathrm{C(H)R}(\mathrm{C}_5\mathrm{H}_4\mathrm{N}}\text{-}2)\}_2\mathrm{Me}_2]$ | X-ray | A | | [48,146] |
| *rac*-$[\overline{\mathrm{Si}\{\mathrm{C(H)R}(\mathrm{C}_5\mathrm{H}_4\mathrm{N}}\text{-}2)\}_2\mathrm{MeCl}]$ | X-ray | A | | [48,146] |
| $[\overline{\mathrm{Si}\{\mathrm{C(Ph)}_2(\mathrm{C}_5\mathrm{H}_4\mathrm{N}}\text{-}2)\}(\mathrm{Me})\mathrm{Cl}_2]$ | $^{1}$H, $^{13}$C, $^{29}$Si, MS and X-ray | A | | [151] |
| $[\overline{\mathrm{Si}\{\mathrm{CR}_2(\mathrm{C}_5\mathrm{H}_3\mathrm{N}}\mathrm{Me}\text{-}6)\text{-}2\}(\mathrm{Me})\mathrm{Cl}_2]$ | $^{1}$H, $^{13}$C and EA | | | [48,146] |
| $[\overline{\mathrm{Si}\{\mathrm{CR}_2(\mathrm{C}_5\mathrm{H}_3\mathrm{N}}\mathrm{Me}\text{-}6)\text{-}2\}(\mathrm{H})\mathrm{Cl}_2]$ | X-ray | A | | [48,146] |
| $[\overline{\mathrm{Si}\{\mathrm{CR}_2(\mathrm{C}_5\mathrm{H}_3\mathrm{N}}\mathrm{Me}\text{-}6)\text{-}2\}\mathrm{Me}_2\mathrm{Cl}]$ | $^{29}$Si | | Five-coord. Si | [48] |
| $[\overline{\mathrm{Si}\{\mathrm{CR}_2(\mathrm{C}_5\mathrm{H}_3\mathrm{N}}\mathrm{Me}\text{-}6)\text{-}2\}\mathrm{Me}_3]$ | $^{29}$Si | | Four-coord. Si | [48] |
| $[\overline{\mathrm{Si}\{\mathrm{CR}_2(\mathrm{C}_5\mathrm{H}_3\mathrm{N}}\mathrm{Me}\text{-}6)\text{-}2\}_2\mathrm{Me}_2]$ | $^{1}$H, $^{13}$C and EA | | | [48] |
| $[\overline{\mathrm{Ge}\{\mathrm{C(R)Ph}(\mathrm{C}_5\mathrm{H}_4\mathrm{N}}\text{-}2)\}_2]$ | $^{1}$H, $^{13}$C, EA, MS and X-ray | A | Monomer | [154] |
| $[\overline{\mathrm{Ge}\{\mathrm{CR}_2(\mathrm{C}_5\mathrm{H}_4\mathrm{N}}\text{-}2)\}_2]$ | $^{1}$H, $^{13}$C, $^{29}$Si, EA, MS and X-ray | A | Monomer | [153] |
| $[\overline{\mathrm{Ge}\{\mathrm{CR}_2(\mathrm{C}_5\mathrm{H}_4\mathrm{N}}\text{-}2)\}_2(=\mathrm{S})]$ | $^{1}$H, $^{13}$C, $^{29}$Si, EA and MS | | | [153] |
| $[\overline{\mathrm{Ge}\{\mathrm{CR}_2(\mathrm{C}_5\mathrm{H}_4\mathrm{N}}\text{-}2)\}\{\mathrm{C(R)}=(\mathrm{C}_5\mathrm{H}_4\mathrm{N}\text{-}2)\}(\mathrm{SR})]$ | $^{1}$H, $^{13}$C, $^{29}$Si, EA, MS and X-ray | A | | [153] |
| $[\overline{\mathrm{Ge}\{\mathrm{CR}_2(\mathrm{C}_5\mathrm{H}_4\mathrm{N}}\text{-}2)\}_2(=\mathrm{Se})]$ | $^{1}$H, $^{13}$C, $^{29}$Si, $^{77}$Se, EA, MS and X-ray | A | | [153] |
| $[\overline{\mathrm{Ge}\{\mathrm{CR}_2(\mathrm{C}_5\mathrm{H}_4\mathrm{N}}\text{-}2)\}\{\mathrm{C(R)}=(\mathrm{C}_5\mathrm{H}_4\mathrm{N}\text{-}2)\}(\mathrm{SeR})]$ | $^{1}$H, $^{13}$C, $^{29}$Si, $^{77}$Se, EA and MS | | | [153] |
| $[\overline{\mathrm{Ge}\{\mathrm{CR}_2(\mathrm{C}_5\mathrm{H}_4\mathrm{N}}\text{-}2)\}_2(=\mathrm{Te})]$ | $^{1}$H, $^{13}$C, $^{29}$Si, $^{125}$Te, EA, MS and X-ray | A | | [153] |
| $[\overline{\mathrm{Sn}\{\mathrm{CR}_2(\mathrm{C}_5\mathrm{H}_4\mathrm{N}}\text{-}2)\}_2]$ | $^{1}$H, $^{13}$C, $^{29}$Si, $^{119}$Sn, EA, MS and X-ray | A | Monomer | [48,125,152] |
| $[\mathrm{Sn}\{\mathrm{C(R)Ph}(\mathrm{C}_5\mathrm{H}_4\mathrm{N}\text{-}2)\}_2]$ | $^{1}$H, $^{13}$C, $^{119}$Sn, MS, EA and X-ray | A | Chelate *trans* | [154] |
| $[\overline{\mathrm{Sn}\{\mu\text{-}\mathrm{N(R)C(Ph)C}}\mathrm{R}\}]_2$ | $^{1}$H, EA, MS and X-ray | E | | [89] |
| $[\overline{\mathrm{Sn}\{\mathrm{N(R)C(Ad)C}}\mathrm{(H)R}\}_2]$ | $^{1}$H, $^{13}$C, $^{29}$Si, $^{119}$Sn, EA, MS and X-ray | B | | [170] |
| $[\mathrm{Sn}\{\mathrm{N(R)C}(^t\mathrm{Bu})\mathrm{CH}(\mathrm{C}_6\mathrm{H}_3\mathrm{Me}_2\text{-}2,5)\}_2]$ | $^{1}$H, $^{13}$C, $^{119}$Sn, $^{29}$Si, EA, MS and X-ray | C | Enamide | [89] |
| *rac*-$[\overline{\mathrm{Sn}\{\mathrm{N(R)C}(^t\mathrm{Bu})\mathrm{C}}\mathrm{(H)R}\}_2]$ | $^{1}$H, $^{13}$C, $^{119}$Sn, EA and X-ray | B | | [32,89] |

Table 1 (*Continued*)

| Complex | Characterisation | Bonding mode [a] | Comments | References |
|---|---|---|---|---|
| $[\mathrm{Sn\{N(R)C(Ph)CH_2\}_2}]$ | $^1$H, $^{13}$C, $^{119}$Sn, MS and EA | | | [81] |
| $[\mathrm{Sn\{N(R)C(Ph)CR_2\}\{N(R)C(Ph){=}CR_2\}}]$ | $^1$H, $^{13}$C, $^{29}$Si, $^{119}$Sn, MS, EA and X-ray | B, C | Monomer, $\eta^1$:$\eta^3$ bound ligands | [33] |
| $[\mathrm{Sn(\mu\text{-}Cl)\{N(R)C(Ph)CR_2\}}]_2$ | $^1$H, $^{13}$C, $^{29}$Si, $^{119}$Sn, MS and EA | | Dimer | [33] |
| $[\mathrm{Sn\{CR_2(C_5H_4N\text{-}2)\}Cl}]$ | $^1$H, $^{13}$C, $^{29}$Si, $^{119}$Sn, EA, MS and X-ray | A | Monomer | [48,125,152] |
| $[\mathrm{Sn\{CR_2(C_5H_4N\text{-}2)\}NR_2}]$ | $^1$H, $^{13}$C, $^{29}$Si, $^{119}$Sn, MS, EA and X-ray | A | Monomer | [48,125,152] |
| $[\mathrm{Sn\{C(H)R(C_9H_6N\text{-}8)\}_2}]$ | $^1$H, $^{13}$C | | | [133,154] |
| $[\mathrm{Sn(\mu\text{-}S)\{C(H)R(C_9H_6N\text{-}8)\}}]_2$ | $^1$H, $^{13}$C | | | [133] |
| $[\mathrm{Sn\{C(H)R(C_9H_6N\text{-}8)\}_2({=}Se)}]$ | $^1$H, $^{13}$C | | | [133] |
| $[\mathrm{Sn\{C(H)R(C_9H_6N\text{-}8)\}_2({=}Te)}]$ | $^1$H, $^{13}$C | | | [133] |
| $[\mathrm{Sn\{C(H)R(C_9H_6N\text{-}8)\}X}]$, X = F, Cl, Br or I | $^1$H, $^{13}$C | | | [166] |
| $[\mathrm{Sn\{C(H)R(C_9H_6N\text{-}8)\}_2X_2}]$, X = F, Cl, Br or I | $^1$H, $^{13}$C | | | [166] |
| $[\mathrm{Pb\{N(R)C(Ph)CR_2\}\{N(R)C(Ph){=}CR_2\}}]$ | $^1$H, $^{13}$C, $^{29}$Si, $^{207}$Pb, MS, EA and X-ray | B, C | Monomer, $\eta^1$:$\eta^3$ bound ligands | [33] |
| $[\mathrm{Pb(\mu\text{-}Cl)\{N(R)C(Ph)CR_2\}}]_2$ | $^1$H, $^{13}$C, $^{29}$Si, $^{207}$Pb, MS, EA and X-ray | A | Pb distorted tbp | [33] |
| $[\mathrm{Pb\{N(R)C(^tBu)C(H)R\}Cl}]$ | $^1$H, $^{13}$C, $^{29}$Si, $^{207}$Pb, MS and EA | | | [33] |
| *Group 15* | | | | |
| *trans*-$[\mathrm{P(Cl)\{NC(^tBu){=}C(H)R\}}]_2$ | $^1$H, $^{13}$C, $^{31}$P, EA and MS | | Diazadiphosphetidine | [64] |
| *trans*-$[\mathrm{P(NMe_2)\{NC(^tBu){=}C(H)R\}}]_2$ | $^1$H, $^{13}$C, $^{31}$P, EA and MS | | Diazadiphosphetidine | [171] |
| $[\mathrm{P\{CR_2(C_5H_4N\text{-}2)Cl_2\}}]$ | $^1$H, $^{13}$C and EA | | | [48,159] |
| $[\mathrm{P\{CR_2(C_5H_3NMe\text{-}6)\text{-}2\}Cl_2}]$ | $^1$H, $^{13}$C and X-ray | | | [48,157] |
| $[\mathrm{As\{CR_2(C_5H_4N\text{-}2)\}Cl_2}]$ | $^1$H and $^{13}$C | | | [122] |
| $[\mathrm{As\{CR_2(C_5H_3NMe\text{-}6)\text{-}2\}Cl_2}]$ | $^1$H, $^{13}$C and X-ray | | | [48,157] |
| $[\mathrm{Sb\{CR_2(C_5H_4N\text{-}2)Cl_2\}}]$ | $^1$H, $^{13}$C, EA and X-ray | A | Monomer | [156] |
| $[\mathrm{Sb\{C(H)R(C_5H_3NMe\text{-}6)\text{-}2\}(\mu\text{-}Cl)Cl}]_2$ | $^1$H, $^{13}$C, EA and X-ray | A | Dimer with bridging Cl | [48,156,157] |

Table 1 (*Continued*)

| Complex | Characterisation | Bonding mode [a] | Comments | References |
|---|---|---|---|---|
| $[Sb\{CPh_2(C_5H_4N\text{-}2)Cl_2\}]$ | $^1H$, $^{13}C$, EA and X-ray | A |  | [48,147] |
| $[Sb\{CR_2(C_5H_3NMe\text{-}6)\text{-}2\}Cl_2]$ | $^1H$, $^{13}C$, EA and X-ray | A | Monomer | [48,146,157] |
| $[Sb\{CR_2(C_5H_3NMe\text{-}6)\text{-}2\}_2Cl]$ | $^1H$, $^{13}C$, EA and X-ray | A |  | [48,146] |
| $[(\{SbCR_2(C_5H_4N\text{-}2)\}_2(\mu\text{-}Cl))(\mu\text{-}Cl)]_n$ | X-ray |  | Polymer | [161] |
| $[Al\{CR_2(C_5H_4N\text{-}2)Sb(Me)CR_2(C_5H_4N\text{-}2)\}Me_2]$ | $^1H$, $^{13}C$, EA and X-ray | D+C |  | [160] |
| $[Bi\{CR_2(C_5H_4N\text{-}2)Cl_2\}]$ | $^1H$, $^{13}C$, EA and MS |  |  | [156] |
| $[Bi\{CR_2(C_5H_3NMe\text{-}6)\text{-}2\}_2Cl]$ | $^1H$ and $^{13}C$ |  | Unstable | [48,157] |
| $[Bi\{CR_2(C_5H_4N\text{-}2)\{CH_2C(H){=}C(R)(C_5H_4N\text{-}2)\}]$ | MS and X-ray | A |  | [156] |
| *Lanthanide and thorium* |  |  |  | [156] |
| $[Ce\{N(R)C(^tBu)C(H)R\}_2Cl(thf)]$ | $^1H$, $^{13}C$, $^{29}Si$, MS and EA |  |  | [49] |
| $[Nd\{N(R)C(^tBu)C(H)R\}_2Cl(thf)]$ | $^1H$, $^{13}C$, $^{29}Si$, MS and EA, |  |  | [49] |
| $[Sm\{N(R)C(^tBu)C(H)R\}_2I(thf)]$ | $^1H$, MS, EA and X-ray | B | Monomer | [49] |
| $[Sm\{N(R)C(^tBu)C(H)R\}_2(thf)]$ | $^1H$, $^{13}C$, $^{29}Si$, MS and EA |  |  | [49] |
| $[Yb\{N(R)C(^tBu)C(H)R\}_2I]$ | $^1H$, $^{13}C$, $^{29}Si$, $^{171}Yb$, MS and EA |  |  | [49] |
| $[Yb\{N(R)C(^tBu)C(H)R\}_2]$ | $^1H$, $^{13}C$, $^{171}Yb$, EA, MS and X-ray | B | *rac*-Isomer crystallised | [30,49,74] |
| $[Yb\{N(R)C(^tBu)C(H)R\}_2(OTf)]$ | $^1H$, $^{13}C$, $^{29}Si$, $^{19}F$, $^{171}Yb$, MS and EA |  | Broad $^{19}F$ as Yb(III) paramagnetic | [49] |
| $[Th\{CH_2(C_5H_3NMe\text{-}6)\text{-}2\}_2(OC_6H_3^tBu_2\text{-}2,6)_2]$ | $^1H$, $^{13}C$ and X-ray | A |  | [135] |
| $[Th\{N(R)C(^tBu)C(H)R\}(\mu_3\text{-}Cl)(\mu\text{-}Cl)_2K(OEt_2)]_n$ | $^1H$, $^{13}C$, MS, EA and X-ray | B |  | [127] |

[a] See Section 3 for the description of bonding modes.

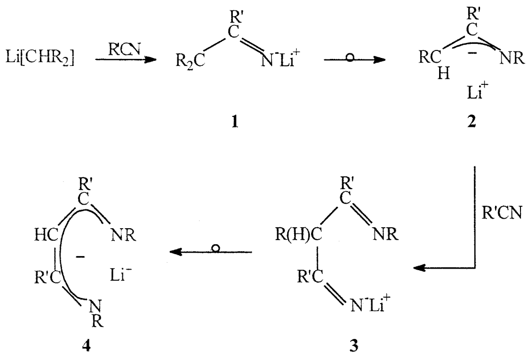

Scheme 1. R′ = Ph or $^t$Bu, R = $SiMe_3$ [28,29,31].

calculations on models showed this was the most stable arrangement [62]. The proposed reaction pathway for the formation of $[\mathrm{Li}\{\mu\text{-}\mathrm{N(R)C(R')C(H)R}\}]_2$ involved nucleophilic attack of $^{-}CHR_2$ on R′CN to give **1** followed by a 1,3-$SiMe_3$ shift to form the lithium-1-azaallyl **2** (Scheme 1). For R = Ph, the 1-azaallyl reacted further with another nitrile molecule to form the β-diketiminate **4** [29,30].

The complex $[\mathrm{Li}\{\mu\text{-}\mathrm{N(R)C(}^t\mathrm{Bu)C(H)R}\}]_2$ crystallises as a dimer with a central $Li_2N_2$ rhombus. The ligand behaves as a bridging/chelate **E**, coordinating $\eta^3$- to one lithium and σ-bonding to the other through the nitrogen atom [29]. The coordination about the lithium is completed by an agostic Li···$CH_3(SiMe_2CH$–) contact.

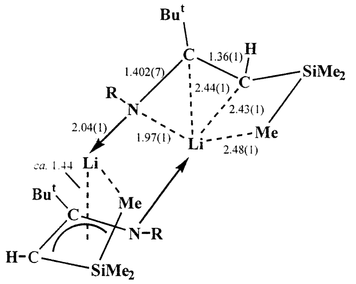

However, $SiMe_3$ migration is not always favoured. In the synthesis of the dilithio derivative of a dianionic cyclopentadienyl ligand, the 1-azaallyl side chain was created from the reaction of $[Li_2\{\eta^5\text{-}C_5H_4Si(Me)_2C(H)R\}(tmen)]$ (R = $SiMe_3$) with $^t$BuCN; two possible pathways were, in principle, available [63]. Ultimately, the crystal structure showed that $\eta^5$-$C_5H_4SiMe_2$ migration was preferred over $SiMe_3$. Similarly, from Li{N($SiMe_3$)$SiMe_2$OMe} and adamantyl (Ad) cyanide the migrating group was not $SiMe_3$; thus the crystalline product was [Li{μ-N($SiMe_2$OMe)C(Ad)C(H)$SiMe_3$}]$_2$, in which each lithium is three-coordinate, being bound to each of the nitrogen atoms but also a methoxy group [64].

By subtle changes in the alkali metal alkyl, nitrile or solvent, this route proved to be a versatile way of 'tuning' metal 1-azaallyls with slightly different steric and electronic properties (see Table 1). For example: (a) the presence of a strong neutral donor L (thf, pmdeta or tmen), in the reaction between $LiCHR_2$ ($R = SiMe_3$) and PhCN afforded the monomeric $[Li\{N(R)C(Ph)C(H)R\}(L)]$ (L = tmen or pmdeta) or dimeric $[Li\{\mu\text{-}N(R)C(Ph)C(H)R\}(thf)]_2$ product (i) in Scheme 2, instead of the lithium β-diketiminate, $[Li\{N(R)C(Ph)C(H)C(Ph)NR\}]_2$ (which resulted if the reaction was carried out in $Et_2O$), (ii) in Scheme 2 [65]; (b) reaction of $LiCHR_2$ with the bulky $^t$BuCN afforded only the lithium 1-azaallyl, (iii) in Scheme 2; more forcing conditions or addition of more nitrile did not result in the β-diketiminate, presumably due to steric reasons [29–31]; (c) $LiCR_3(thf)_2$ ($R = SiMe_3$) treated with PhCN afforded the 1-azaallyl $[Li\{N(R)C(Ph)CR_2\}(thf)]$ but did not react further to form the β-diketiminate but with $^t$BuCN yielded the 1:1 adduct, Eq. (3) [33,65].

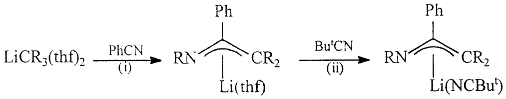

(3)

The 1-azaallyl $[Li\{\mu\text{-}N(R)C(Ph)C(H)R\}(thf)]_2$, Fig. 2, is a centrosymmetric dimer containing as core a nearly planar LiNLiN ring with the angles subtended at the nitrogen atoms narrower (74.1(1)°) than those at the Li atoms (106.0(1)°) with closely similar Li–N distances (2.051(3) and 2.063(3) Å). This structure is very similar to the one observed for the dimeric solvent-free 1-azaallyl complex $[Li\{\mu\text{-}N(R)C(Ad)C(H)R\}]_2$ (Ad = adamantyl) [66].

The presence of an extra trimethylsilyl group gave rise to the monomeric, crystalline $[Li\{N(R)C(C_6H_4Br\text{-}4)CR_2\}(thf)]$ with the ligand bonded in an unsymmetrical $\eta^3$-fashion to the metal and the coordination about the lithium completed by one thf molecule and a weak agostic interaction between Li and a methyl group. The short Li–N and Li–O bonds of 1.93(2) and 1.84(2) Å, respectively, and N–Li–O angle of 142° indicate that N and O are the principal donor atoms to the lithium.

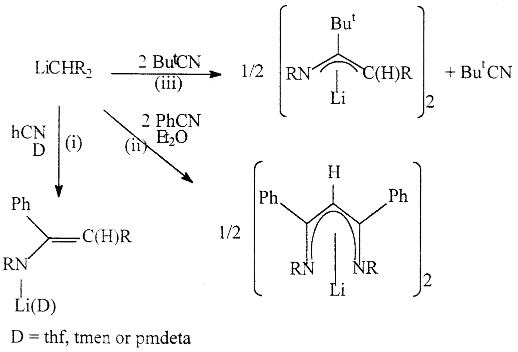

Scheme 2. Synthetic routes to 'tuning' lithium 1-azaallyls [29–31,33,65].

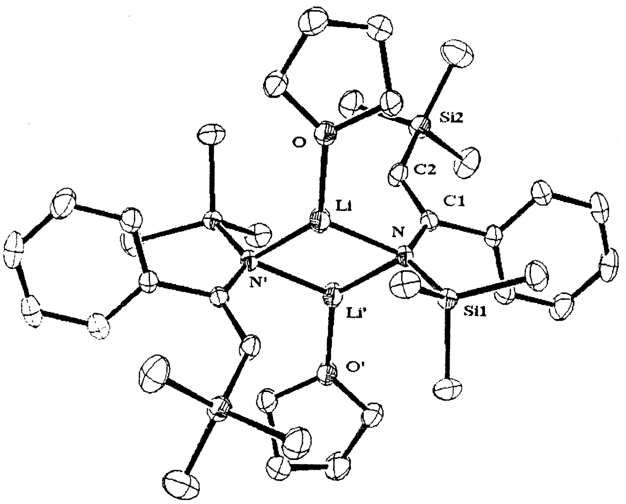

Fig. 2. The molecular structure of crystalline $[Li\{\mu\text{-}N(R)C(Ph)C(H)R\}(thf)]_2$ [28].

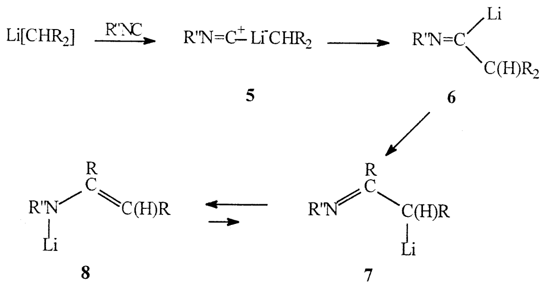

Scheme 3. Proposed pathway in the $LiCHR_2/R''NC$ system ($R'' = C_6H_3Me_2$-2,6, $R = SiMe_3$) [67].

Recently, it was discovered that the reaction of bis(trimethylsilyl)methyllithium with an isonitrile R″NC (R″ = Ph or $C_6H_3Me_2$-2,6) in the presence of a strong neutral donor afforded a lithium 1-azaallyl, Scheme 3 [67]. A 1:1 adduct was proposed as the initial product **5**, which was transformed into the lithioaldimine **6**, followed by a 1,2-$SiMe_3$ shift yielding the lithium 1-azaallyl **7**. Further reactions with a nitrile or isonitrile afforded a β-diketiminate or its 1,3-diazaallyl isomer. As with the $LiCHR_2/R'CN$ system, the nature of the products obtained was dependent upon stoichiometry, solvent and isonitrile. Other examples of such an isonitrile insertion reaction using $^t$BuNC or $CNC_6H_3Me_2$-2,6 have yielded the compounds $[Li\{N(Ph)C(R)C(H)R'\}(tmen)]$ ($R' = {}^t$Bu or $C_6H_3Me_2$-2,6) [68] and $[Li_2(\{N(^tBu)C(R)C(H)\}_2C_6H_4\text{-}1,4)(tmen)_2]$ [69] or its 1,2-isomer [70].

### 4.2.2. Reactions of lithium metal 1-azaallyls

Lithium 1-azaallyls have proved to be useful ligand transfer reagents. However, $[Li\{N(H)C(^tBu)CH_2\}(HMPA)]_2$ with $[Zr(\eta^2\text{-}C_5H_5)_2Cl_2]$ yielded the Zr ketimide [173]. $[Li\{\mu\text{-}N(R)C(^tBu)C(H)R\}]_2$ underwent an insertion reaction with benzonitrile affording the lithium β-diketiminate $[Li\{\mu\text{-}N(R)C(^tBu)C(H)C(Ph)N(R)\}]_2$, likewise a useful ligand transfer reagent [29–31], Scheme 4. Analogous reactions were observed for tungsten [71], zirconium [29,72], magnesium [73] and ytterbium-1-azaallyl complexes [74].

From Scheme 4, it is evident that $[Li\{\mu\text{-}N(R)C(^tBu)C(H)R\}]_2$ behaves as either a *C*- or *N*-centred nucleophile [29]. Hydrolysis afforded the imine, $RCH_2C(^tBu){=}NR$, while treatment with $CH_2Br_2$ followed by $Li^nBu$ gave $[Li\{N(R)C(^tBu)C(H)CH(R)^n\text{-}Bu\}]_2$, via an unusual 1,2-H/$SiMe_3$ dyotropic exchange [75]. The reaction with certain phosphorus(III) chlorides yielded *trans-P,P′*-dichlorodiazaphosphetidines, phosphonium salts, ketimines or enamines [76].

Treatment of $[Li\{\mu\text{-}N(R)C(^tBu)C(H)R\}]_2$ with $PCl_3$ afforded the *trans-P,P′*-dichlorodiazaphosphetidine $ClPN(R')P(Cl)NR'$ ($R' = C(^tBu){=}C(H)SiMe_3$) in poor yield. A possible reaction pathway involved the 1-azaallyl ligand behaving as an *N*-centred nucleophile attacking $PCl_3$ to give $Cl_2PN{=}C(^tBu)C(H)R_2$, which in turn eliminated $SiMe_3Cl$ affording $ClP{=}NC(^tBu){=}C(H)R$; which then underwent a [2 + 2] cyclodimerisation [76]. A higher yielding route involved reaction of the imine $RCH_2C(^tBu){=}NR$ with $PCl_3$ affording $Cl_2PN{=}C(^tBu)C(H)R_2$, which upon thermolysis was converted into the dichlorodiazaphosphetidine. If $PPh_2Cl$ was used in place of $PCl_3$, the imine $RN{=}C(^tBu)CH(R)PPh_2$ was obtained, which proved to be a useful precursor to an enamine (via thermolysis) or the cyclic phosphonium salts

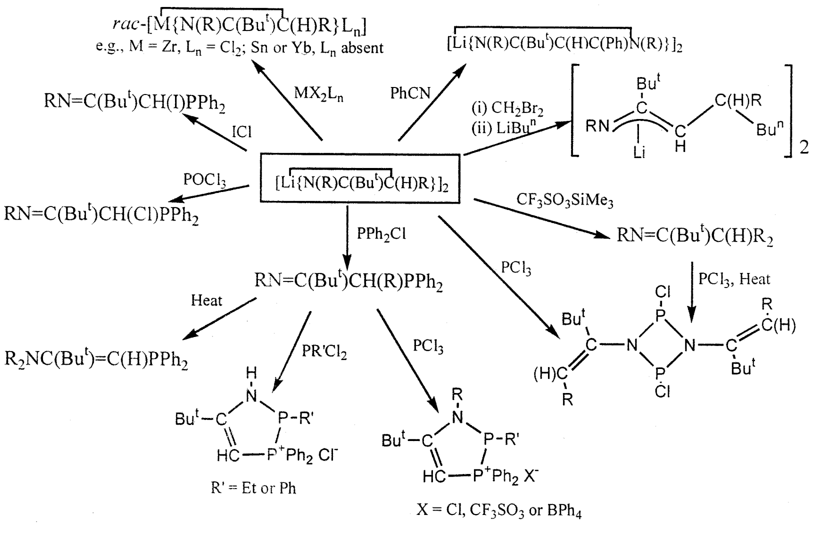

Scheme 4. Selected reactions of $[Li\{\mu\text{-}N(R)C(^tBu)C(H)R\}]_2$ ($R = SiMe_3$) [29–31,76].

$Ph_2PP(R')N(H)C(^tBu)=CH]Cl$ (R′ = Ph or Et) or $[Ph_2PP(Cl)N(SiMe_3)C(^tBu)=CH]X$ (X = Cl, $CF_3SO_3$ or $BPh_4$) by reaction with $R'PCl_2$ or $PCl_3$, respectively. Other reported reactions of $[Li\{\mu\text{-}N(R)C(^tBu)C(H)R\}]_2$ included those with $POCl_3$ or ICl affording the ketimine, $RN=C(^tBu)CH(X)R$ (X = Cl or I).

Surprisingly, thermolysis in benzene of a series of substituted monomeric lithium 1-azaallyls $[Li\{N(R)C(C_6H_4R'\text{-}4)CR_2\}(thf)]$ (R′ = H, F, Br, OMe or $^t$Bu, R = $SiMe_3$), followed by quenching with methanol provided a new route to arylacetylenes, in moderate to high yields, Eq. (4) (R′ = H, F, Br, OMe or $^t$Bu) [65]. Limitations to this reaction sequence depended upon the R′ substituent. Groups responsive to nucleophilic attack (e.g. R′ = $NO_2$ or F) or with acidic protons gave side products. Prolonged thermolysis of $[Li\{\mu\text{-}N(R)C(^tBu)C(H)R\}]_2$ showed no evidence of acetylene formation [65]. This synthesis is an alkyne analogue of Peterson olefinations, e.g. $LiCH_2SiMe_3 + Ph_2CO \rightarrow Ph_2C=CH_2 + LiOSiMe_3$ [77]. An interesting insertion reaction of a lithium enamide is shown in Eq. (5) [78].

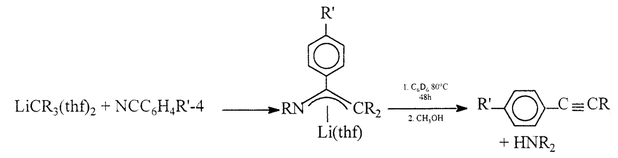

(4)

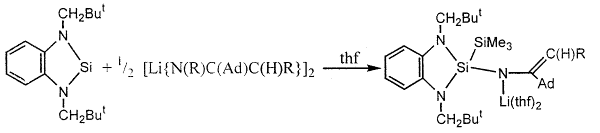

(5)

### 4.2.3. *Synthesis, structures and reactions of the heavier Group 1 metal 1-azaallyls*

Sodium and potassium 1-azaallyls were prepared by metathesis between $MO^tBu$ (M = Na or K) and the lithium 1-azaallyl [29], or from the metal alkyl $MCHR_2$ with the nitrile affording $[M\{N(R)C(^tBu)C(H)R\}]_n$ or $[M\{N(R)C(Ph)C(H)R\}]_n$ (M = Na or K), respectively [79]. The X-ray molecular structure of

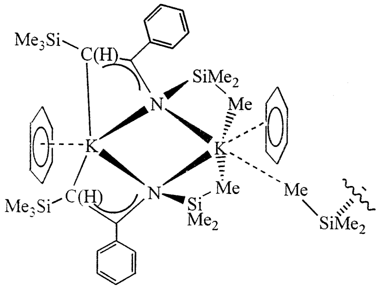

Fig. 3. Schematic representation of the crystalline $[K\{N(R)C(Ph)C(H)R\}]_n$ (R = $SiMe_3$) [79].

$[\overline{\mathrm{K\{N(R)C(Ph)C}}\mathrm{(H)R\}]_n}$, Fig. 3, is interesting in that it crystallises as a polymeric dimer with the N atoms bridging the two metal centres, one molecule of benzene and an agostic K···Me interaction completing the coordination environment about K. The ligand terminally chelates to the metal, adopting an enamido structure characterised by short C–C and long N–C bond lengths [79].

Not only the lithium, but also the sodium and particularly potassium [30,32,33,49,73,74,79,89,127], 1-azaallyls have been used as ligand transfer reagents to generate 1-azaallyls of a variety of metals, including complexes of Mg, Al, Ca, Ti(III), Cu(I), Ni(II), Sr, Zr(IV), Nb(IV), Pd(II), Sn(II), Ba, Sm(III), Yb(II), Hf(IV), Au(I), Hg(II), Pb(II) and Th(IV) [29–31,33,47,50,63,66,81, 82,84,85,90,112,119–122,167,170]. From $\mathrm{[Cs\{\mu\text{-}CHR_2\}\{O(^tBu)Me\}]_2}$ and $\mathrm{^tBuCN}$, the caesium complex $\mathrm{Cs\{N(R)C(^tBu)C(H)R\}}$ was prepared [172].

## 4.3. Group 2 metal 1-azaallyls

Monomeric alkaline earth metal complexes containing monoanionic bidentate ligands are rare. Four-coordinate examples have been based upon an alkyl-functionalised pyridyl ligand $[\mathrm{M}\overline{\mathrm{g\{CR_2(C_5H_4N}}\mathrm{\text{-}2)\}_2}]$ (Section 5 [80]). Magnesium, calcium, strontium and barium bis-1-azaallyls $[\mathrm{A}\overline{\mathrm{e\{N(R)C(^tBu)C}}\mathrm{(H)R\}_2(thf)_n}]$ ($\mathrm{R = SiMe_3}$, Ae = Mg, $n = 0$; Ae = Ca, Sr or Ba, $n = 2$) were derived from $[\mathrm{K\{}\overline{\mathrm{N(R)C(^tBu)C}}\mathrm{(H)R\}]_n}$ and the alkaline earth metal halide $\mathrm{AeBr_2}$ [73]. X-ray diffraction studies of $[\mathrm{M}\overline{\mathrm{g\{N(R)C(^tBu)C}}\mathrm{(H)R\}_2}]$, Fig. 4, showed the Mg to be in a planar environment, confirmed by computational studies (cf. the distorted tetrahedral geometry in $[\mathrm{M}\overline{\mathrm{g\{CR_2(C_5H_4N}}\mathrm{\text{-}2)\}_2}]$ [80]). The ligands are bonded in a *trans*-chelate fashion forming with the magnesium atom a chair skeletal conformation.

Surprisingly, the reaction between $\mathrm{MgBr_2}$ and $[\mathrm{L}\overline{\mathrm{i\{\mu\text{-}N(R)C(^tBu)C}}\mathrm{(H)R\}]_2}$ afforded only $[\mathrm{M}\overline{\mathrm{g(Br)\{N(R)C(^tBu)C}}\mathrm{(H)R\}(NC^tBu)}]$ [81]. Treatment of $[\mathrm{M}\overline{\mathrm{g\{N(R)C(^tBu)C}}\mathrm{(H)R\}_2}]$ with PhCN yielded the unsymmetrical β-diketiminate $\mathrm{[Mg(\{N(R)C(^tBu)C(H)C(Ph)NR\}_2]}$ [73].

## 4.4. Group 4 metal 1-azaallyls

Group 4 metal 1-azaallyls can be prepared by: (i) a LiCl elimination reaction between titanocene(III) [47] or zirconocene(IV) chloride (or $\mathrm{ZrCl_4}$) and the lithiated

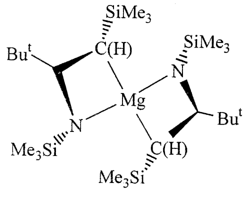

Fig. 4. Schematic representation of the crystalline $[\mathrm{M}\overline{\mathrm{g\{N(R)C(^tBu)C}}\mathrm{(H)R\}_2}]$ [73].

1-azaallyl $[Li\{\mu\text{-}N(R)C(^tBu)C(H)R\}]_2$, e.g. Eq. (6) [29–31,82]; (ii) cleavage of cyclopropane by a zirconocene-$\eta^2$-imine, Eq. (7) [42]; (iii) β-hydride transfer to the metal from an unstable zirconocene-$\eta^2$- imine, Eq. (8) [43]; or (iv) treatment of a titanocene-$\eta^2$-imine with dihydrogen, water or $[Et_3NH]Cl$, Eq. (9) affording the 1-azaallyl $[Ti\{N(Ar)C(H)CPh_2\}(X)Cp_2]$ or the enamide $[Ti\{N(Ar)C(H){=}CPh_2\}(H)Cp_2]$ ($Ar = C_6H_4Me\text{-}4$, $X = Cl$ or OH, $Cp = \eta^5\text{-}C_5H_5$) [83]. Hydrolysis of these compounds afforded *N*-(2,2-diphenylvinyl)-4-methylaniline. Section 5 discusses the Group 4 metal complexes containing the $[CR_2(C_5H_4N\text{-}2)]^-$ ligand and related derivatives.

$$ZrCl_4 + [Li(\mu\text{-}N(R)C(^tBu)C(H)R\}]_2 \rightarrow [Zr\{N(R)C(^tBu)C(H)R\}_2Cl_2] \quad (6)$$

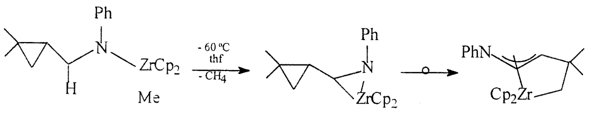

(7)

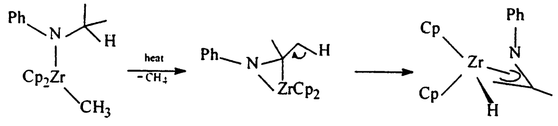

(8)

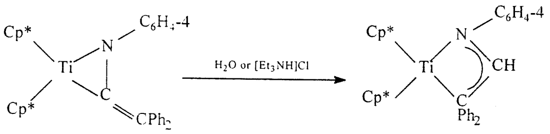

(9)

Structural evidence for $\eta^3$-1-azaallyl coordination has been shown in $[Zr\{N(R)C(^tBu)C(H)Ph\}Cl_3]$ [29–31,84], $[Zr(\{N(R)C(^tBu)CH\}_2C_6H_4\text{-}1,2)Cl_2]$ [30,31,85], *rac*-$[Zr\{N(R)C(^tBu)C(H)R\}_2Cl_2]$ and $[\{Zr(N(R)C(^tBu)C(H)R)(\mu\text{-}Cl)Cl_2\}_2]$ [29–31,82]. Due to the prochiral nature of the central carbon of the 1-azaallyl moiety, diastereoisomers are possible. However, $[Zr\{N(R)C(^tBu)C(H)R\}_2Cl_2]$ crystallises as the *rac*-diastereoisomer (cf. Ref. [30];

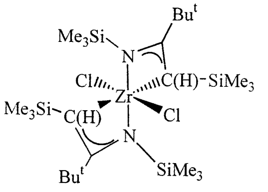

Fig. 5. Schematic representation of the crystalline *rac*-$[Zr\{N(R)C(^tBu)C(H)R\}_2Cl_2]$ [29–31,82].

similarly for Sn(II) and Yb(II) analogues), illustrated in Fig. 5, and is shown to be a monomer with the zirconium in a distorted tetrahedral environment (if taking the 1-azaallyl as occupying a single coordination site). The ligand exhibits $\eta^3$-coordination to the metal centre with the Zr–C(terminal) distance longer than Zr–C(central). A similar feature is observed in $[\{Zr(N(R)C(^tBu)C(H)R)(\mu\text{-}Cl)Cl_2\}_2]$, except that in this case the complex is a dimer. The $[N(R)C(^tBu)C(H)R]^-$ ligand is exceptionally sterically demanding especially when compared with the corresponding polymeric cyclopentadienyl complex $[\{Zr(\eta^5\text{-}C_5H_5)Cl(\mu\text{-}Cl)_2\}_\infty]$ [86].

The complexes $[Zr\{N(R)C(^tBu)C(H)Ph\}Cl_3]$ and $[Zr(\{N(R)C(^tBu)CH\}_2\text{-}C_6H_4\text{-}1,2)Cl_2]$ showed significant catalytic activity in the presence of MAO (methylaluminoxane) towards the polymerisation of ethylene under slight $C_2H_4$ pressure (6–10 bar); the former complex was also effective for propene, producing highly monodisperse atactic polypropylene under ambient conditions [30,85].

Cationic zirconium 1-azaallyl complexes were generated by C–H activation of *N*-heterocycles lacking $\alpha$-hydrogen, e.g. 2,3-benzoquinoline, phenazine or 2,6-dimethylpyridine, by treatment with $[Zr(\eta^5\text{-}C_5H_5)_2(Me)(thf)]^+$, exemplified in Eq. (10). The resulting four-membered heterocycles contained a labile thf molecule and hence were dissociated extensively in $CD_2Cl_2$ solution, confirmed by low-temperature NMR spectroscopic studies [87].

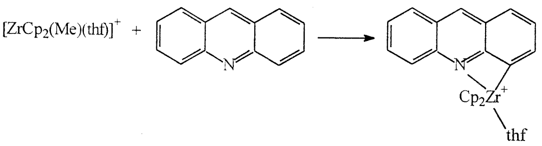

(10)

When the zwitterionic amide $[^+Zr\{N(R)CH(Ph)(CH_2)_2{}^-B(C_6F_5)_3\}Cp_2]$ was set aside in $CD_2Cl_2$, NMR spectroscopic evidence supported its conversion into the zwitterionic zirconium 1-azaallyl $[^+Zr\{N(R)C(Ph)C(H)CH_2^-B(C_6F_5)_3Cp_2]$ [88].

### 4.5. Group 5 metal 1-azaallyls

The vanadium 1-azaallyls $[V(N\{Si(^tBu)_2C(Me)_2CH_2\}C(R'')C(H)R'')(=NR')(HNR')]$ ($R'' = Me$ or Et) were obtained from the thermolysis of $[VMe(NR')(HNR')_2]$ ($R' = Si^tBu_3$) in the presence of $R''C{\equiv}CR''$, Scheme 5 [44].

The X-ray molecular structure of the latter, illustrated in Fig. 6, was one of the first early transition metal $\eta^3$-1-azaallyls to be described [44]. The vanadium atom is in a distorted tetrahedral environment (assuming the 1-azaallyl ligand occupies a single coordination site), coordinated by amido, imido and the unusual highly asymmetric 1-azaallyl-alkyl ligands. The V–N(1) bond of 2.043(3) Å is significantly shorter than the V–C (2.335–2.384 Å). This asymmetric $\eta^3$-1-azaallyl bonding contrasts sharply with those of less-electrophilic transition metals, having nearly equivalent M–N and M–C distances [25,52,61,89]. The near planarity at the nitrogen (sum of angles 357.4°), as well as the asymmetric bonding, may be due to the steric constraints of the ligand. The lengthening of the metal–amido and

–imido distances reflects the fact that there may be steric crowding also around the vanadium atom. The $^1$H (C*H*R) and $^{13}$C{$^1$H} (*C*R and *C*HR) NMR spectral shifts for the 1-azaallyl fragments indicated that the $\eta^3$-coordination was also retained in solution.

The same compounds were obtained under milder conditions from [V(=NR′)$_2$(HNR′)(OEt$_2$)]. NMR spectral monitoring of the reaction with but-2-yne showed the formation of an isolable intermediate having a 2-azavanadacyclobutene structure. The driving force for the transfer of a hydrogen from the Si$^t$Bu$_3$ group to the four-membered ring could be due to the increase in electron-donating ability of the ligand [44].

NMR spectroscopic evidence served to identify the niobium(III) 1-azaallyl [Nb{N(R)C($^t$Bu)CH$_2$}($\eta^5$-C$_5$H$_4$SiMe$_3$)$_2$], prepared from the X-ray-characterised lithium-1azaallyl [Li{N(R)C($^t$Bu)CH$_2$}]$_3$ [90]. Additionally, [Nb{N(R)C($^t$Bu)CH$_2$}-Cl($\eta^5$-C$_5$H$_4$SiMe$_3$)$_2$] was characterised by IR and elemental analysis [90]. To date these appear to be the only examples of niobium-1-azaallyls; tantalum-1-azaallyl are still unknown.

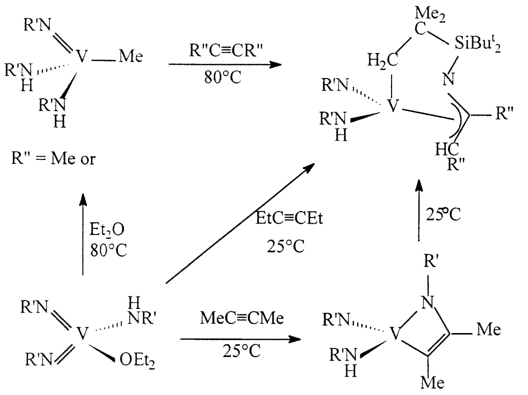

Scheme 5. Synthetic routes to vanadium 1-azaallyls (R′ = $^t$Bu, R″ = Me or Et) [44].

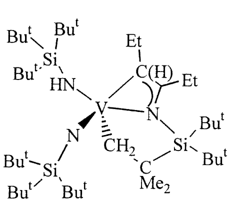

Fig. 6. Schematic representation of the crystalline [V(N{Si(Bu$^t$)$_2$C(Me)$_2$CH$_2$}C(Et)C(H)Et)-(=NR′)(HNR′)] (R′ = Si$^t$Bu$_3$) [44].

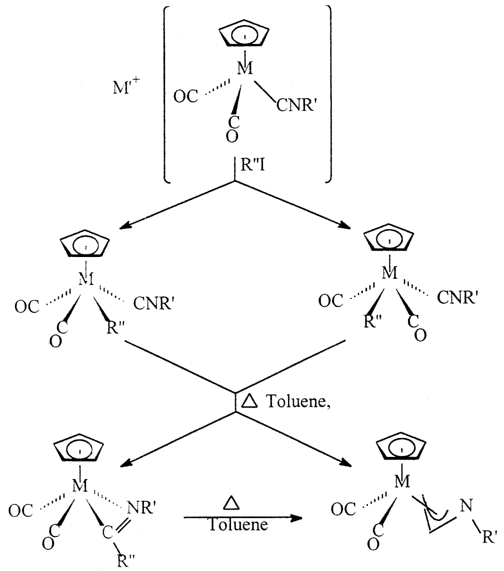

Scheme 6. Synthesis of molybdenum and tungsten 1-azaallyls (M′ = Na, M = Mo or W) [35–40].

### 4.6. *Group 6 metal 1-azaallyls*

Electron-rich complexes of molybdenum and tungsten and their involvement in metal-mediated C–C coupling reactions have been studied widely; in these, the 1-azaallyl ligand has played an important role. Three principal synthetic routes have been employed in their formation: (i) the reaction of $[Mo_2(CO)_4(\eta^5\text{-}C_5H_5)_2]$ with a substituted 2-azirine, Eq. (11) [34]; (ii) condensation of a carbon-bound metal enolate with a primary amine, Eq. (12) [41]; or (iii) thermal isomerisation of a metal isonitrile complex involving a 1,2-hydrogen shift, Scheme 6 [35–40].

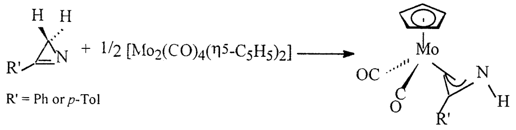

(11)

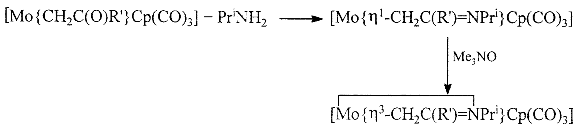

$$\begin{tikzcd}[Mo\{CH_2C(O)R'\}Cp(CO)_3] - Pr^iNH_2 \arrow[r] & [Mo\{\eta^1\text{-}CH_2C(R')=NPr^i\}Cp(CO)_3] \arrow[d, "Me_3NO"] \\ & [Mo\{\eta^3\text{-}CH_2C(R')=NPr^i\}Cp(CO)_3]\end{tikzcd} \qquad (12)$$

The third route has yielded the majority of Mo and W 1-azaallyls. The mechanism for their formation has been explored extensively. Alkylation of the metallates $M'[MCp^*(CO)_2(CNR')]$ ($M' = Na$ or K, M = Mo or W, $R' = Me$, Et, ${}^i$Pr or ${}^t$Bu and $Cp^* = \eta^5\text{-}C_5H_5$ or $\eta^5\text{-}C_5Me_5$) by $R''I$ ($R'' = Me$ or Et) afforded alkyl complexes $[MCp^*(CO)_2R''(CNR')]$, which upon thermolysis isomerised into isolable metal-$\eta^2$-iminoacyls and/or 1-azaallyls, $[M\{\eta^2\text{-}C(NR')R''\}Cp^*(CO)_2]$ or $[M\{\eta^3\text{-}CH_2C(H)NR'\}\text{-}Cp^*(CO)_2]$ Scheme 6 [35–40]. The kinetic stability of the alkyls towards rearrangement was dependent upon the nature of M, R′ and the solvent [37,39]. For M = Mo, bulky R′ groups (e.g. $^t$Bu) and polar solvents (e.g. pyridine or acetonitrile) favoured the formation of stable $\eta^2$-iminoacyls, while 1-azaallyl formation occurred with tungsten and small R′ groups (e.g. Me or Et) in aromatic hydrocarbons. The 1-azaallyl isomer was preferred thermodynamically, being formed from the $\eta^2$-iminoacyl upon refluxing in toluene [36,37,39]. This rearrangement involved a 1,2-hydrogen shift from the carbon-bonded alkyl substituent to the iminoacyl carbon. UV-photoelectron spectroscopic investigations indicated that the two lowest energy bands were due to the orbitals containing the four electrons and that the ionisation energy of the $\eta^2$-iminoacyl was ca. 0.5 eV lower than that of the 1-azaallyl [91].

NMR spectroscopic studies of the molybdenum and tungsten 1-azaallyls showed them to have the *syn*, *endo* configuration [35–37,39]. This was confirmed in several structures and is exemplified in $[Mo\{N(^tBu)C(H)CH_2\}Cp(CO)_2]$, Fig. 7; the $^t$Bu group adopts a *syn* position, possibly to minimise adverse steric interactions with the Cp ring [39]. The C(8)–C(9) and C(8)–N(1) bond lengths lie in the range between single and double bonds. The Mo–C and Mo–N bond lengths are similar to those in other Group 6 metal examples with Mo–C(8) (2.317(3) Å) slightly longer than Mo–(C9) (2.288(4) Å).

Substitution of a cyclopentadienyl by an indenyl ($\eta^5$-$C_9H_7$) ligand favoured $\eta^2$ clobop|-iminoacyl formation [40]. A room temperature fluxional process was observed for $[W\{N(^tBu)C(H)CH_2\}(\eta^5\text{-}C_9H_7)]$. The mechanism is outlined in Scheme

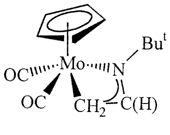

Fig. 7. Schematic representation of the crystalline $[Mo\{N(^tBu)C(H)CH_2\}Cp(CO)_2]$ [39].

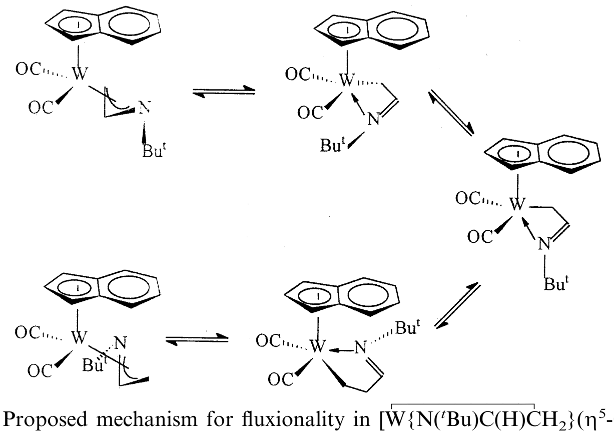

Scheme 7. Proposed mechanism for fluxionality in $[W\{N(^tBu)C(H)CH_2\}(\eta^5\text{-}C_9H_7)]$ [40].

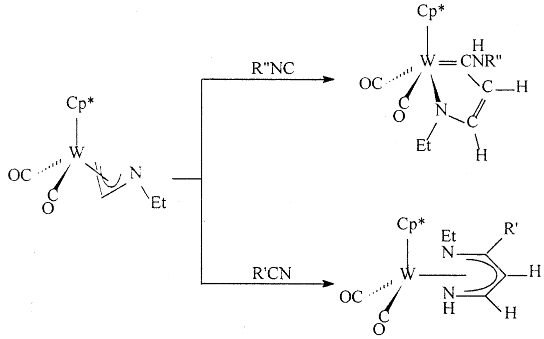

Scheme 8. Reaction of [$W\{N(Et)C(H)CH_2\}Cp^*(CO)_2$] with R″NC or R′CN (R″ = Me or Et, R′ = Me or Ph) [71].

7, implicating a transient planar metal-azacyclobutenyl species which underwent pseudo-rotation to the *syn*, *endo* $\eta^3$-allylic system. The alternative mechanism of dissociation of a ligating atom, followed by an $\mu$-$\eta^1$-rotation generating an electron-deficient intermediate was discounted as being higher in energy.

The complex [$W\{N(Et)C(H)CH_2\}Cp^*(CO)_2$] ($Cp^* = \eta^5$-$C_5Me_5$) underwent facile C–C bond-forming reactions with an isonitrile R″NC to give the cyclic aminocarbene complex [$W\{=C(NHR'')C(H)=C(H)N(Et)\}Cp^*(CO)_2$] [37] or with a nitrile R′CN to yield the *N*,*N*-β-diketiminato complex, [$W\{N(H)C(R'')C(H)C(H)N(Et)\}Cp^*(CO)_2$], Scheme 8) [71].

The aminocarbyne complex [$W\{\equiv CNEt_2\}Cp^*(CO)_2$] reacted in a selective [2 + 2] cycloaddition fashion with the nitrilium salt [$MeCNMe_2$][$BF_4$] to afford the iminocarbene complex [$W\{N(Me)C(Me)C(NEt_2)Cp^*(CO)_2$] [92]. From [$Mo(CO)_3(NCMe)_3$] and $HBF_4 \cdot OEt_2$ in acetonitrile [$Mo\{\eta^3$-$N(H)C(H)CH_2\}(CO)_2(NCMe)_3$][$BF_4$] was obtained [93]. If the reaction was conducted under an atmosphere of dihydrogen, the yield was improved dramatically. A similar cationic complex was prepared by methylation of [$Mo\{N(H)C(Ph)CH_2\}Cp(CO)_2$] by $CF_3SO_3Me$ [34].

### 4.7. Groups 7 and 8 metal 1-azaallyls

The first Fe(II) 1-azaallyls were prepared from the reaction of [$Fe_2(CO)_9$] with a substituted 2-azirine in the presence of an alkyne, Eq. (13) (R′ = COOMe or Ph) [94].

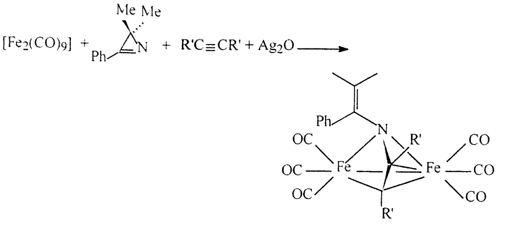

(13)

The X-ray molecular structure $[Fe_2\{\mu\text{-}N\{C(Ph)CMe_2\}C(CO_2Me)C(CO_2Me)\}(CO)_6]$ shows the terminal C and N of the 1-azaallyl ligand to be bonded to both Fe atoms, while the central C of the N$\overset{\cdots}{-}$C$\overset{\cdots}{-}$C moiety binds to only one metal centre [94]. The short Fe–Fe bond length of 2.453(4) Å was attributed to a bent bond between the two metal atoms. NMR spectroscopic studies identified two dynamic processes, one intramolecular ('flip-flopping' of the azaallyl ligand between the two Fe atoms) and an intermolecular scrambling of the CO molecules [94,95].

Similarly, a bimetallic MnFe-1-azaallyl complex was prepared and X-ray characterised as shown in Fig. 8 [96].

Another route involved the reaction of $[Fe_2(\mu\text{-}CH_2)(CO)_8]$ with a phosphine imine $R'N{=}PR''_3$ ($R' = {}^tBu$, $R'' = Ph$; $R' = R'' = Ph$) under a CO atmosphere [97,98]. The initial products were 3-ferra-4-pyrrolin-2-ones which slowly eliminated CO affording the 1-azaallyl complexes, Scheme 9. Formation of the 1-azaallyl complexes was favoured if the reaction was conducted in the absence of CO or $R' = Ph$. The slower elimination when $R' = {}^tBu$ was explained by the electron-donating ${}^tBu$ group strengthening the C–N bond, thereby decreasing the tendency for bond cleavage. Phosphine imines had been previously proposed to deoxygenate carbonyls [97,98]. The structure of $[Fe_2\{\eta\text{-}N({}^tBu)C(H)C(H)\}(CO)_6]$ shows two independent molecules, one contains a puckered metallacycle while the other is planar.

These Fe(II) 1-azaallyls underwent reversible carbonylation reactions, forming isomeric ferrapyrolinones, dependent upon whether photolysis or thermolysis was employed [99,100]. The analogous reaction with an alkyne afforded a ferrapyridine, in which the alkyne molecule had inserted into the Fe–C bond.

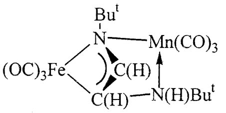

Fig. 8. Schematic representation of the crystalline $[FeMn\{\mu\text{-}N(Bu^t)C(H)C(H)N(H)Bu^t\}(CO)_6]$ [96].

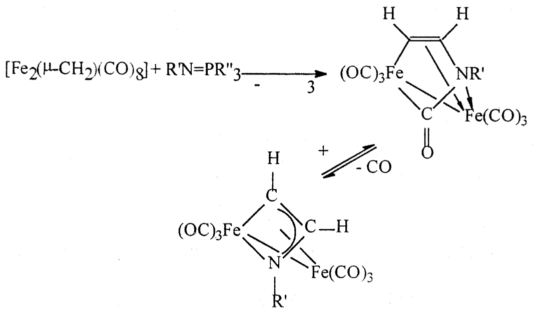

Scheme 9. Formation of $[Fe_2\{\mu\text{-}N(R')C(H)C(H)\}(CO)_6]$ [97,98].

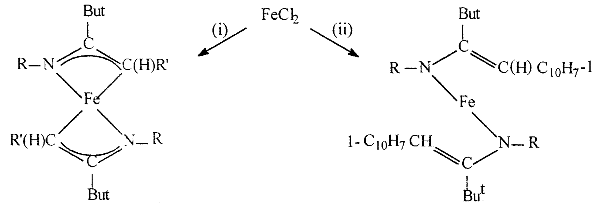

Scheme 10. Synthetic routes to iron(II) 1-azaallyls: (i) $(2/n)[\mathrm{K}\{\mathrm{N(R)C(^{t}Bu)C(H)C_6H_4Me\text{-}4}\}]_n$ or $[\mathrm{Li}\{\mu\text{-}\mathrm{N(R)C(^{t}Bu)C(H)R}\}]_2$; (ii) $(2/n)[\mathrm{K}\{\mathrm{N(R)C(^{t}Bu)C(H)C_{10}H_7\text{-}1}\}]_n$ [89].

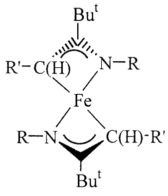

Fig. 9. Schematic representation of the crystalline $[\mathrm{Fe_2}\{\mathrm{N(R)C(^{t}Bu)C(H)R'}\}_2]$ ($\mathrm{R'} = \mathrm{R}$ or $\mathrm{C_6H_4Me\text{-}4}$) [89].

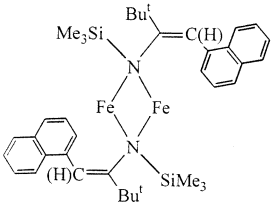

Fig. 10. Schematic representation of the crystalline $[\mathrm{Fe_2}\{\mathrm{N(R)C(^{t}Bu)C(H)C_{10}H_7\text{-}1}\}]_2$ [89].

Mononuclear iron(II) bis(1-azaallyl)s were obtained by treatment of $\mathrm{FeCl_2}$ with a sterically hindered alkali metal 1-azaallyl, Scheme 10 ($\mathrm{R'} = \mathrm{R}$ or $\mathrm{C_6H_4Me\text{-}4}$) [89].

Different bonding modes and coordination about the metal atom were observed in some iron(II) 1-azaallyls, dependening upon the nature of the ligands. Thus, $\eta^3$-bonding was observed in $[\mathrm{Fe_2}\{\mu\text{-}\mathrm{N}\{\mathrm{C(Ph)CMe_2}\}\mathrm{C(CO_2Me)C(CO_2Me)}\}\mathrm{(CO)_6}]$ [94], $[\mathrm{Fe_2}\{\mu\text{-}\mathrm{N(^{t}Bu)C(H)C(H)}\}\mathrm{(CO)_6}]$ [97,98], and $[\mathrm{Fe}\{\mathrm{N(R)C(^{t}Bu)C(H)R'}\}_2]$, Fig. 9 ($\mathrm{R'} = \mathrm{R}$ or $\mathrm{C_6H_4Me\text{-}4}$) [89]. In the final *p*-tolyl, unlike the trimethylsilyl, complex Fe–C(1) is shorter than Fe–C(2) and this was attributed to the electron-releasing *p*-tolyl group delocalising electrons towards the more favoured enamido ligation giving N–C(1) more single and C(1)–C(2) more double bond character. For $[\mathrm{Fe}\{\mathrm{N(R)C(^{t}Bu)C(H)C_{10}H_7\text{-}1}\}]_2$, Fig. 10, a true enamido structure was observed. The N–M–N bond angle deviates slightly from linearity (cf. Fe amides [101–103]).

The magnetic moments of the mononuclear compounds were consistent with a $\mathrm{d^6}$ $\mathrm{Fe^{2+}}$ high-spin configuration, as in high-spin Fe(II) silylamides [102,103].

1-Azaallyl complexes of ruthenium have been known for some time and exhibit $\eta^3$-asymmetric coordination to the metal centre. Two methods have been employed in their synthesis. Thermolysis of $[Ru_3(CO)_{12}]$ with $R^1C(H){=}C(H)C(H){=}NR^2$ afforded four- or five-membered ruthenacycles, Scheme 11 [104,105]. When $R^1$ and $R^2$ were bulky groups, bridging 1-azaallyl complexes were favoured; upon further heating they were converted into five-membered heterocycles retaining a bridging $\eta^3$-1-azaallyl ligand [95,104,105]. These ruthenium-1-azaallyls were fluxional in solution, with 'flipping' of the 1-azaallyl ligand between the metal centres, Eq. (14) [95], (cf. $[Fe_2\{\mu\text{-}N\{C(Ph)CMe_2\}C(CO_2Me)C(CO_2Me)\}(CO)_6]$ [94]). Reaction of $[Ru_3(CO)_{12}]$ with a 1,4-diazabuta-1,3-diene or ketene [106,107], or by insertion of CO into a ruthenium 1-azaallyl [104,105], afforded five-membered metallacycles also containing a bridging 1-azaallyl fragment. Structural characterisation showed asymmetric bonding of the two Ru centres by the 1-azaallyl ligand [104–107]. The heterobimetallic complex $[FeMn\{\mu\text{-}N(Bu^t)C(H)C(H)N(H)Bu^t\}(CO)_6]$ also exhibited an $\mu,\eta^3$-azaallyl fragment within the terdentate ligand [96].

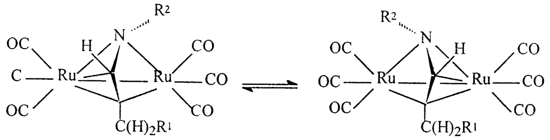

(14)

An attempt to create an unsaturated ruthenium amide, in order to examine its ability to react with a species containing aryl or vinyl C–H bonds, resulted in an unexpected product, Eq. (15) [45,46]. The molecular structure revealed a bridging nitrogen with one intact isopropyl group and the other doubly dehydrogenated, alternatively viewed as a bridging 1-azaallyl [45,46]. The ${}^iPrN{-}CMe$ and $MeC{-}CH_2$ bonds lengths lie in the range between single and double bonds. The nitrogen is bound to both ruthenium centres, while both the azaallylic carbons atoms are bound to Ru(2), leaving Ru(1) unsaturated, this being alleviated by an agostic interaction. Mechanistic and NMR spectroscopic studies showed that the complex had formed by β-C–H and γ-C–H activation, followed by dehydrochlorination. The compound underwent adduct formation with CO or a phosphine, the $\mu,\eta^3$-1-azaallyl structure being maintained in each product [46].

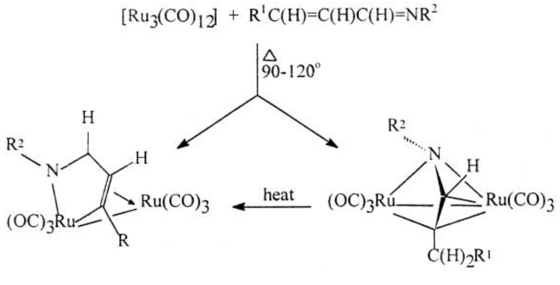

Scheme 11. Routes to ruthenium 1-azaallyls [95,104–107].

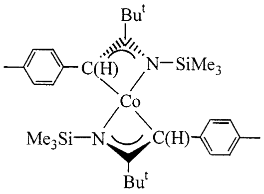

Fig. 11. Schematic representation of the crystalline $[Co\{N(R)C(^tBu)C(H)C_6H_4Me\text{-}4\}_2]$ [89].

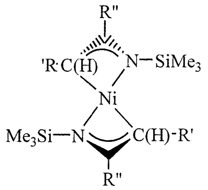

Fig. 12. The molecular structure of crystalline $[Ni\{N(R)C(R'')C(H)R'\}_2]$ ($R'' = Ph$, $R' = R$ [79]; or $R'' = {}^tBu$, $R' = C_6H_4Me\text{-}4$ [89]).

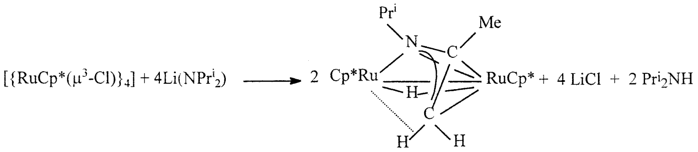

(15)

## 4.8. Cobalt 1-azaallyls

Complexes containing cobalt–carbon σ bonds have been notoriously difficult to synthesise due to their low thermal stability. Prior to 1993, $[CoMe_2(PMe_3)_3]$ was the only known cobalt alkyl complex [108]. Reaction of $CoCl_2$ with the lithium analogue of the following bulky ligands $[CR_2(C_5H_4N\text{-}2)]^-$ and $[C(Ph)R(C_5H_4N\text{-}2)]^-$ afforded the thermally stable complexes $[Co\{CR_2(C_5H_4N\text{-}2)\}_2]$ and $[Co\{C(Ph)R(C_5H_4N\text{-}2)\}_2]$, respectively, and are discussed further in Section 5 [109,110].

The mononuclear cobalt bis(1-azaallyl) complexes $[Co\{N(R)C(^tBu)C(H)\text{-}C_6H_4Me\text{-}4\}_2]$ and $[Co\{N(R)C(^tBu)C(H)R\}_2]$ have been synthesised, in which the cobalt atom is situated in a distorted octahedral environment, bound in true $\eta^3$-fashion by the N$\cdots$C$\cdots$C moiety; the structure of the former is illustrated in Fig. 11 and is similar to that of the Fe(II) analogues discussed in Section 4.7. Magnetic moments for these pseudo-octahedral cobalt complexes were in the range of 2.1–2.9 $\mu_B$, appropriate for one unpaired electron in a low spin $d^7$ complex. The value for $[Co\{N(R)C(^tBu)C(H)C_6H_4Me\text{-}4\}_2]$ was higher than the spin-only theoretical value, attributed to unquenched orbital contributions from the first excited state.

### 4.9. Group 10 metal 1-azaallyls

Structural characterisation has been obtained for nickel bis(1-azaallyl)s of Fig. 12 ($R'' = Ph$, $R' = R$ [79]; or $R'' = {}^tBu$, $R' = C_6H_4Me$-4 [89]), synthesised by potassium halide elimination reactions. Each structure shows the nickel to be in a six-coordinate environment, $\eta^3$-bound by each 1-azaallyl ligand. NMR spectroscopic studies of the *p*-tolyl complex showed the presence of three isomers; the molecular structure of the major isomer had both ligands adopting the *anti*-conformation in a *trans*-configuration. The complex $[Ni\{N(R)C(Ph)C(H)R\}_2]$ existed as two isomers in solution, but the solid state structure showed the ligands to be arranged in a *cis*, *anti*-orientation.

The complexes $[Ni\{N(R)C({}^tBu)C(H)R\}I]$ and $[Ni\{N(R)C({}^tBu)C(H)R\}I(PPh_3)]$ were prepared from the iodoalkyl imine $N(R){=}C({}^tBu)CH(R)I$ and nickel and also $PPh_3$ for the latter [47], which crystallises as a monomer with the nickel $\eta^3$-bonded to the 1-azaallyl ligand, Fig. 13.

Although palladium and platinum $\eta^3$-allyl complexes have been studied extensively, surprisingly few examples containing the 1-azaallyl ligand have been reported. $\eta^1$-1-Enamido fragments were observed in the five-membered metallacycles $[Pt\{N(COMe)C({=}C(R')H)C(O)O\}L_2]$ [$R' = Ph$ and $L_2 = (PPh_3)_2$, $(PMePh_2)_2$, $(PMe_2Ph)_2$ or $Ph_2P\{CH_2\}_nPPh_2$ ($n = 1$–4); $R' = H$ and $L_2 = (PMePh_2)_2$, $(PMe_2Ph)_2$ or $(Ph_2PCH_2PPh_2)$] and $[Pd\{N(COMe)C({=}C(R')H)C(O)O\}L_2]$ ($L_2 = Ph_2P\{CH_2\}_3PPh_2$) [111].

Recent research in Sussex has generated the homo- and heteroleptic palladium complexes $[Pd\{N(R)C({}^tBu)C(H)R\}I]$ and $[Pd\{N(R)C({}^tBu)C(H)R\}I(PPh_3)]$ [47]. No structural evidence exists at present, but presumably the former complex crystallises as a monomer, analogous to the nickel complex.

### 4.10. Group 11 metal 1-azaallyls

The metal(I) complexes $[Cu\{\mu\text{-}N(R)C({}^tBu)C(H)R\}]_2$ [50] and $[M\{N(R)C(Ph)CR_2\}]_2$ (M = Cu or Au) [112], synthesised by salt elimination reactions, showed remarkable thermal stability. Their spectroscopic (UV–vis, NMR, ESR) and electrochemical properties were documented [112]. Their solid-state structures show centrosymmetric dimers with one half as the asymmetric unit, the other being generated by an inversion centre, as exemplified in Fig. 14. The $\eta^2$-ligands *C*,*N*-bridge the two metal centres, the resultant eight-membered ring

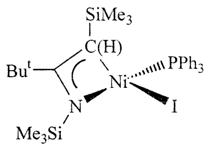

Fig. 13. Schematic representation of the crystalline $[Ni\{N(R)C({}^tBu)C(H)R\}I(PPh_3)]$ [47].

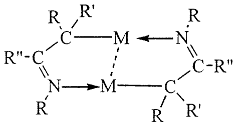

Fig. 14. Schematic representation of the crystalline [M{μ-N(R)C(R″)C(R′)}]$_2$ (M = Cu, R′ = H, R″ = $^t$Bu [50]; M = Au, R′ = R, R″ = Ph [112]).

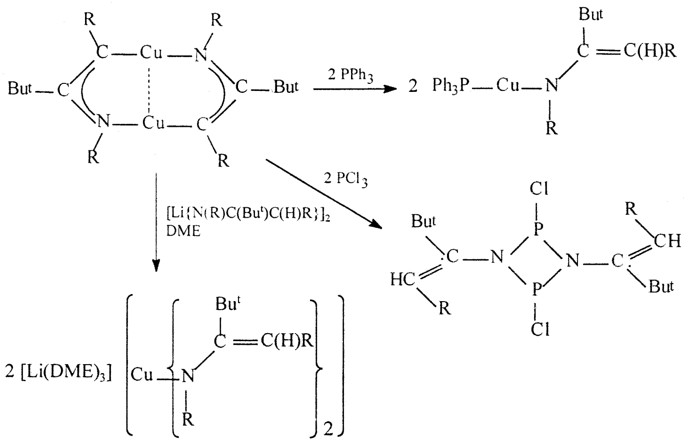

Scheme 12. Selected reactions of [Cu{μ-N(R)C($^t$Bu)C(H)R}]$_2$ [50].

being nearly coplanar. All structures exhibit N–M–C bond angles close to the ideal linear value and short M···M contacts, possibly due to the geometry of the ligands, although the values are interesting in view of theoretical discussions about d$^{10}$–d$^{10}$ closed shell interactions between Cu(I) atoms [113–115]. In both compounds the short C–N and long C–C bond lengths suggest that the ligand behaves in a bridging iminoalkyl fashion.

The copper(I) 1-azaallyl [Cu{μ-N(R)C($^t$Bu)C(H)R}]$_2$ underwent the reactions shown in Scheme 12. For [Li(DME)$_3$][Cu{N(R)C($^t$Bu)C(H)R}$_2$], the presence of a strong neutral donor was essential in shifting the equilibrium towards this product. If the experiment was carried out in pentane with cooling, [Cu{μ-N(R)C($^t$Bu)C(H)R}]$_2$ crystallised out first, thereby shifting the equilibrium towards the starting materials.

The complexes [Cu{N(R)C($^t$Bu)C(H)R}(PPh$_3$)] and [Li(DME)$_3$][Cu{N(R)C($^t$Bu)C(H)R}$_2$] crystallised as monomers. In each case, the 1-azaallyl ligand behaves as an enamide with long C–N and short C–C bonds. They showed reduced thermal stability and increased sensitivity towards dioxygen compared to [Cu{μ-N(R)C($^t$Bu)C(H)R}]$_2$, probably because their monomeric structure was retained in solution, thus shielding the copper atom less effectively. Previous examples of Li–Cu mixed complexes include [Li(thf)$_4$][{Cu{N(SiMePh$_2$)$_2$}$_2$] [116] and [Li(thf)$_4$][Cu{C(SiMe$_3$)$_3$}$_2$] [117].

Although $[\mathrm{Cu\{CR_2(C_5H_4N\text{-}2)\}}]_2$ was oxidised electrochemically [118], attempts to synthesise the related Cu(II) 1-azaallyl were unsuccessful, generally resulting in formation of the Cu(I) 1-azaallyl and an organic coupled product [89].

### 4.11. Group 13 metal 1-azaallyls

Group 13 metal 1-azaallyls are rather rare. The first examples were reported in 1999 [119–122]. Treatment of the appropriate lithium-1-azallyls $[\mathrm{Li\{N(R)C(Ph)CR_2\}(thf)}]$, $[\mathrm{Li\{N(R)C(Ph)C(H)R\}(thf)}]$, $[\mathrm{Li\overline{\{\mu\text{-}N(R)C({}^tBu)C}(H)R\}}]_2$ in the correct stoichiometry with the appropriate $\mathrm{AlMe}_n\mathrm{X}_{3-n}$ afforded, respectively, the aluminium 1-azaallyls $[\mathrm{Al\{N(R)C(Ph)CR_2\}Me}_n\mathrm{X}_{2-n}(\mathrm{thf})_m]$ ($n = 2$, $m = 0$; $n = 1$, X = Cl, $m = 0$ or 1; $n = 0$, X = Cl, $m = 0$ or 1; X = Br, $m = 0$] and $[\mathrm{Al\{N(R)C({}^tBu)C(H)R\}}_n\mathrm{Me}_{3-n}(\mathrm{thf})_m]$ ($n = 1$, $m = 0$ or 1 or $n = 2$ and $m = 1$). Fluoro- and iodo-1-azaallyls $[\mathrm{Al\overline{\{N(R)C(Ph)C}R_2\}F(\mu\text{-}F)}]_2$ and $[\mathrm{Al\overline{\{N(R)C(Ph)C}R_2\}I_2}]$ were prepared by treatment of $[\mathrm{Al\overline{\{N(R)C(Ph)C}R_2\}Me_2}]$ with two equivalents of $\mathrm{Me_3SnF}$ or $\mathrm{I_2}$, respectively [120]. $[\mathrm{Al\overline{\{N(R)C(Ph)C}R_2\}F(\mu\text{-}F)}]_2$ is the first example of a dimeric aluminium difluoride, in which two bridging F atoms reside on the pseudo-twofold axis of the ca. $C_2$ symmetric molecule. $[\mathrm{Al\{N(R)C(Ph)CR_2\}H(\mu\text{-}H)}]_2$, obtained from the 1-azaallylaluminium dibromide and $[\mathrm{LiAlH_4}]$, afforded $[\mathrm{Al\{N(R)C(Ph)CR_2\}(\mu\text{-}E)}]_2$ when treated with E (E = Se or Te) [121]. X-ray studies of the complexes $[\mathrm{Al\overline{\{N(R)C(Ph)C}R_2\}Cl_2}]$ and

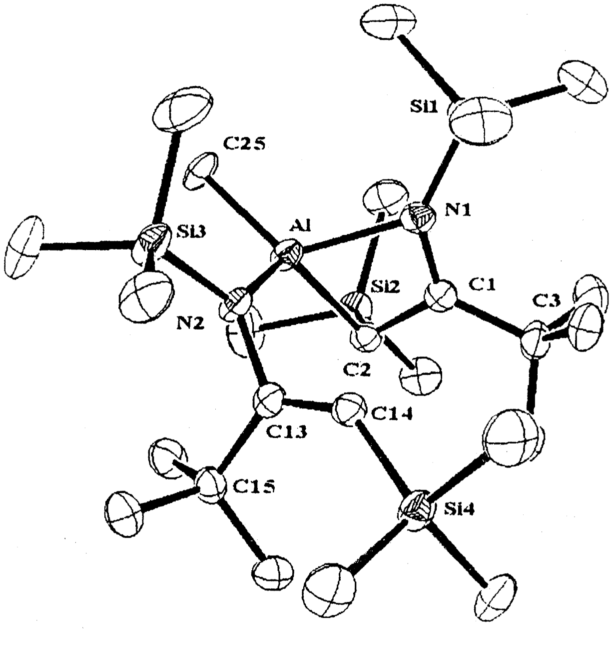

Fig. 15. The molecular structure of $[\mathrm{Al\overline{\{N(R)C({}^tBu)C}(H)R\}\{N(R)C({}^tBu){=}C(H)R\}Me}]$ [119].

$[\mathrm{Al}\{\mathrm{N(R)C(Ph)CR_2}\}\mathrm{F}(\mu\text{-}\mathrm{F})]_2$ showed the 1-azaallyl ligand was $\eta^3$-bonded to the Al atom, whereas in $[\mathrm{Al}\{\mathrm{N(R)C(Ph)CR_2}\}\mathrm{Cl_2(thf)}]$ it is enamido [120].

The molecular structure of $[\mathrm{Al}\{\mathrm{N(R)C(^tBu)C(H)R}\}\{\mathrm{N(R)C(^tBu){=}C(H)R}\}\mathrm{Me}]$ is illustrated, Fig. 15, showing the presence of both tautomeric 1-azaallyl ligands in the crystalline molecule, one being $\eta^3$-bonded to the aluminium atom, the other enamido [119]. The Al–N(1) bond of 1.998(2) Å is significantly longer than the Al–N(2) of 1.839(2) Å, as is the C(1)–C(2) compared with the C(13)–C(14) bond (1.468(3) and 1.347(3) Å, respectively). Multinuclear NMR spectroscopic experiments showed that the structure was retained in solution with the two 1-azaallyl ligands exchanging rapidly, the $^1$H-NMR coalescence temperature of 302 K corresponded to a $\Delta G$ of 60.7 kJ mol$^{-1}$. The presence in a single crystalline molecule of two tautomeric 1-azaallyl ligands had been previously observed in $[\mathrm{Sn}\{\mathrm{N(R)C(Ph)CR_2}\}\{\mathrm{N(R)C(Ph){=}CR_2}\}]$, see Section 4.12 [32].

A bis(aluminium-1-azaallyl) was prepared by reduction with potassium of an in situ-prepared mixture of the azaallyls $[\mathrm{Al}\{\mathrm{N(R)C(Ph)CR_2}\}\mathrm{I_2}]$ and $[\mathrm{Al}\{\mathrm{N(R)C(Ph)CR_2}\}\mathrm{(Cl)I}]$ [122]. The X-ray crystal structure shows the shortest Al–Al bond reported so far for a neutral compound, at 2.593(3) Å.

Reaction of $\mathrm{GaCl_3}$ with the lithium azaallyl $[\mathrm{Li}\{\mathrm{N(R)C(Ph)CR_2}\}\mathrm{(thf)}]$ afforded the first gallium azaallyl $[\mathrm{Ga}\{\mathrm{N(R)C(Ph)CR_2}\}\mathrm{Cl_2}]$. Reduction with Na–K alloy afforded the digallane compound $[\mathrm{Ga}\{\mathrm{N(R)C(Ph)CR_2}\}\mathrm{Cl}]_2$ [122]. Both were characterised by X-ray as was $[\mathrm{In}\{\mathrm{N(R)C(Ph)CR_2}\}\mathrm{Br}]_2$, obtained from InBr and the lithium 1-azaallyl [122].

### 4.12. Group 14 metal 1-azaallyls

The number of structurally characterised examples of hydrocarbyls of bivalent germanium, tin and lead decreases in the sequence $\mathrm{Sn} > \mathrm{Ge} \gg \mathrm{Pb}$, with very few thermally stable organolead compounds. Use of the 1-azaallyl ligand has significantly increased knowledge in this area, with several structures demonstrating a number of different bonding modes of the ligands. The following bis(1-azaallyl) complexes have been synthesised: *rac*-$[\mathrm{Sn}\{\mathrm{N(R)C(^tBu)C(H)R}\}_2]$ [32], $[\mathrm{M}\{\mathrm{N(R)C(Ph)CR_2}\}\{\mathrm{N(R)C(Ph){=}CR_2}\}]$ (M = Sn or Pb) [33] and $[\mathrm{Sn}\{\mathrm{N(R)C(^tBu){=}C(H)C_6H_3Me_2\text{-}2,5}\}_2]$ [32], illustrated in Scheme 13. The unusual compound $[\mathrm{Sn}\{\mu\text{-}\mathrm{N(R){=}C(Ph)CPh}\}]_2$ was obtained from $\mathrm{SnBr_2}$ and $2[\mathrm{K}\{\mathrm{N(R)C(Ph)C(H)Ph}\}]$ in thf [89]. Its X-ray structure is shown in Fig. 16.

In these metal complexes, the size of the substituents on the ligands plays an important role in determining the bonding to the metal centre. Bonding modes demonstrated include (i) an $\eta^1$-enamide, in $[\mathrm{Sn}\{\mathrm{N(R)C(^tBu){=}C(H)C_6H_3Me_2\text{-}2,5}\}_2]$, evident from short Sn–N(1), long N(1)–C(1) and short C(1)–C(2) bond distances, the lone pair of electrons pointing away from the ligands; (ii) an $\eta^3$-1-azaallyl, in *rac*-$[\mathrm{Sn}\{\mathrm{N(R)C(^tBu)C(H)R}\}_2]$, the C(1) atom being bent towards the metal. An alternative description for *rac*-$[\mathrm{Sn}\{\mathrm{N(R)C(^tBu)C(H)R}\}_2]$ is as a bent sandwich compound (cf. $\mathrm{Sn}(\eta^5\text{-}\mathrm{C_5Me_5})_2$ [123,124]); and (iii) $[\mathrm{Sn}\{\mathrm{N(R)C(Ph)CR_2}\}$-

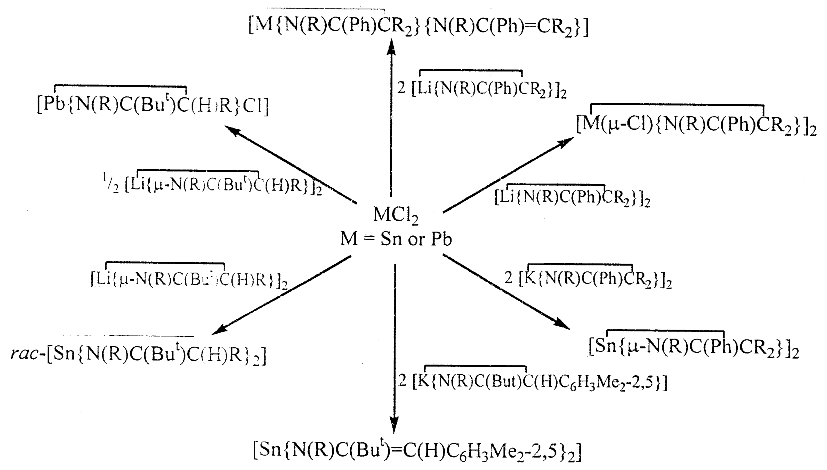

Scheme 13. Synthetic routes to Group 14 metal 1-azaallyls [32,33,89].

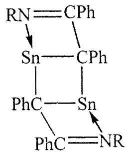

Fig. 16. Schematic representation of the crystalline $[Sn\{\mu\text{-}N(R)=C(Ph)CPh\}]_2$ [89].

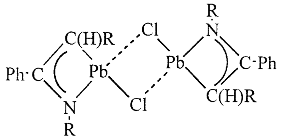

Fig. 17. Schematic representation of the crystalline $[Pb(\mu\text{-}Cl)\{N(R)C(Ph)CR_2\}]_2$ [33].

$\{N(R)C(Ph)=CR_2\}]$, the presence of an additional trimethylsilyl group on the terminal carbon increases the steric demand of the ligand and to accommodate both ligands about the tin, one ligand is $\eta^3$- while the other is $\eta^1$-coordinated, with Sn–N bond distances of 2.288(4) and 2.153(4) Å, respectively. The C(Ph)–$CR_2$ bond lengths are 1.461(6) and 1.365(3) Å, respectively [32].

A variety of heteroleptic metal-1-azaallyls was obtained from treatment of $MCl_2$ (M = Sn or Pb) with one equivalent of the appropriate lithium reagent $[Li\{N(R)C(Ph)CR_2\}(thf)]$ or $[Li\{\mu\text{-}N(R)C({}^tBu)C(H)R\}]_2$, Scheme 13. The solid-state structure of $[Pb(\mu\text{-}Cl)\{N(R)C(Ph)CR_2\}]_2$, Fig. 17, shows a loosely bound centrosymmetric dimer with significantly different Pb–Cl bond lengths; the lead atom is best described as being in a distorted trigonal bipyramidal geometry [33]. The central carbon of the 1-azaallyl ligand is bent towards the metal, as in *rac*-$[Sn\{N(R)C({}^tBu)C(H)R\}_2]$ [32].

Fluxional processes in solution were observed on the NMR spectroscopic time-scale for $[\mathrm{M}(\mu\text{-Cl})\{\mathrm{N(R)C(Ph)CR_2}\}]_2$ and $[\mathrm{M}\{\mathrm{N(R)C(Ph)CR_2}\}\{\mathrm{N(R)C(Ph){=}CR_2}\}]$ (M = Sn or Pb). For the chlorides, splitting of the broad $\mathrm{SiMe_3}$ singlet at low temperatures, similar to the situation in $[\mathrm{Sn}\{\mathrm{CR_2(C_5H_4N\text{-}2)}\}\mathrm{Cl}]$ and $[\mathrm{Sn}\{\mathrm{CR_2(C_5H_4N\text{-}2)}\}\mathrm{NR_2}]$ [125], was observed. Two possible explanations for the non-equivalent $\mathrm{SiMe_3}$ signals are: (i) the scission of M–N bond and subsequent rotation of the ligand about M–C bond, making the two $\mathrm{SiMe_3}$ groups inequivalent; or (ii) a rapid monomer–dimer equilibrium with exchange of bridging chlorides; (ii) was favoured. In the case of $[\mathrm{Sn}\{\mathrm{N(R)C(Ph)CR_2}\}\{\mathrm{N(R)C(Ph){=}CR_2}\}]$, the broad $\mathrm{SiMe_3}$ signals did not split down to − 90°C in toluene-$d_8$, indicative of more rapid exchange between the $\eta^1$- and $\eta^3$-ligands than observed for the related aluminium complex $[\mathrm{Al}\{\mathrm{N(R)C(^tBu)C(H)R}\}\{\mathrm{N(R)C(^tBu){=}C(H)R}\}\mathrm{Me}]$ [119].

### 4.13. Lanthanide metal and thorium 1-azaallyls

Several 1-azaallyl complexes of the lanthanides have been prepared via potassium halide elimination reactions, Scheme 14 [49].

The X-ray molecular structure of $[\mathrm{Sm}\{\mathrm{N(R)C(^tBu)C(H)R}\}_2\mathrm{I(thf)}]$ shows that if the $\eta^3$-ligand $\{\mathrm{N(R)C(^tBu)C(H)R}\}^-$ is taken as occupying a single site, the samarium atom is in a distorted tetrahedral geometry. The two Sm–C distances are approximately equal.

The lanthanide(II) 1-azaallyls $[\mathrm{Sm}\{\mathrm{N(R)C(^tBu)C(H)R}\}_2\mathrm{(thf)}]$ and $[\mathrm{Yb}\{\mathrm{N(R)C(^tBu)C(H)R}\}_2]$ were prepared from the reaction of $\mathrm{SmI_2(thf)_2}$ or $\mathrm{YbI_2}$ with $[\mathrm{K}\{\mathrm{N(R)C(^tBu)C(H)R}\}]_n$ in diethyl ether, (iv) and (v) in Scheme 14. The Yb compound was also obtained by insertion of two equivalents of $^t$BuCN into the

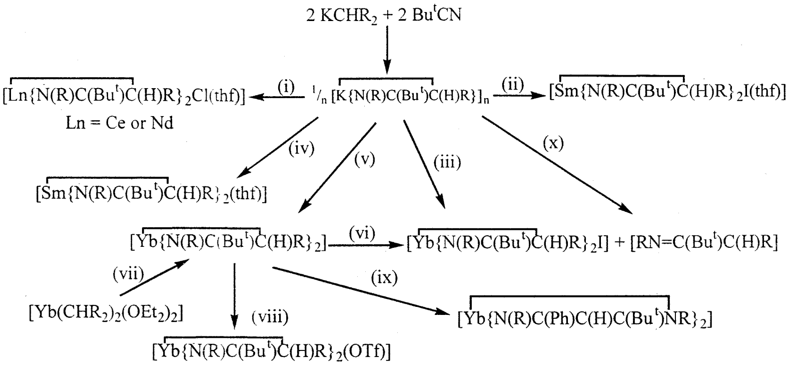

Scheme 14. Synthetic routes to lanthanide 1-azaallyls at ca. 25°C: (i) $\mathrm{LnCl_3}$ (Ln = Ce or Nd), thf, reflux, 12 h; (ii) $\mathrm{SmI_3(thf)_2}$, $\mathrm{Et_2O}$, 36 h; (iii) $\mathrm{YbI_3}$, $\mathrm{Et_2O}$, 36 h; (iv) $\mathrm{SmI_2(thf)_2}$, thf, 18 h; (v) $\mathrm{YbI_2}$, $\mathrm{Et_2O}$, 24 h; (vi) $\frac{1}{2}\mathrm{I_2}$, $\mathrm{Et_2O}$, 12 h; (vii) 2$^t$BuCN, $\mathrm{Et_2O}$, 12 h; (viii) Ag(OTf), toluene, 12 h; (ix) 2PhCN, $\mathrm{Et_2O}$, 12 h; (x) $\mathrm{I_2}$, $\mathrm{Et_2O}$, 8 h (R = $\mathrm{SiMe_3}$, OTf = $\mathrm{OSO_2CF_3}$) [49].

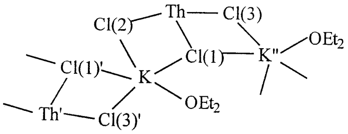

Fig. 18. Schematic representation of the crystalline $[\mathrm{Th\{N(R)C({}^{t}Bu)C(H)R\}(\mu_3\text{-}Cl)(\mu\text{-}Cl)_2K(OEt_2)}]_n$, with the $\{\mathrm{N(R)C({}^{t}Bu)C(H)R}\}^-$ ligands omitted for clarity [127].

Yb–C bonds of $[\mathrm{Yb(CHR_2)_2(OEt_2)_2}]$, (vii) in Scheme 14. The $^1$H-NMR spectrum showed two signals corresponding to each group; this was attributed to the asymmetry of the $\{\mathrm{N(R)C({}^{t}Bu)C(H)R}\}^-$ ligand giving rise to a mixture of *meso* and *rac* diastereoisomers [74]. The compound $[\mathrm{Yb\{N(R)C({}^{t}Bu)C(H)R\}_2}]$ crystallises as the *rac*-diastereoisomer with two independent molecules in each unit cell. Bonding of the 1-azaallyl ligand to the ytterbium atom was essentially identical to that in $[\mathrm{Sm\{N(R)C({}^{t}Bu)C(H)R\}_2I(thf)}]$; however, the distance of the ytterbium atom to the central carbon of the N$\overset{\cdots}{-}$C$\overset{\cdots}{-}$C moiety is longer than that to the terminal carbon [49,74]. The average Yb–N distances of 2.335(14) Å are shorter than those in the benzamidinate $[\mathrm{Yb\{(NR)_2C(Ph)\}_2(thf)_2}]$, 2.473(2) Å [126].

Compound $[\mathrm{Yb\{N(R)C({}^{t}Bu)C(H)R\}_2}]$ underwent: (a) an insertion reaction with two equivalents of benzonitrile affording the unsymmetrical β-diketiminate $[\mathrm{Yb\{N(R)C(Ph)C(H)C({}^{t}Bu)NR\}_2}]$, (ix) in Scheme 14; (b) oxidation with Ag(OTf), affording $[\mathrm{Yb\{N(R)C({}^{t}Bu)C(H)R\}_2(OTf)}]$, (viii) in Scheme 14; or (c) reaction with one equivalent of diiodine to give $[\mathrm{Yb\{N(R)C({}^{t}Bu)C(H)R\}_2I}]$ as the major product (determined by elemental analyses and mass spectrometry) and as a minor product $[\mathrm{RN{=}C({}^{t}Bu)C(H)R}]_2$, identified by X-ray crystallography, probably formed by a ligand radical coupling reaction, (vi) in Scheme 14. Treatment of $[\mathrm{K\{N(R)C({}^{t}Bu)C(H)R\}}]_n$ with one equivalent of diiodine also gave the same ligand-coupled product, (x) in Scheme 14.

$\eta^3$-1-Azaallyl coordination was found in a heterobimetallic thorium/potassium compound. Treatment of $\mathrm{ThCl_4}$ with two equivalents of $[\mathrm{K\{N(R)C({}^{t}Bu)C(H)R\}}]_n$ in diethyl ether afforded the polymeric thorium(IV)–potassium chloride complex of Eq. (16) [127].

$$2\mathrm{ThCl_4} + \frac{1}{n}[\mathrm{K\{N(R)C({}^{t}Bu)C(H)R\}}]_n \xrightarrow[\text{48 h, 25°C}]{\mathrm{Et_2O}} \frac{1}{n}[\mathrm{Th\{N(R)C({}^{t}Bu)C(H)R\}(\mu_3\text{-}Cl)(\mu\text{-}Cl)_2K(OEt_2)}]_n \qquad (16)$$

The X-ray molecular structure is illustrated in Fig. 18, showing a *rac*-diastereoisomeric unit of the polymer, with the $^t$Bu groups of the $\{\mathrm{N(R)C({}^{t}Bu)C(H)R}\}^-$ ligands pointing away from each other [127]. The thorium atom is coordinated by three chlorides in a pseudo-T-shaped geometry. The two 1-azaallyl ligands, which 'sandwich' the $\mathrm{ThCl_3}$ unit, are $\eta^3$-bonded to the thorium, with the thorium distance to the central carbon being slightly shorter than that to the terminal carbon. Each potassium atom has four $Cl^-$ nearest neighbours from two adjacent $ThCl_2$ moieties. Attempts to reduce $[\mathrm{Th}\{\mathrm{N(R)C(^tBu)C(H)R}\}(\mu_3\text{-Cl})(\mu\text{-Cl})_2\mathrm{K(OEt_2)}]_n$ with K–Na alloy in thf were unsuccessful.

## 5. Metal complexes based on the $[CR_2(C_5H_4N\text{-}2)]^-$ and related ligands

### 5.1. Introduction

This section discusses the metal complexes involving the alkyl-functionalised pyridyl ligand $[CR_2(C_5H_4N\text{-}2)]^-$ and its derivatives.

### 5.2. Lithium and notes on Na, K and Mg 2-pyridylalkyls

Metallation of 2-picoline using various lithium reagents was reported as early as 1974 [128]. The first structurally characterised examples of lithium derivatives were synthesised by lithiation of $[C(H)R_2(C_5H_4N\text{-}2)]$, Scheme 15 [51]. In non-polar solvents the 1:1 metallated: non-metallated adduct, $[\mathrm{Li}\{CR_2(C_5H_4N\text{-}2)\}\text{-}\{NC_5H_4C(H)R_2\text{-}2\}]$ was obtained, while the presence of a catalytic amount of diethyl ether in the reaction mixture afforded $[\mathrm{Li}\{\mu\text{-}CR_2(C_5H_4N\text{-}2)\}]_2$, free of $Et_2O$,

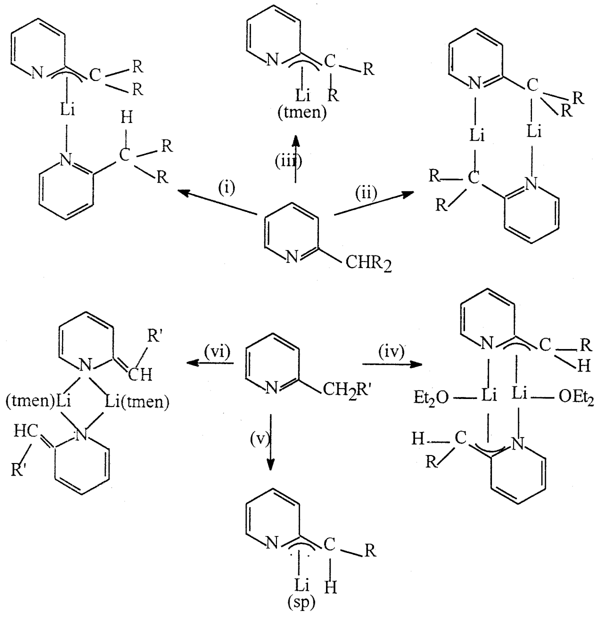

Scheme 15. Synthetic routes to lithium 2-pyridylmethyls: (i) $\mathrm{Li^nBu}$, hexane, ca. 0°C; (ii) and (iv) $\mathrm{Li^nBu}$, hexane–$OEt_2$, ca. 20°C; (iii) and (vi) $[\mathrm{Li^nBu(tmen)}]$, hexane, ca. 0°C; (v) $[\mathrm{Li^nBu(sp)}]$, hexane–$OEt_2$, ca. 0°C ($R = SiMe_3$, $R' = R$, $SiMe_2^t$Bu or Ph, sp = (−)-sparteine) [51–53].

or the thf recrystallisation solvent. The monomer [Li{CR$_2$(C$_5$H$_4$N-2)}(tmen)] exhibited no evidence of dimerisation, presumably due to the metal centre being coordinatively saturated. With the use of the slightly less-sterically hindered ligand, [C(H)R(C$_5$H$_4$N-2)]$^-$, the presence of polar solvents was required to fully metallate the ligand. Monomeric and dimeric structures were found in [Li{C(H)R(C$_5$H$_4$N-2)}(−)-sparteine] and [Li{$\mu$-C(H)R(C$_5$H$_4$N-2)}(tmen)]$_2$, respectively [51–53].

The nature of the lithium–ligand interactions, electron density distribution within the ligand and degree of aggregation was dependent upon: (a) the steric and electronic nature of the group at the *ipso*-carbon; (b) the degree of substitution at the *ipso*-carbon; and (c) the nature and presence of ancillary bases, e.g. tmen [53]. Key bonding features of the [CR$_2$(C$_5$H$_4$N-2)]$^-$ and [C(H)R(C$_5$H$_4$N-2)]$^-$ ligands in the lithium complexes were that they could act as: (a) $\eta^1$-alkyls (with dative pyridyl links to another lithium), exemplified in the dimeric [Li{$\mu$-CR$_2$(C$_5$H$_4$N-2)}]$_2$, which forms an eight-membered step-like ring; (b) $\eta^3$-azaallyls (in the majority of the compounds); (c) $\eta^3$-azaallyl — $\sigma$-donors, in [Li{C(H)R(C$_5$H$_4$N-2)}-{NC$_5$H$_4$C(H)R$_2$-2}]$_2$ or [Li{$\mu$-C(H)R(C$_5$H$_4$N-2)}(OEt$_2$)]$_2$, in which the *ipso*-carbons were coplanar with the aromatic rings and the Et$_2$O molecules were situated above and below the plane; and (d) a bridging enamido group in [Li{$\mu$-C(H)R(C$_5$H$_4$N-2)}(tmen)]$_2$ (R = SiMe$_3$, Ph or SiMe$_2^t$Bu) [51–53,129], with the negative charge of the ligand localised at the nitrogen atom. Supporting evidence was provided by the sp$^2$ geometry about the $\alpha$-carbon, an exocyclic double bond, and localised double and single bonds in the pyridyl ring. NMR spectroscopic solution data on [Li{$\mu$-C(H)R(C$_5$H$_4$N)-2}(tmen)]$_2$ (R = SiMe$_3$) indicated the presence of the $\eta^3$-azaallyl fragment [51–53].

A dilithium bis(1-azaallyl) was generated by metallation of [CH$_2$R{C$_5$H$_3$(C(H)R-6)-2}] in which the two lithium atoms occupied $\eta^3$-azaallyl positions on opposite sides of the pyridyl ring to minimise dipolar repulsion, Eq. (17) [130].

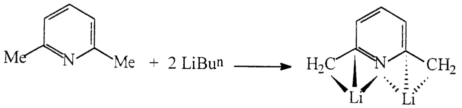

(17)

The crystalline sodium and potassium analogues [Na{NC$_5$H$_4$(CPh$_2$)-2}(thf)$_3$] and [K{NC$_5$H$_4$(CPh$_2$)-2}(pmdeta)] showed the alkali metals to be bound directly to the nitrogen suggesting the negative charge of the ligand was almost totally localised at the nitrogen [131].

The above lithium complexes proved to be useful ligand transfer reagents in synthesising thermally stable, low valent, mononuclear complexes of Fe(II), Co(II) or Ni(II) [109,110,132,133]. Each of the complexes [Li{$\mu$-CR$_2$(C$_5$H$_4$N-2)}]$_2$ and [Li{$\mu$-C(H)R(C$_5$H$_4$N-2)}(OEt$_2$)]$_2$ underwent an insertion reaction with the $\alpha$-H-free nitrile R′CN (R′ = $^t$Bu or Ph), exemplified in Eq. (18) [134].

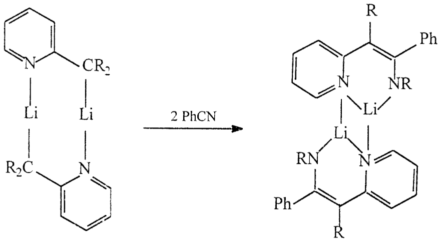

(18)

Unless, otherwise stated, the following complexes were synthesised by a lithium halide elimination reaction between the metal halide and the appropriate lithium reagent bearing SiMe$_3$ (≡R) groups. Thermally stable [Mg{CR$_2$(C$_5$H$_4$N-2)}]$_2$ was synthesised from Mg$^s$Bu$^n$Bu and two equivalents of [C(H)R$_2$(C$_5$H$_4$N-2)] [80]. The X-ray molecular structure shows the complex to be a monomer with the magnesium atom situated in a distorted tetrahedral environment, having mean bond angles of N–Mg–N 117.4(9)° and C–Mg–C 157.0(7)°. The ligand coordinates to the magnesium atom in a *C*,*N*-chelating fashion with no interaction between the magnesium atom and the central carbon of the 1-azaallyl moiety. The alkali metal enamides [Na(r)(pmdeta)], [K(r)(pmdeta)]$_2$, [Na(r)(tmen)]$_2$, [Li(r′)(pmdeta)] and [Mg(r)$_2$(HMPA)$_2$] were prepared and crystallographically characterised [r = C(H)R(C$_5$H$_4$N-2), r′ = C(H)R{C$_5$H$_3$NMe-6}-2] [174].

### 5.3. Group 4 metal 2-pyridylalkyls

Group 4 metal complexes of [CR$_2$(C$_5$H$_4$N-2)]$^-$ and its derivatives contain the ligand bound in a *C*,*N*-chelating fashion, exemplified in [Hf{CH$_2$(C$_5$H$_3$NMe-6)-2}$_2$(OC$_6$H$_3^t$Bu$_2$-2,6)$_2$] [135] and [Zr{C(H)R(C$_5$H$_4$N-2)}Cp$_2$Cl] [136]. Interestingly, in the 6-methyl substituted complex [Zr{CH$_2$(C$_5$H$_3$NMe-6)-2}$_2$Cp$_2$], one ligand is *C*,*N*-bonded while the other is coordinated only through the *C*-atom to give an 18-electron complex [137]. Detailed variable-temperature NMR spectral studies were carried out to assess the structure in solution; it was concluded that the *C*,*N*-chelated structure was maintained in all cases.

The possibility of $\eta^3$-coordination was proposed for [Zr{C(H)R(C$_5$H$_4$N-2)}Cp$_2$] (from reaction of [Zr{C(H)R(C$_5$H$_4$N-2)}Cp$_2$Cl] with Na/K in thf), for which a solid state structure was not available [137]. This was based upon the EPR spectrum exhibiting no nitrogen or hydrogen hyperfine coupling (usually associated with polyhapto ligands, such as $\eta^5$-C$_5$H$_5$); chelate ring formation would have been unfavourable. However, for the related d$^2$ species [Mo{C(H)Me(C$_5$H$_4$N-2)}$_2$Cp$_2$], the chelate structure was assigned [138].

The insertion chemistry of Group 4 metal three-membered metallacycles has been well investigated; less has been reported for the related four-membered metallacycles. The zirconium and hafnium chelates [M{CH$_2$(C$_5$H$_3$NMe-6)-2}$_2$Cp$_2$] (M = Zr or Hf, Cp = $\eta^5$-C$_5$H$_5$) underwent facile insertion reactions with some polar and non-polar substrates [87], exemplified by reaction with 2,6-dimethylphenyl isonitrile,

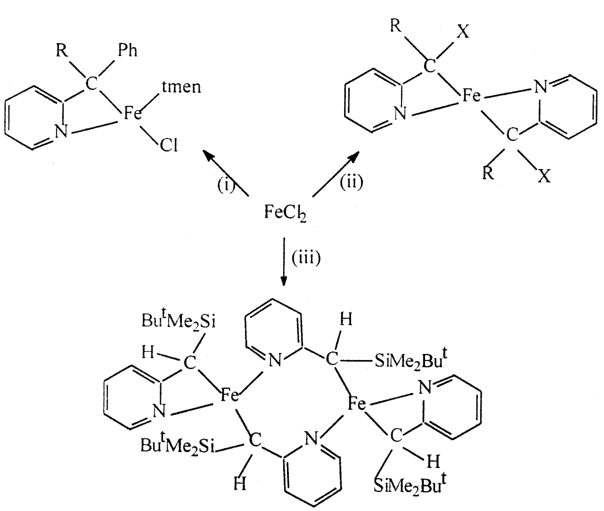

Scheme 16. Synthetic routes to iron(II) complexes: (i) $\frac{1}{2}[Li\{\mu\text{-}C(R)Ph(C_5H_4N\text{-}2)\}(tmen)]_2$, $Et_2O$; (ii) $[Li\{\mu\text{-}CR_2(C_5H_4N\text{-}2)\}]_2$ or $[Li\{\mu\text{-}C(R)Ph(C_5H_4N\text{-}2)\}(tmen)]_2$, $Et_2O$; (iii) $[Li\{C(SiMe^t_2Bu)H(C_5H_4N\text{-}2)\}(tmen)]_2$, $Et_2O$ [132,141].

affording an $\eta^2$-iminoacyl, which was readily converted at ambient temperatures to the mono- and bis(enamides) $[M\{N(Ar)C(H){=}C(H)(C_5H_3NMe\text{-}6)\text{-}2\}\{CH_2\text{-}(C_5H_3Me\text{-}6)\text{-}2\}\}Cp_2]$ and $[M\{N(Ar)C(H){=}C(H)(C_5H_3NMe\text{-}6)\text{-}2\}_2Cp_2]$ ($M = Zr$ or $Hf$, $Ar = C_6H_3Me_2\text{-}2,6$, $Cp = \eta^5\text{-}C_5H_5$), via a 1,2-hydrogen shift [135,139]. The cationic $[Zr\{CH_2(C_5H_3NMe\text{-}6)\text{-}2\}_2Cp_2]^+$ underwent insertion reactions with olefins to yield a variety of six-membered metallacycles; treatment with acetonitrile gave the β-diketiminate, $[Zr\{(C_5H_3NMe\text{-}6)C(H)C(Me)N(H)\}Cp_2]^+$, Eq. (19) [72]: the reaction between $[Zr\{N(R)C(^tBu)C(H)R\}Cl_3]$, and PhCN afforded the crystalline β-deketiminate $[Zr\{N(R)C(^tBu)C(H)C(Ph)N(R)\}Cl_3]$ [140].

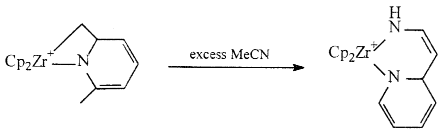 (19)

## 5.4. Groups 8–11 metal 2-pyridylalkyls

Use of $[CRR'(C_5H_4N\text{-}2)]^-$ ($R' = R$ or $Ph$) afforded thermally stable, low valent, monomeric Fe(II) complexes, Scheme 16 ($X = R$ or $Ph$) [132,141]. Careful control of stoichiometry yielded $[Fe\{C(R)Ph(C_5H_4N\text{-}2)\}Cl(tmen)]$ [141].

As with the Group 4 metal complexes, *C*,*N*-chelate formation was observed in crystalline $[Fe\{CR_2(C_5H_4N\text{-}2)\}_2]$ [132] and $[Fe\{CR_2(C_5H_4N\text{-}2)\}Cl(tmen)]$ [141].

Both *C*,*N*-bridging and *C*,*N*-terminal chelate bonding modes were observed in the dimeric complex $[Fe\{C(H)(SiMe^t_2Bu)(C_5H_4N\text{-}2)\}_2]_2$, containing an eight-membered $Fe_2(CCN)_2$ core, adopting a stair-like conformation [141]. The Fe–C(terminal) and Fe–C(bridging) bond lengths lie between 2.160(2) and 2.163(2) Å, while the Fe–C bond lengths in $[Fe\{CR_2(C_5H_4N\text{-}2)\}_2]$ are in the range of 2.129(7)–2.154(8) Å; the shorter bonds may be attributed to stabilisation of the negative charge on the ligand by the two trimethylsilyl groups [132,141].

Protolysis of $[Fe\{CR_2(C_5H_4N\text{-}2)\}_2]$ by $Ar^{Me}OH$ or ArSH ($Ar^{Me} = C_6H_2{}^tBu_2$-2,6-Me-4, $Ar = C_6H_2{}^tBu_3$-2,4,6) afforded the 12-electron monomeric, three-coordinate iron(II) complex, $[Fe(OAr^{Me})_2\{NC_5H_4C(H)R_2\text{-}2\}]$ or $[Fe(SAr)_2\{NC_5H_4C(H)R_2\text{-}2\}]$, respectively [132,141]. The presence of the chelating neutral $[C(H)R_2(C_5H_4N\text{-}2)]$ in these complexes was believed to be required in order to prevent oligomerisation.

The cobalt(II) complexes $[Co\{CR_2(C_5H_4N\text{-}2)\}_2]$ and $[Co\{C(Ph)R(C_5H_4N\text{-}2)\}_2]$, are mononuclear, four-coordinate complexes with the cobalt being in a planar environment, each ligand bonded as a *C*,*N*-chelate [109,110]. The fifth and sixth octahedral sites are occupied by the $SiMe_3$ groups, one from each ligand, effectively blocking the cobalt atom from further attack and accounting for the stability of the complexes. The resulting compound $[Co\{C(H)(SiMe_2{}^tBu)(C_5H_4N\text{-}2)\}_2]_2$ is a dimer, the cobalt being in a quasi-tetrahedral environment and isostructural to the Fe(II) analogue [132,141]. The dimeric structure is probably due to the less bulky nature of the ligand. Unlike the Fe(II) analogues, these cobalt 1-azaallyls were inert towards bulky alcohols or thiols, attributed to the effective shielding of the metal centre by the ligands.

Early attempts to synthesise the nickel(II) analogues from $NiCl_2$ and the appropriate lithium reagent were ineffective, affording alkyl-coupled products, believed to have arisen from intramolecular reductive coupling within the initially formed thermally unstable nickel alkyl compounds [142]. Addition of an excess of triethylphosphine (greater than four equivalents per mole of Ni) led to the isolation of $[Ni\{CR_2(C_5H_4N\text{-}2)\}_2]$, stable towards, air, heat, light or hydrolysis. No structural characterisation was obtained, but the diamagnetic nature of the compound suggested a planar geometry, with presumably the $SiMe_3$ groups situated above and below the nickel preventing attack by a nucleophile [143].

The diamagnetic, half-sandwich compounds $[Ni\{CR_2(C_5H_4N\text{-}2)\}Cp]$, $[Ni\{C(H)R(C_5H_4N\text{-}2)\}Cp]$ and $[Ni\{CR_2(C_5H_4N\text{-}2)\}(\eta^5\text{-}C_5H_3R_2\text{-}1,3)]$ were also prepared [142]. The X-ray molecular structure of $[Ni\{N(R)C({}^tBu)C(H)C_6H_4Me\text{-}4\}_2]$ shows the ligand coordinated to the nickel in a *C*,*N*-terminal chelating fashion. The five Ni–C(ring) distances are unequal. A variable temperature $^1H$-NMR spectral study of $[Co\{C(H)(SiMe_2{}^tBu)(C_5H_4N\text{-}2)\}_2]_2$ indicated that free rotation of the cyclopentadienyl about Ni was not hindered by the ligand. In the $^1H$-NMR spectrum of $[Ni\{C(H)R(C_5H_4N\text{-}2)\}Cp]$, the surprisingly large shift to higher frequency, for C*H* $\delta$ 4.39 (compared to $\delta$ 2.31 in the free ligand) suggested $\eta^3$-1-azaallyl bonding [142].

Group 11 metal complexes $[M\{CR_2(C_5H_4N\text{-}2)\}]_2$ (M = Cu, Ag or Au) [51,118,144] and $[M\{CR_2(C_5H_3NMe\text{-}6)\text{-}2\}]_2$ (M = Cu, Ag or Au) showed remarkable thermal stability; the presence of a methyl group on the pyridyl ring in

$[\mathrm{M\{CR_2(C_5H_3NMe\text{-}6)\text{-}2\}}]_2$ (M = Cu, Ag or Au) significantly enhanced such stability [48,145]. Their core is structurally similar to $[\mathrm{Cu\{\mu\text{-}N(R)C(^{t}Bu)C(H)R\}}]_2$ [50] and a related Au compound [112]. Use of the less-sterically hindered ligand $[\mathrm{C(H)R(C_5H_4N\text{-}2)}]^-$ afforded the tetramer $[\mathrm{Cu\{C(H)R(C_5H_4N\text{-}2)\}}]_4$ in which the ligand bridges successive metal atoms to form a macrocyclic structure with $\mathrm{SiMe_3}$ groups alternating above and below the plane [118].

### 5.5. Group 12 metal 2-pyridylalkyls

The first reported examples of Group 12 metal 1-azaallyl complexes were $[\mathrm{M\{CR_2(C_5H_4N\text{-}2)\}}]_2$ (M = Zn, Cd or Hg) [48,80], prepared from the lithium reagent and the appropriate metal chloride. The crystalline Zn and Cd complexes are isostructural with the magnesium analogue $[\mathrm{Mg\{CR_2(C_5H_4N\text{-}2)\}}]_2$, each metal being the centre of a distorted tetrahedron. Crystalline $[\mathrm{Hg\{CR_2(C_5H_4N\text{-}2)\}}]_2$, however, shows a coordination number of two about the metal [80]. Thus, the dative M–N interaction weakens progressively down the group, indicated by the increasing M–N bond lengths and opening of the C–M–C angles: Zn 2.29(4) Å, 164.0(0)°; Cd, 2.49 Å, 174.0(3)°; Hg, 2.78 Å, 179.5(3)°; this reflects the increasingly soft character for the heavier $\mathrm{M}^{2+}$ ions [80]. A similar structural trend was also observed for the methyl-substituted compounds $[\mathrm{M\{CR_2(C_5H_3NMe\text{-}6)\text{-}2\}}]_2$ (M = Zn, Cd or Hg) [48,146,147], the most noticeable difference being the decrease in N–M–N bond angle to minimise steric interaction between the trimethylsilyl group and methyl group on the pyridyl ring.

The crystalline cadmium complex $[\mathrm{Cd\{C(H)R(C_5H_3NMe\text{-}6)\text{-}2\}_2(tmen)}]$ is the *rac*-isomer, with a longer Cd–N bond, 2.605(5) Å than in the bis(silylated) analogue [48,145].

The heteroleptic complexes of the Group 12 metals, $[\mathrm{Hg\{CR_2(C_5H_4N\text{-}2)\}Cl}]_2$ and $[\mathrm{M\{C(H)R(C_5H_3NMe\text{-}6)\text{-}2\}Cl}]_2$ (M = Zn or Hg) were prepared using equimolar portions of the lithium reagent and the Group 12 metal chloride, or via a redistribution reaction of the homoleptic compound with one equivalent of the metal chloride [48,145,148]. Crystalline $[\mathrm{Hg\{CR_2(C_5H_4N\text{-}2)\}Cl}]_2$ shows near linear C–Hg–Cl coordination and a weak Hg···Cl interaction of 3.588(4) Å across the centre of symmetry [48,146,147].

### 5.6. Groups 13 and 14 metal 2-pyridylalkyls

For Group 13 metals, three types of M(III) compounds have been synthesised, Scheme 17: (a) the five-coordinate species $[\mathrm{M\{CR_2(C_5H_4N\text{-}2)\}_2Cl}]$ and $[\mathrm{M\{CR_2(C_5H_3NMe\text{-}6)\text{-}2\}_2Cl}]$ (M = Al, Ga or In) [48,145,149]; (b) the four-coordinate $[\mathrm{M\{CR_2(C_5H_3NMe\text{-}6)\text{-}2\}Cl_2}]$ (M = Al or In) (the indium analogue was also obtained from a conproportionation reaction of $[\mathrm{In\{CR_2(C_5H_3NMe\text{-}6)\text{-}2\}_2Cl}]$ and $\mathrm{InCl_3}$) [48,145]; and (c) the four-coordinate cation in the salt $[\mathrm{M\{CR_2(C_5H_4N\text{-}}$

$2)\}]_2[MCl_4]$ (M = Al or Ga) from $[M\{CR_2(C_5H_4N\text{-}2)\}_2Cl]$ with $MCl_3$, which formed ligand clathrates in benzene with complex–solvent composition of 1:12 and 1:6 for Al and Ga, respectively [150].

Several of the compounds were authenticated structurally; the ligands behaved as chelates forming strained four-membered ring systems. The X-ray molecular structure of $[Ga\{CR_2(C_5H_4N\text{-}2)\}_2Cl]$, shows the gallium in a distorted trigonal bipyramidal environment with the N-atoms situated in the axial positions and the complex devoid of any multicentre bonding [150]. The ambient temperature $^1H$-NMR spectrum of $[Al\{CR_2(C_5H_4N\text{-}2)\}_2Cl]$ showed non-equivalent $SiMe_3$ groups, consistent with the rigid chelate ring structure being retained in solution. However, the indium and gallium analogues were fluxional in solution. The presence of a methyl group on the pyridyl rings had little effect upon the arrangement of the ligands about the metal centre.

In $[Al\{CR_2(C_5H_4N\text{-}2)\}_2][AlCl_4]$, the metal atom in the cation is situated on a twofold crystallographic axis; the overall environment about the metal in $[Al\{CR_2(C_5H_4N\text{-}2)\}_2]^+$ is distorted tetrahedral [150].

Reduction of $[M\{CR_2(C_5H_3NMe\text{-}6)\text{-}2\}_2Cl]$ (M = Al or Ga) with Na–K alloy in thf afforded highly coloured solutions containing the paramagnetic $[M\{CR_2(C_5H_4N\text{-}2)\}_2]$, which combined to form the tail-to-tail coupled product, (vii) in Scheme 17.

Silicon compounds of the formula $[Si\{CR'_2(C_5H_4N\text{-}2)\}Cl_2X]$ (R′ = R or Ph, X = Me or H) and $[Si\{C(R)R'(C_5H_3NMe\text{-}6)\text{-}2\}Cl_2X]$ (R′ = R or H, X = Me or H)

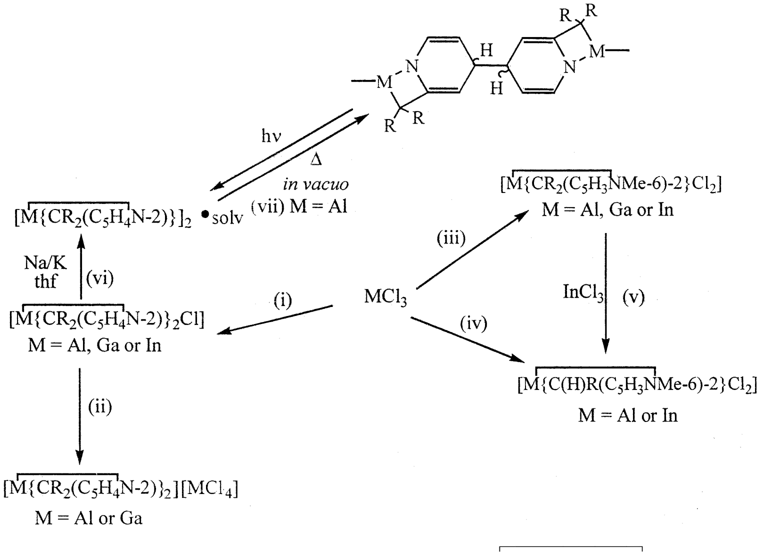

Scheme 17. Synthetic routes to Group 13 metal complexes: (i) $[Li\{\mu\text{-}CR_2(C_5H_4N\text{-}2)\}]_2$, $Et_2O$; (ii) $MCl_3$, $C_6H_6$; (iii) $2[Li\{CR_2(C_5H_3NMe\text{-}6)\text{-}2\}]$; (iv) $[Li\{CR_2(C_5H_3NMe\text{-}6)\text{-}2\}]$; (v) $InCl_3$; (vi) Na–K, thf; (vii) heat [48,149,150].

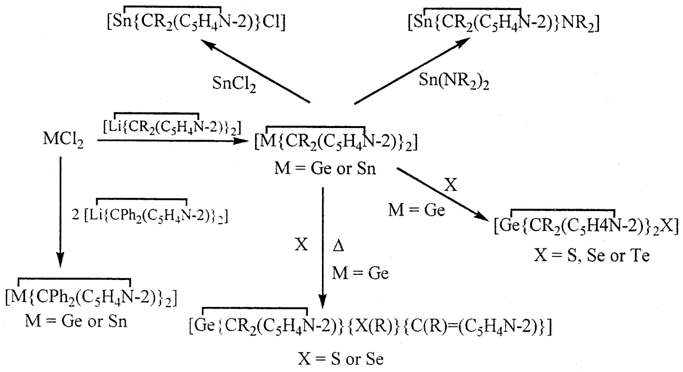

Scheme 18. Synthetic routes to germanium and tin complexes and selected reactions [125,152–154].

were synthesised from the appropriate chlorosilane and lithium reagent [48,146,147,151]. The X-ray molecular structure of the five-coordinate species [Si{$CR_2(C_5H_4N$-2)}(H)$Cl_2$], shows the silicon in a trigonal bipyramidal environment with a strong intramolecular interaction to the pyridyl N (Si–N 2.066(9) Å) to give a strained four-membered ring [151]. The two $SiMe_3$ groups are *cis* and *trans* with respect to H and Cl. The room temperature $^{29}Si\{^1H\}$-NMR spectrum showed two distinct $SiMe_3$ resonances consistent with the solid-state structure persisting in solution. The $^{29}Si\{^1H\}$-NMR spectrum of [Si{$CR_2(C_5H_4N$-2)}(Me)$Cl_2$] was temperature-dependent, with one $SiMe_3$ signal observed at room temperature and two at − 70°C, indicating the presence of an equilibrium between the four- and five-coordinate structures in solution. The addition of a methyl group on the pyridyl ring in [Si{$CR_2(C_5H_3NMe$-6)-2}$_2$(H)$Cl_2$] did not appear significantly to affect the solid state structure. The phenyl derivatives [Si{$CPh_2(C_5H_4N$-2)}$Cl_2X$] (X = Me or H) were devoid of such Si–N interactions; thus, the Si–N interaction in the trimethylsilyl analogues [Si{$CR_2(C_5H_3NMe$-6)-2}$_2$(H)$Cl_2$] was suggested to be due to minimisation of steric interaction between the $SiMe_3$ groups and the C(2) proton on the pyridyl ring, thereby directing the N-centre towards the silicon.

Preparation of bivalent germanium and tin compounds is illustrated in Scheme 18, with some selected reactions [125,152–154].

As usual, the ligand behaved as a *C*,*N*-chelate, M being in a distorted tetrahedral environment (M = Ge or Sn) [154]. The complexes [M{$CR_2(C_5H_4N$-2)}$_2$] (M = Ge or Sn, R = $SiMe_3$), surprisingly, are isostructural with [Ga{$CR_2(C_5H_4N$-2)}$_2$Cl], with the quasi-square-pyramidal Group 14 metal atoms having a stereochemically active lone pair of electrons [125,152–154].

Two types of reactions were investigated: (i) conproportionation of [Sn{$CR_2(C_5H_4N$-2)}$_2$] with $SnCl_2$ or $Sn(NR_2)_2$ afforded [Sn{$CR_2(C_5H_4N$-2)}Cl] or [Sn{$CR_2(C_5H_4N$-2)}$NR_2$], respectively [125,152]; or (ii) oxidation of [Ge{$CR_2(C_5H_4N$-2)}$_2$] with the chalcogen S, Se or Te yielding stable germanethiones, -selenones or -tellurones, $[Ge\{CR_2(C_5H_4N\text{-}2)\}_2X]$ ($X = S$, Se or Te), exceedingly rare examples of $M = X$ ($X =$ chalcogen) compounds [153]. In the case of (ii), if the reaction was carried out at elevated temperatures, one trimethylsilyl group underwent a 1,3-shift to the chalcogen affording the thermodynamical isomer $[Ge\{CR_2(C_5H_4N\text{-}2)\}\{X(R)\}\{C(R)=(C_5H_4N\text{-}2)\}]$ ($X = S$ or Se). The thione, selenone and tellurone structures are related to $[Ge\{CR_2(C_5H_4N)\text{-}2\}_2]$, with the chalcogen atom occupying the site of the stereochemically pair of electrons in the latter. The migration of the $SiMe_3$ group in $[Ge\{CR_2(C_5H_4N\text{-}2)\}\{X(R)\}\{C(R)=(C_5H_4N\text{-}2)\}]$ results in one ligand acting as a *C*,*N*-chelate, while the other has iminoalkyl coordination.

Fluxional processes in solution were observed on the NMR spectral time-scale for $[Sn\{CR_2(C_5H_4N\text{-}2)\}Cl]$ and $[Sn\{CR_2(C_5H_4N\text{-}2)\}NR_2]$, with splitting of $SiMe_3$ (in $CR_2$) signals at low temperatures [125,152]. This was attributed to cleavage of the Sn–N bond of the $[CR_2C_5H_4N\text{-}2)]^-$ ligand and subsequent rotation about the Sn–C bond.

A mixed tin–osmium cluster $[Os_3(\mu\text{-}H)Sn\{CR_2(C_5H_4N\text{-}2)\}(CO)_{10}]$ was prepared from $[Os_3(H)_2(CO)_{10}]$ and $[Sn\{CR_2(C_5H_4N\text{-}2)\}_2]$ [155]. The proposed reaction pathway was by attack from one of the H atoms cleaving a ligand group from the tin compound to give a transient $Sn\{CR_2(C_5H_4N\text{-}2)\}^-$ which then replaced the other bridging H atom to give the product.

### *5.7. Group 15 metal 2-pyridylalkyls*

Complexes of the formula $[M\{CR_2(C_5H_4N\text{-}2)Cl_2\}]$ ($M = P$, As, Sb or Bi, $R = SiMe_3$) were obtained from equimolar portions of the lithium reagent and the appropriate $MCl_3$; the phosphorus (m.p. (dec.) $> -78$°C) and arsenic (m.p. (dec.) $> 20$°C) compounds were thermally unstable with respect to $SiMe_3Cl$ elimination [156]. The bismuth complex was photosensitive and afforded a bismuth mirror in thf. The P, As and Sb analogues having a 6-methyl substituent were characterised by X-ray; the P compound showed the shortest $N\cdots P$ dative bond of 2.238(1) Å.

Crystalline $[Sb\{CR_2(C_5H_3NMe\text{-}6)\text{-}2\}Cl_2]$ is monomeric. The coordination environment about the metal atom is affected by a stereochemically active lone pair of electrons and is best described as distorted trigonal bipyramidal with Sb, Cl(1), C(6) atoms and the lone pair of electrons approximating to an equatorial plane. The ligand chelates to the metal atom and the long Sb–N bond of 2.371(7) Å was attributed to the steric strain in the four-membered chelate ring [48]. Similar structural features are evident in the bismuth analogue.

Use of the related $[CPh_2(C_5H_4N\text{-}2)]^-$ ligand, devoid of trimethylsilyl groups, thereby removing the opportunity for $SiMe_3Cl$ elimination, afforded a phosphorus derivative, stable at ambient temperatures [158]. The potential for novel chemistry has been demonstrated by the reaction of $[P\{CR_2(C_5H_4N\text{-}2)Cl_2\}]$ with M(COT) ($M = Ca$, Sr or Ba; COT = cyclooctatriene) affording a stable phosphacyclopropane, Eq. (20) [134]. Reduction of $[\overline{P\{CR_2(C_5H_3N}Me\text{-}6)\text{-}2\}Cl_2]$ with $Li[AlH_4]$ yielded an *N*-functionalised disecondary diphosphine, Eq. (21) [159].

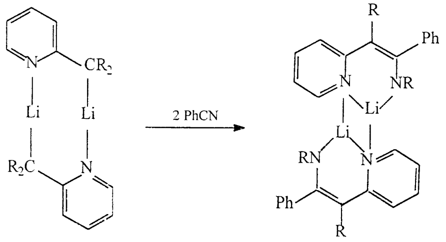

(20)

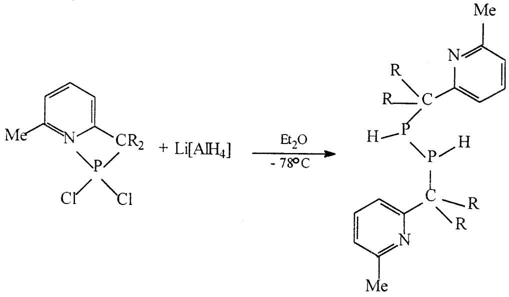

(21)

Comparison of the above compounds with the mono-silylated, methyl-substituted $[\overline{Sb\{C(H)R(C_5H_3N}Me\text{-}6)\text{-}2\}(\mu\text{-}Cl)Cl]_2$, which is dimeric with chloride bridges and has a stereochemically active lone pair of electrons demonstrates the need for bulky ligands to restrict the formation of oligomeric or polymeric species [146,147,157].

Attempts to form the monochloro complexes $[\overline{M\{CR_2(C_5H_4N}\text{-}2)_2Cl\}]_2$ (M = As, Sb or Bi) from two equivalents of the lithium reagent and one of the appropriate $MCl_3$ were unsuccessful in the cases of As and Sb, because of rapid loss of $SiMe_3Cl$ and formation of an intractable red oil [156]. Addition of $AlMe_3$ to the red Sb oil afforded the X-ray-characterised compound

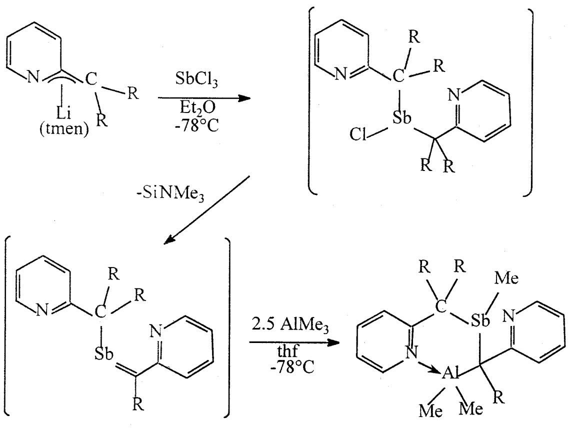

Scheme 19. Proposed pathway for formation of a mixed Al–Sb complex [160].

$[Al\{CR_2(C_5H_4N\text{-}2)Sb(Me)CR_2(C_5H_4N\text{-}2)\}Me_2]$, Scheme 19 [160]. The proposed intermediate was a stibene.

The reaction of $[Bi\{CR_2(C_5H_4N\text{-}2)Cl_2\}]$ with another equivalent of the lithium reagent afforded a red solid (m.p. (dec.) $>0°C$), which was identified as the insertion product $[Bi\{CR_2(C_5H_4N\text{-}2)\}\{CH_2C(H){=}C(R)(C_5H_4N\text{-}2)\}]$, Eq. (22), from X-ray crystallography (bismuth atom in a distorted trigonal bipyramidal environment) and mass spectrometry [156].

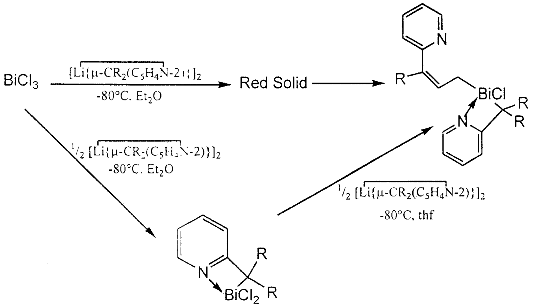

(22)

Thermal $SiClMe_3$ elimination from $[Sb\{CR_2(C_5H_4N\text{-}2)Cl_2\}]$ afforded the chloro-bridged polymeric *C*-centred geminal distibene, $[(\{SbCR_2(C_5H_4N\text{-}2)\}_2(\mu\text{-}Cl))(\mu\text{-}Cl)]_n$ [161]. The structure remains one of the few authenticated examples of a distibene [162–164]; the polymer contains a repeating $C_2Sb_2$ unit internally bridged by one chloride with the other chloride linking the units. Each Sb(III) centre is formally five-coordinate, bound to the two geminal carbons, a pyridyl *N*, a bridging and a linking chloride; the stereochemically active lone pair of electrons occupies the *trans* position to one of the geminal *C*-centres [161].

Attempts to form a trialkylated bismuth complex resulted in the head-to-tail coupled product, characterised by X-ray crystallography, presumed to have arisen from reductive coupling and/or nucleophilic attack of a coordinated ligand followed by a rearrangement [156]. The presence of a radical species was ruled out, as this would have resulted in 'tail-to-tail' coupling (cf. Ga and Al [149]). Reaction of $NiCl_2$ with $[Li\{\mu\text{-}CR_2(C_5H_4N\text{-}2)\}]_2$ also gave a 'head-to-tail' product [142].

### 5.8. Thorium 2-pyridylalkyls

The X-ray molecular structure of $[Th\{CH_2(C_5H_3NMe\text{-}6)\text{-}2\}_2(OC_6H_3^tBu_2\text{-}2,6)_2]$, prepared from $ThCl_4$ with successively $[Li\{CR_2(C_5H_3NMe\text{-}6)\text{-}2\}]$ and then $Li(OC_6H_3^tBu_2\text{-}2,6)$, is isomorphous and isostructural with its hafnium analogue [135]. Both pyridyl-methyl ligands are *C*,*N*-chelating with the geometry about the thorium best described as trigonal prismatic, the triangular faces being formed by O, C and N atoms. The M–N bonds are longer than the M–C bonds, indicating a dative pyridyl link. The thorium lies considerably out of plane of the pyridine ring, presumably to reduce steric effects, although this does not maximise overlap of the nitrogen lone pair of electrons with the heterocyclic ring.

### *5.9. Metal quinolylalkyls*

Closely related to the above ligand system is the quinolyl-1-azaallyl ligand $[\mathrm{C(H)R(C_9H_6N\text{-}8)}]^-$ ($\mathrm{R = SiMe_3}$). To date, lithium [134,165], zirconium [165], tin [133,154], lead [154] and iron [141] complexes have been prepared. The tin complex $[\overline{\mathrm{Sn\{C(H)R(C_9H_6N}}\mathrm{\text{-}8)\}_2}]$ underwent reaction with chalcogens forming a dimeric stannanethione $[\overline{\mathrm{Sn(\mu\text{-}S)C(H)R(C_9H_6N}}\mathrm{\text{-}8)\}]_2$, monomeric stannane–selenone or tellurone $[\overline{\mathrm{Sn\{C(H)R(C_9H_6N}}\mathrm{\text{-}8)\}_2({=}E)}]$ ($\mathrm{E = Se}$ or Te) [133], (cf. $[\overline{\mathrm{Ge\{CR_2(C_5H_4N}}\mathrm{\text{-}2)\}_2X}]$ $\mathrm{X = S}$, Se or Te [153]). Redistribution reactions of $[\overline{\mathrm{Sn\{C(H)R(C_9H_6N}}\mathrm{\text{-}8)\}_2}]$ with $\mathrm{SnX_2}$ ($\mathrm{X = F}$, Cl, Br or I) afforded $[\mathrm{\{C(H)R(C_9H_6N\text{-}8)\}_2Sn \rightarrow SnCl_2}]$ (the first structurally characterised example of a stable donor–acceptor complex between two tin centres), $[\overline{\mathrm{Sn\{C(H)R(C_9H_6N}}\mathrm{\text{-}8)\}X}]$ or $[\overline{\mathrm{Sn\{C(H)R(C_9H_6N}}\mathrm{\text{-}8)\}_2X_2}]$ ($\mathrm{X = F}$, Cl, Br or I), dependening on the reaction conditions [166].

## 6. Concluding remarks

The aim of this article is to provide a comprehensive review of the synthesis, characterisation and reactions of all metal 1-azaallyls. Two principal routes to lithium 1-azaallyls are known: (i) metallation of an imine, ketimine or other unsaturated species or (ii) reaction of $\mathrm{LiCHR_2}$ ($\mathrm{R = SiMe_3}$) or a related α-silylmethyllithium compound with an α-H-free nitrile (e.g. $^t$Bu affording $[\overline{\mathrm{Li\{\mu\text{-}N(R)C(^tBu)C}}\mathrm{(H)R\}}]_2$). Route (ii) is extremely versatile for 'tuning' 1-azaallyl ligands with specific stereoelectronic properties. Lithium (or Na or K) 1-azaallyls are effective ligand transfer reagents and their reaction with the appropriate metal halide provided the principal synthetic route to main group, d- and f-block metal 1-azaallyls. Further reactions of lithium 1-azaallyls have also been discussed. Other reported synthetic routes to metal 1-azaallyl complexes included (i) the reaction of $[\mathrm{Mo_2(CO)_4(\eta^5\text{-}C_5H_5)_2}]$ or $[\mathrm{Fe_2(CO)_9}]$ with a substituted 2-azirine; (ii) thermal isomerisation of a Mo or W alkyl-containing isonitrile ligands, or of Mo or W $\eta^2$-iminoacyl complexes; (iii) decarbonylation of a Group 6 metal $\eta^2$-imine; (iv) reaction of a titanocene-$\eta^2$-imine with $\mathrm{H_2}$, $\mathrm{H_2O}$ or $[\mathrm{Et_3NH}]\mathrm{Cl}$; (v) cleavage of cyclopropane by a zirconocene-$\eta^2$-imine; (vi) β-hydride transfer to the metal from an unstable zirconocene-$\eta^2$-imine; (vii) thermolysis of a vanadium imide complex; (viii) reaction of $[\mathrm{Fe_2(\mu\text{-}CH_2)(CO)_8}]$ with a phosphine imine; (ix) β- and γ-CH-dehydrogenation of an amine in a ruthenium complex; (x) reaction of $[\mathrm{Ru_3(CO)_{12}}]$ with a monoazadiene; and (xi) insertion reaction of $[\mathrm{Yb(CHR_2)_2(OEt_2)_2}]$ with two equivalents of *tert*-butyl cyanide affording $[\overline{\mathrm{Yb\{N(R)C(^tBu)C}}\mathrm{(H)R\}_2}]$.

A diversity of bonding modes is evident in the complexes. $\eta^3$-Coordination is inevitably asymmetric due to the differing electronic properties of the nitrogen and carbon atoms, and was observed most frequently in the transition metal complexes. Another feature is lability of the $\mathrm{SiMe_3}$ substituents and the prochiral nature at the central carbon of the 1-azaallyl moiety, leading to the possibility of diastereoisomers in bis(1-azaallyl)metal compounds (cf. Al, Sn, Zr or Yb) or diastereoselectivity.

As the data of Table 1 amply demonstrate, thermally stable 1-azaallyls of a wide range of elements in a variety of metal oxidation states have been prepared and characterised. This is attributed to the kinetic stabilisation afforded by bulky substituents (often $SiMe_3$) at the 1- and 3-positions and the presence of the hard 1-(*N*–) and soft 3-(*C*–) potential ligating centres. This significant versatility is a feature not associated with its isolobal and structurally related ligands: the allyl **II**, carboxylato **V**, 1-oxaallyl **VI** or 1,3-diazaallyl **VII**. As an illustration, we note that homoleptic 1-azaallyls of Fe(II), Co(II) and Ni(II) are thermally stable (Sections 4.7, 4.8 and 4.9); corresponding allyls are unknown.

The final section discussed the complexes synthesised from the alkyl-functionalised pyridyl ligand $\{CR_2(C_5H_4N\text{-}2)\}^-$ ($R = SiMe_3$) and its related derivatives. $\eta^3$-Coordination, *C*,*N*-chelate and *C*,*N*-bridging modes were observed in a variety of lithium complexes; such a ligand behaved as a *C*,*N*-chelate in the majority of the main group and transition metal analogues forming strained four-membered metallacycles.

## Acknowledgements

We are grateful to EPSRC and FMC Corporation (Bromsgrove and Dr F. Reed) for a CASE award for C.F.C., the European Commission for the award of a Marie Curie Fellowship for P.G.M., and our collaborators at Sussex for their valuable research contributions.

## References

[1] A.J. Pearson, Synlett (1990) 10.
[2] S.L. Blystone, Chem. Rev. 89 (1989) 1663.
[3] J.W. Faller, K.-H. Chao, J. Am. Chem. Soc. 105 (1983) 3893.
[4] K. Yamamoto, J. Tsuji, Tetrahedron Lett. 23 (1982) 3089.
[5] B.M. Trost, Tetrahedron 33 (1977) 2615.
[6] B.M. Trost, T.R. Verhoeven, Comprehensive Organomet. Chem. 8 (1982) 799 (and references therein).
[7] R.D. Adams, D.F. Chodosh, J.W. Faller, A.M. Rosan, J. Am. Chem. Soc. 101 (1979) 2571.
[8] J.J. Doney, R.G. Bergman, C.H. Heathcock, J. Am. Chem. Soc. 107 (1985) 3274.
[9] E.R. Burkhardt, J.J. Doney, R.G. Bergman, C.H. Heathcock, J. Am. Chem. Soc. 109 (1987) 2022.
[10] F. Mercier, J. Fischer, F. Mathey, Angew. Chem. Int. Ed. Engl. 25 (1986) 357.
[11] F. Mercier, C. Hugel-Le Goff, L. Ricard, F. Mathey, Organometallics 7 (1988) 955.
[12] C. Hugel-Le Goff, F. Mercier, L. Ricard, F. Mathey, J. Organomet. Chem. 363 (1989) 325.
[13] F. Mercier, F. Mathey, Organometallics 9 (1990) 863.
[14] R. Appel, W. Schuln, M. Nieger, Angew. Chem. Int. Ed. Engl. 27 (1988) 416 (and references therein).
[15] J. Barker, M. Kilner, Coord. Chem. Rev. 133 (1994) 219.
[16] F.T. Edelmann, Coord. Chem. Rev. 137 (1994) 403.
[17] H.R. Keable, M. Kilner, J. Chem. Soc. Dalton Trans. (1972) 153.
[18] T. Inglis, M. Kilner, T. Reynoldson, E.E. Robertson, J. Chem. Soc. Dalton Trans. (1975) 924.

[19] T. Inglis, M. Kilner, J. Chem. Soc. Dalton Trans. (1975) 930 (and references therein).
[20] J.K. Whitesell, M.A. Whitesell, Synthesis (1983) 517 (and references therein).
[21] S. Nückel, P. Bürger, Organometallics 19 (2000) 3305.
[22] G. Wittig, H.D. Frommeld, P. Suchanek, Angew. Chem. 75 (1963) 978.
[23] G. Wittig, H. Reiff, Angew. Chem. 80 (1968) 8.
[24] G. Stork, S.R. Dowd, J. Am. Chem. Soc. 85 (1963) 2178.
[25] L.M. Jackson, L.M. Scarmoutzos, B.D. Smith, P.G. Williard, J. Am. Chem. Soc. 110 (1988) 6058.
[26] K.N. Houk, R.W. Strozier, N.G. Rondan, R.R. Fraser, N. Chuaqui-Offermanns, J. Am. Chem. Soc. 102 (1980) 1427.
[27] R.R. Fraser, N. Chuaqui-Offermanns, K.N. Houk, N.G. Rondan, J. Organomet. Chem. 206 (1981) 131.
[28] P.B. Hitchcock, M.F. Lappert, M. Layh, D.S. Liu, R. Sablong, T. Shun, J. Chem. Soc. Dalton Trans. (2000) 2301.
[29] P.B. Hitchcock, M.F. Lappert, D.S. Liu, J. Chem. Soc. Chem. Commun. (1994) 2637.
[30] M.F. Lappert, D.S. Liu, J. Organomet. Chem. 500 (1995) 203.
[31] P.B. Hitchcock, J. Hu, M.F. Lappert, M. Layh, D.S. Liu, J.R. Severn, T. Shun, Anal. Quim. Int. Ed. 92 (1996) 186.
[32] P.B. Hitchcock, J. Hu, M.F. Lappert, M. Layh, J. Severn, Chem. Commun. (1997) 1189.
[33] P.B. Hitchcock, M.F. Lappert, M. Layh, Inorg. Chim. Acta 269 (1998) 181.
[34] M. Green, R.J. Mercer, C.E. Morton, A.G. Orpen, Angew. Chem. Int. Ed. Engl. 24 (1985) 422.
[35] E. Carmona, P.J. Daff, A. Monge, P. Palma, M.L. Poveda, C. Ruiz, J. Chem. Soc. Chem. Commun. (1991) 1503.
[36] A.C. Filippou, W. Grünleitner, P. Kiprof, J. Organomet. Chem. 415 (1991) 175.
[37] A.C. Filippou, W. Grünleitner, C. Völkl, P. Kiprof, J. Organomet. Chem. 413 (1991) 181.
[38] A.C. Filippou, W. Grünleitner, E.O. Fischer, J. Organomet. Chem. 428 (1992) C37.
[39] P.J. Daff, A. Monge, P. Palma, M.L. Poveda, C. Ruiz, P. Valerga, E. Carmona, Organometallics 16 (1997) 2263.
[40] U. Amador, P.J. Daff, M.L. Poveda, C. Ruiz, E. Carmona, J. Chem. Soc. Dalton Trans. (1997) 3145.
[41] G.-M. Yang, G.-H. Lee, S.-M. Peng, R.-S. Liu, Organometallics 10 (1991) 1305.
[42] P.W. Dimmock, R.J. Whitby, J. Chem. Soc. Chem. Commun. (1994) 2323.
[43] N. Coles, M.C.J. Harris, R.J. Whitby, J. Blagg, Organometallics 13 (1994) 190.
[44] J. de With, A.D. Horton, A.G. Orpen, Organometallics 12 (1993) 1493.
[45] R. Kuhlman, K. Steib, K.G. Caulton, J. Am. Chem. Soc. 115 (1993) 5813.
[46] R. Kuhlman, K. Folting, K.G. Caulton, Organometallics 14 (1995) 3188.
[47] P.B. Hitchcock, M.F. Lappert, M. Layh, Z. Anorg. Allg. Chem. 626 (2000) 1081.
[48] T.R. van den Ancker, C.L. Raston, J. Organomet. Chem. 500 (1995) 289 (and references therein).
[49] P.B. Hitchcock, M.F. Lappert, S. Tian, J. Organomet. Chem. 549 (1997) 1.
[50] P.B. Hitchcock, M.F. Lappert, M. Layh, J. Chem. Soc. Dalton Trans. (1998) 1619.
[51] R.I. Papasergio, C.L. Raston, A.H. White, J. Chem. Soc. Chem. Commun. (1983) 1419.
[52] D. Colgan, R. Papasergio, C.L. Raston, A.H. White, J. Chem. Soc. Chem. Commun. (1984) 1708.
[53] R.I. Papasergio, B.W. Skelton, P. Twiss, A.H. White, C.L. Raston, J. Chem. Soc. Dalton Trans. (1990) 1161.
[54] W.N. Setzer, P.v.R. Schleyer, Adv. Organomet. Chem. 24 (1985) 353.
[55] N. Kallman, D.B. Collum, J. Am. Chem. Soc. 109 (1987) 7466.
[56] R.A. Wanat, D.B. Collum, G. Van Duyne, J. Clardy, R.T. DePue, J. Am. Chem. Soc. 108 (1986) 3415.
[57] H. Dietrich, W. Mahdi, R. Knorr, J. Am. Chem. Soc. 108 (1986) 2462.
[58] T.J. Lynch, M. Newcomb, D.E. Bergbreiter, M.B. Hall, J. Org. Chem. 45 (1980) 5005.
[59] D. Enders, G. Bachstäder, K.A.M. Kramer, M. Marsch, K. Harms, G. Boche, Angew. Chem. Int. Ed. Engl. 27 (1988) 1522.
[60] D.B. Collum, D. Kahne, S.A. Gut, R.T. DePue, F. Mahamadi, R.A. Wanat, J. Clardy, G. Van Duyne, J. Am. Chem. Soc. 106 (1984) 4865.
[61] P.C. Andrews, D.R. Armstrong, M. MacGregor, R.E. Mulvey, D. Reed, J. Chem. Soc. Chem. Commun. (1989) 1341.

[62] D.R. Armstrong, W. Clegg, L. Dunbar, S.T. Liddle, M. MacGregor, R.E. Mulvey, D. Reed, S.A. Quinn, J. Chem. Soc. Dalton Trans. (1998) 3431.
[63] P.B. Hitchcock, J. Hu, M.F. Lappert, Chem. Commun. (1998) 143.
[64] F. Antolini, P.B. Hitchcock, M.F. Lappert, unpublished work.
[65] P.B. Hitchcock, M.F. Lappert, M. Layh, Tetrahedron Lett. 39 (1998) 4745.
[66] L. Bourget, P.B. Hitchcock, M.F. Lappert, unpublished work.
[67] P.B. Hitchcock, M.F. Lappert, M. Layh, Chem. Commun. (1998) 201.
[68] P.B. Hitchcock, M.F. Lappert, M. Layh, J. Chem. Soc. Dalton Trans. (2001), in press.
[69] W.-P. Leung, H. Cheng, R.-B. Huang, Q.-C. Yang, T.C.W. Mak, Chem. Commun. (2000) 451.
[70] W.-P. Leung, H. Cheng, D.-S. Liu, Q.-G. Wang, T.C.W. Mak, Organometallics 19 (2000) 3001.
[71] A.C. Filippou, C. Völkl, R.D. Rogers, J. Organomet. Chem. 463 (1993) 135.
[72] A.S. Guram, R.F. Jordan, D.F. Taylor, J. Am. Chem. Soc. 113 (1991) 1833.
[73] C.F. Caro, P.B. Hitchcock, M.F. Lappert, Chem. Commun. (1999) 1433.
[74] P.B. Hitchcock, S.A. Holmes, M.F. Lappert, S. Tian, J. Chem. Soc. Chem. Commun. (1994) 2691.
[75] M.T. Reetz, Adv. Organomet. Chem. 16 (1977) 23.
[76] P.B. Hitchcock, M.F. Lappert, M. Layh, J. Organomet. Chem. 529 (1997) 243.
[77] D.J. Peterson, J. Org. Chem 33 (1968) 780.
[78] B. Gehrhus, P.B. Hitchcock, M.F. Lappert, P.G. Merle, unpublished work.
[79] P.B. Hitchcock, M.F. Lappert, R. Sablong, unpublished work.
[80] M.J. Henderson, R.I. Papasergio, C.L. Raston, A.H. White, M.F. Lappert, J. Chem. Soc. Chem. Commun. (1986) 672.
[81] C.F. Caro, D.Phil. Thesis, University of Sussex, 1998.
[82] P.B. Hitchcock, M.F. Lappert, D.S. Liu, E.J. Ryan, Polyhedron 14 (1995) 2745.
[83] R. Fandos, M. Lanfranchi, A. Otero, M.A. Pellinghelli, M.J. Ruiz, J.H. Teuben, Organometallics 16 (1997) 5283.
[84] M.F. Lappert, D.S. Liu, Neth. Pat. Appl. 9500085, 1995.
[85] M.F. Lappert, D.S. Liu, Neth. Pat. Appl. 9401515, 1994.
[86] L.M. Engelhardt, R.I. Papasergio, C.L. Raston, A.H. White, Organometallics 3 (1984) 18.
[87] A.S. Guram, R.F. Jordan, Organometallics 9 (1990) 2116.
[88] C.J. Harlan, B.M. Bridgewater, T. Hascall, J.R. Norton, Organometallics 18 (1999) 3827.
[89] J.R. Severn, D.Phil. Thesis, University of Sussex, 1998.
[90] A. Antiñolo, C. Huertas, I. delHierro, M.F. Lappert, A. Otero, S. Prashar, A.M. Rodriguez, E. Villaseñor, Organometallics 17 (1998) 5874.
[91] P.J. Daff, N. Kaltsoyannis, J. Chem. Soc. Dalton Trans. (1995) 1925.
[92] A.C. Filippou, B. Lungwitz, C. Völkl, E. Herdtweck, J. Organomet. Chem. 502 (1995) 131.
[93] B.S. McGilligan, T.C. Wright, G. Wilkinson, M. Motevalli, M.B. Hursthouse, J. Chem. Soc. Dalton Trans. (1988) 1737.
[94] Y. Nakamura, K. Bachmann, H. Heimgartner, H. Schmid, J.J. Daly, Helv. Chim. Acta 61 (1978) 589.
[95] W.P. Mul, C.J. Elsevier, L.H. Polm, K. Vrieze, M.C. Zoutberg, Heijdenrijk, C.H. Stam, Organometallics 10 (1991) 2247.
[96] J. Keijsper, J. Mul, G. van Koten, K. Vrieze, H.C. Ubbels, C.H. Stam, Organometallics 3 (1984) 1732.
[97] C.A. Mirkin, K.-L. Lu, G.L. Geoffroy, A.L. Rheingold, D.L. Staley, J. Am. Chem. Soc. 111 (1989) 7279.
[98] C.A. Mirkin, K.-L. Lu, T.E. Snead, B.A. Young, G.L. Geoffroy, A.L. Rheingold, B.S. Haggerty, J. Am. Chem. Soc. 113 (1991) 3800.
[99] C.A. Mirkin, K.-L. Lu, T.E. Snead, G.L. Geoffroy, J. Am. Chem. Soc. 112 (1990) 2809.
[100] C.A. Mirkin, T.J. Oyer, M.S. Wrighton, T.E. Snead, G.L. Geoffroy, J. Am. Chem. Soc. 114 (1992) 1256.
[101] M.M. Olmstead, P.P. Power, S.C. Schoner, Inorg. Chem. 30 (1991) 2547.
[102] H. Hope, M.M. Olmstead, B.D. Murray, P.P. Power, J. Am. Chem. Soc. 109 (1985) 712.
[103] H. Chen, R.A. Bartlett, H.V.R. Dias, M.M. Olmstead, P.P. Power, J. Am. Chem. Soc. 111 (1989) 4339.

[104] C.J. Elsevier, W.P. Mul, K. Vrieze, Inorg. Chim. Acta 200 (1992) 689.
[105] L. Polm, C.J. Elsevier, W.P. Mul, K. Vrieze, M.J.N. Cristophersen, F. Muller, C.H. Stam, Polyhedron 7 (1988) 2521.
[106] O.C.P. Beers, J.G.P. Delis, W.P. Mul, K. Vrieze, C.J. Elsevier, W.J.J. Smeets, A.L. Spek, Inorg. Chem. 32 (1993) 3640.
[107] L.H. Polm, G. van Koten, K. Vrieze, C.H. Stam, W.C.J. van Tunen, J. Chem. Soc. Chem. Commun. (1983) 1177.
[108] H.F. Klein, H.H. Karsch, Chem. Ber. 109 (1976) 1453.
[109] W.-P. Leung, H.-K. Lee, L.-H. Weng, Z.-Y. Zhou, T.C.W. Mak, J. Organomet. Chem. 443 (1993) C39.
[110] W.-P. Leung, H.-K. Lee, L.-H. Weng, Z.-Y. Zhou, T.C.W. Mak, J. Chem. Soc. Dalton Trans. (1997) 779.
[111] R.D.W. Kemmitt, S. Mason, D.R. Russell, J. Organomet. Chem. 415 (1991) C9.
[112] P.B. Hitchcock, M.F. Lappert, M. Layh, A. Klein, J. Chem. Soc. Dalton Trans. (1999) 1455.
[113] F.A. Cotton, X. Feng, M. Matusz, R. Poli, J. Am. Chem. Soc. 110 (1988) 7077.
[114] P.K. Mehrotra, R. Hoffmann, Inorg. Chem. 17 (1978) 2187.
[115] Y. Jiang, S. Alvarez, R. Hoffmann, Inorg. Chem. 24 (1985) 749.
[116] P.P. Power, K. Ruhlandt-Senge, S.C. Schoner, Inorg. Chem. 30 (1991) 5013.
[117] C. Eaborn, P.B. Hitchcock, J.D. Smith, A.C. Sullivan, J. Organomet. Chem. 263 (1984) C23.
[118] R.I. Papasergio, C.L. Raston, A.H. White, J. Chem. Soc. Dalton Trans. (1987) 3085.
[119] L. Bourget, P.B. Hitchcock, M.F. Lappert, J. Chem. Soc. Dalton Trans. (1999) 2645.
[120] C. Cui, H.W. Roesky, M. Noltemeyer, M.F. Lappert, H.-G. Schmidt, Organometallics 18 (1999) 2256.
[121] C. Cui, H.W. Roesky, M. Noltemeyer, H.-G. Schmidt, Organometallics 18 (1999) 5120.
[122] K.S. Klimek, C. Cui, H.W. Roesky, M. Noltemeyer, H.-G. Schmidt, Organometallics 19 (2000) 3085.
[123] P. Jutzi, F. Kohl, P. Hofmann, C. Krüger, Y.-H. Tsay, Chem. Ber. 113 (1980) 757.
[124] J.L. Atwood, W.E. Hunter, A.H. Cowley, R.A. Jones, J. Chem. Soc. Chem. Commun. (1981) 925.
[125] B.S. Jolly, M.F. Lappert, L.M. Engelhardt, A.H. White, C.L. Raston, J. Chem. Soc. Dalton Trans. (1993) 2653.
[126] A. Recknagel, F. Knösel, H. Gornitzka, M. Noltemeyer, F.T. Edelmann, U. Behrens, J. Organomet. Chem. 417 (1991) 363.
[127] P.B. Hitchcock, J. Hu, M.F. Lappert, S. Tian, J. Organomet. Chem. 536 (1997) 473.
[128] D.F. Beumel, W.N. Smith, B. Ryballka, Synthesis (1974) 43.
[129] W.-P. Leung, L.-H. Weng, R.-J. Wang, T.C.W. Mak, Organometallics 14 (1995) 4832.
[130] R. Hacker, P.v.R. Schleyer, G. Reber, G. Müller, L. Brandsma, J. Organomet. Chem. 316 (1986) C4.
[131] U. Pieper, D. Stalke, Organometallics 12 (1993) 1201.
[132] H.-K. Lee, B.-S. Luo, T.C.W. Mak, W.-P. Leung, J. Organomet. Chem. 489 (1995) C71.
[133] W.-P. Leung, W.-H. Kwok, L.T.C. Law, Z.-Y. Zhou, T.C.W. Mak, Chem. Commun. (1996) 505.
[134] B.-J. Deelman, M.F. Lappert, H.-K. Lee, T.C.W. Mak, W.-P. Leung, P.-R. Wei, Organometallics 16 (1997) 1247.
[135] S.M. Beshouri, P.E. Fanwick, I.P. Rothwell, J.C. Huffman, Organometallics 6 (1987) 2498.
[136] S.I. Bailey, D. Colgan, L.M. Engelhardt, W.-P. Leung, R.I. Papasergio, C.L. Raston, A.H. White, J. Chem. Soc. Dalton Trans. (1986) 603.
[137] S.M. Beshouri, P.E. Fanwick, I.P. Rothwell, J.C. Huffman, Organometallics 6 (1987) 891.
[138] M.J. Calhorda, A.R. Dias, J. Organomet. Chem. 198 (1980) 41.
[139] S.M. Beshouri, D.E. Chebi, P.E. Fanwick, I.P. Rothwell, Organometallics 9 (1990) 2375.
[140] M.F. Lappert, D.S. Liu, Neth. Pat. Appl. 9500202, 1995.
[141] W.-P. Leung, H.-K. Lee, L.-H. Weng, B.-S. Luo, Z.-Y. Zhou, T.C.W. Mak, Organometallics 15 (1996) 1785.
[142] W.-P. Leung, H.-K. Lee, Z.-Y. Zhou, T.C.W. Mak, J. Organomet. Chem. 462 (1993) 7.
[143] K.J. Izod, P. Thornton, Polyhedron 12 (1993) 1613.
[144] R.I. Papasergio, C.L. Raston, A.H. White, J. Chem. Soc. Chem. Commun. (1984) 612.

[145] T.R. van den Ancker, C.L. Raston, Griffith University, Australia, unpublished work.
[146] T.R. van den Ancker, L.M. Engelhardt, C.L. Raston, B.W. Skelton, A.N. Sobolev, A.H. White, Griffith University, Australia, unpublished work.
[147] L.M. Engelhardt, D.S. Hutchings, C. Jones, C.L. Raston, A.H. White, Griffith University, Australia, unpublished work.
[148] M.J. Henderson, C.L. Raston, Griffith University, Australia, unpublished work.
[149] L.M. Engelhardt, U. Kynast, C.L. Raston, A.H. White, Angew. Chem. Int. Ed. Engl. 26 (1987) 681.
[150] U. Kynast, B.W. Skelton, A.H. White, M.J. Henderson, C.L. Raston, J. Organomet. Chem. 384 (1990) C1.
[151] T.R. van den Ancker, B.S. Jolly, M.F. Lappert, C.L. Raston, B.W. Skelton, A.H. White, J. Chem. Soc. Chem. Commun. (1990) 1007; T.R. van den Ancker, C.L. Raston, B.W. Skelton, A.H. White, Organometallics 19 (2000) 4437.
[152] L.M. Engelhardt, B.S. Jolly, M.F. Lappert, C.L. Raston, A.H. White, J. Chem. Soc. Chem. Commun. (1988) 336.
[153] G. Ossig, A. Meller, C. Brönneke, O. Müller, M. Schäffer, R. Herbst-Irmer, Organometallics 16 (1997) 2116.
[154] W.-P. Leung, W.-H. Kwok, L.-H. Weng, L.T.C. Law, Z.-Y. Zhou, T.C.W. Mak, J. Chem. Soc. Dalton Trans. (1997) 4301.
[155] C.J. Cardin, D.J. Cardin, M.A. Convery, M.M. Devereux, J. Chem. Soc. Chem. Commun. (1991) 687.
[156] C. Jones, L.M. Engelhardt, P.C. Junk, D.S. Hutchings, W.C. Patalinghug, C.L. Raston, A.H. White, J. Chem. Soc. Chem. Commun. (1991) 1560.
[157] T.R. van den Ancker, P.C. Andrews, S.J. King, J.E. McGrady, C.L. Raston, B.A. Roberts, B.W. Skelton, A.H. White, J. Organomet. Chem. 607 (2000) 213.
[158] D.S. Hutchings, P.C. Junk, W.C. Patalinghug, C.L. Raston, A.H. White, J. Chem. Soc. Chem. Commun. (1989) 974.
[159] P.C. Andrews, S.J. King, C.L. Raston, B.A. Roberts, Chem. Commun. (1998) 547.
[160] P.C. Andrews, C.L. Raston, B.W. Skelton, A.H. White, Chem. Commun. (1997) 1183.
[161] P.C. Andrews, C.L. Raston, B.W. Skelton, V.-A. Tolhurst, A.H. White, Chem. Commun. (1998) 575.
[162] W. Schwarz, W. Kolandra, J. Weidlein, J. Organomet. Chem. 260 (1984) C1.
[163] H. Schmidbaur, B. Milewski-Mahrla, G. Müller, C. Krüger, Organometallics 3 (1984) 38.
[164] A.F. Chiffey, J. Evans, W. Levason, M. Webster, Organometallics 14 (1995) 1522.
[165] B.-J. Deelman, P.B. Hitchcock, M.F. Lappert, H.-K. Lee, W.-P. Leung, J. Organomet. Chem. 513 (1996) 281.
[166] W.-P. Leung, W.-H. Kwok, F. Xue, T.C.W. Mak, J. Am. Chem. Soc. 119 (1997) 1145.
[167] M.F. Lappert, D.S. Liu, Neth. Pat. Appl. 9400919, 1994.
[168] B.-J. Deelman, P.B. Hitchcock, M.F. Lappert, W.-P. Leung, H.-K. Lee, T.C.W. Mak, Organometallics 18 (1999) 1444.
[169] K.W. Chiu, R.A. Jones, G. Wilkinson, A.M.R. Galas, M.B. Hursthouse, J. Chem. Soc. Dalton Trans. (1981) 2088.
[170] P.B. Hitchcock, M.F. Lappert, P.G. Merle, unpublished work.
[171] P.B. Hitchcock, M.F. Lappert, M. Layh, Eur. J. Inorg. Chem. (1998) 751.
[172] W.M. Boesveld, P.B. Hitchcock, M.F. Lappert, D.-S. Liu, S. Tian, Organometallics 19 (2000) 4030.
[173] D.R. Armstrong, K.W. Henderson, I. Little, C. Jenny, A.R. Kennedy, A.E. McKeown, R.E. Mulvey, Organometallics 19 (2000) 4369.
[174] P.C. Andrews, Y.R. Armstrong, C.L. Raston, B.A. Roberts, B.W. Skelton, A.H. White, J. Chem. Soc. Dalton Trans. (2001) 996.